# Impacts of Human Interventions on the Water Cycle and its Extremes in Europe

Sigrid Jørgensen Bakke


Thesis submitted for the degree of
Master in Physical Geography, Hydrology and Geomatics
(Hydrology)
60 credits

Department of Geosciences
Faculty of Mathematics and Natural Sciences

UNIVERSITY OF OSLO

Spring 2018

# Impacts of Human Interventions on the Water Cycle and its Extremes in Europe

Sigrid Jørgensen Bakke

Impacts of Human Interventions on the Water Cycle and its Extremes in Europe

http://www.duo.uio.no/

Printed: X-press printing house

# Abstract

The water cycle and its extremes are heavily affected by human activities, such as reservoirs operations and water abstractions. The aim of this study was to evaluate impacts of human interventions (HI) on the water cycle in Europe, with a special focus on changes in high and low flows. Impacts of HI on runoff (based on water balance at the grid-cell scale) and discharge (i.e. routed runoff) were analysed using time series simulated with the global hydrological model PCR-GLOBWB 2 at 0.5° resolution for 1901–2001. Three model scenarios were run; no HI (i.e. natural conditions), transient (i.e. annually introduced) HI and current HI (i.e. HI per 2010). Four meteorological forcing data sets were used to assess the results' sensitivity to the choice of forcing data. Simulated discharge was validated against 316 observed discharge time series, and adequate performance were found for all forcing data sets. Time series of regional median runoff percentiles were assessed to investigate impact of transient and current HI on flow percentiles and flow variability. Impacts of current HI on water gains and losses for the whole period were investigated by using the metrics ecosurplus (water gain) and ecodeficit (water loss) for the water cycle in general ($0^{th}$–$100^{th}$ percentile), the low flow end ($0^{th}$–$10^{th}$ percentile) and the high flow end ($90^{th}$–$100^{th}$ percentile). Regional percentiles revealed only minor impacts due to HI, partly due to the regional aggregation of different types of HI. Ecosurplus and ecodeficit proved to be valuable metrics for detecting areas highly impacted by HI. For runoff, the largest impacts were water gains found in highly irrigated areas in southern Europe and north-west of the Black Sea. In these regions, water gains of more than 10% was found for the low flow end. For discharge, as much as one third of Europe had water losses of more than 10% for the low flow end, and one fifth of Europe had water gains of more than 10% for the low flow end due to current HI. Water losses in discharge reflect the impacts of water use accumulating downstream. Areas affected by upstream reservoirs had generally water gains in the low flow end and water losses in the high flow end, reflecting dam operations that retain water during high flows and release water during low flows. Deviating results for runoff and discharge were found, and are mainly caused by abstraction of surface water and introduction of reservoirs in the case of discharge. Such differences demonstrate the importance of distinguishing between runoff and discharge when investigating impacts of HI on the water cycle. All results were sensitive to the choice of forcing data, especially for high flows and in cold regions. The findings of this study revealed various impacts of HI across Europe, and how HI can affect the two flow extremes differently.

# Acknowledgements

First and foremost, I wish to thank my main supervisor Lena Merete Tallaksen, for her expert guidance and encouragements, for introducing me to the international hydrological community, and for giving me the opportunity to go to conferences and international research meetings. I also want to thank my co-supervisors, Niko Wanders and Christel Prudhomme, for sharing their expertise and for even visiting Norway to discuss the results.

A great thanks to the Department of Physical Geography at Utrecht University for hosting me October-November 2017 and making the data underlying this study available to me, and to Niko for all the time he spent during my visit (and in the time after) patiently introducing me to the field of large scale hydrological modelling, and to PCR-GLOBWB 2 in particular.

I am very grateful to the Panta Rhei *Drought in the Anthropocene* working group and the FRIEND *Northern European Low Flow and Drought* group for letting me be part of their networks, and for letting me contribute with posters to their meetings in October 2017.

Moreover, I thank Norsk Hydrologiråd, Industrial Liaison and the European Geosciences Union that gave me financial support allowing me to attend conferences and meetings.

I want to thank the Hydrological Modelling Section at the Norwegian Water Resources and Energy Directorate and the Department of Hydrology and Water Resource Engineering at Wuhan University for letting me present my thesis work for them.

Finally, I want to thank my family and friends for all the encouragements along the way. A special thanks to my husband, for his support and cheering, and for showing interest in the work. I also want to thank my fellow students in study room 214 for our shared moments of joy and frustrations over the past year. The work would be so much harder without Friday cake and three-o'clock ice creams with you.

# Abbreviations

| | |
|---|---|
| **FDC** | Flow Duration Curve |
| **GHM** | Global Hydrological Model |
| **GSWP3** | Meteorological forcing data set from the Global Soil Wetness Project Phase 3 |
| **HI** | Human Interventions |
| **PCR-GLOBWB 2** | PCRaster GLOBal Water Balance model version 2 |
| **PGMFDv2** | Princeton Global Meteorological Forcing Dataset for land surface modeling version 2 |
| **WFD** | The Water and global change project's meteorological Forcing Data set based on reanalysis ERA-40 |
| **WFDEI** | The Water and global change project's meteorological Forcing Data set based on reanalysis ERA-Interim from 1979, and ERA-40 before 1979 |

# Table of Contents

# List of Figures

# List of Tables

# 1 Introduction

Humans have always been vitally reliant on freshwater, for drinking, livestock, agriculture, energy production and well-being among others. A thorough understanding of the hydrological system enables sustainable water use, advantageous water management and better preparedness in case of hydrological anomalies, like droughts and floods. Accordingly, there is a sustained interest in knowledge about water resources and availability.

The global population is increasing, resulting in a rapid increase in the global water demand. To meet the needs of a growing population, reservoir storages have been constructed, natural vegetation replaced with agricultural land and water abstracted from surface- and groundwater (Wood et al. 2011). As a consequence we have left a large footprint on the terrestrial water cycle, with only a small percentage of the land area remaining unaffected (Wood et al. 2011). The recognition of the extent of the human imprint on the environment and earth systems has given rise to a new term for the era we live in; Anthropocene (Steffen et al. 2011, Savenije et al. 2014).

Even though European citizens do not suffer as much from extreme water shortages and poor water quality as other regions of the world, they are still affected. Many areas in Europe experience reduced river flows, lowered lake and groundwater levels and wetlands drying up. We observe an overexploitation by economic sectors that threatens water availability and quality, and water scarcity is widely reported within Europe. Diminishing water resources also have a damaging impacts on fish, birds, and freshwater ecology among others (EEA 2009).

Construction and operation of reservoirs and dams for hydropower production and water supply significantly alters the natural discharge regime, enhance the evapotranspiration from open water, affects ecosystems and migrating fish, and enhances sedimentation in major river systems (Vörösmarty et al. 2003, Döll et al. 2009). On the other hand, dams that retain water (and thus reduce the downstream streamflow) during high flow periods and release water (and thus increase the downstream streamflow) during low flow periods, complying with the Water Framework Directive (WFD 2000), can have a positive effect on our exposure to hydrological extremes (EEA 2017).

In addition to changes in human interventions, there are changes in the climate system that impact the water balance components and the occurrence of hydrological extremes (i.e. floods and droughts). Increasing frequencies of droughts caused by increases in temperature and evapotranspiration are observed in southern Europe, whereas decreas-

ing drought frequencies due to increased precipitation are observed in northern Europe (Stagge et al. 2017). The intensification of droughts are projected to increase in southern Europe (Prudhomme et al. 2014). The pattern of change is more mixed for floods, however in a summary of recent flood change studies, Hall et al. (2014) found a general pattern of decreasing floods in eastern Europe, increases in central and atlantic regions, and both increases and decreases in southern Europe. Floods are projected to increase in large areas of western Europe due to a pronounced increase in (extreme) rainfall, and decrease in Poland and Southern Sweden, among others, due to a reduction in snow-melt induced floods (Rojas et al. 2012).

Stakeholders as well as scientific communities stress the importance of improving our knowledge on the human-water interface to enable sustainable water use. This will aid our water management and improve preparedness in case of hydrological anomalies, like droughts and floods (Rosenzweig et al. 2017). A blueprint to safeguard Europe's water resources by the European Commission (2012) states that "the ecological and chemical status of EU waters is threatened, more parts of the EU are at risk of water scarcity, and the water ecosystems – on whose services our societies depend – may become more vulnerable to extreme events such as floods and droughts.". It further stresses the importance of addressing these challenges to preserve the nature, economy and human health.

Reliable pan-European assessments are needed to improve the overview of the causes, location and scale of changes in the hydrological system, to approach a sustainable water resource management in the coming century (EEA 2009, Montanari et al. 2013). Research communities have several ongoing efforts targeting these topics. The International Association of Hydrological Sciences (IAHS) introduced a scientific decade (2013-2022) entitled "Panta Rhei – Everything flows" dedicated to research addressing changes in the dynamics of the water cycle connected to related societal changes (Montanari et al. 2013). The Water and Global Change (WATCH) project is an international initiative to increase the understanding of the impacts of climate change and human interventions on current and future water cycle (Harding & Blyth 2009). Another example, is the Inter-Sectoral Impact Model Intercomparison Project (ISIMIP), a community-driven climate-impacts modeling initiative that aims at strengthen the understanding of cross-sectoral impacts, herein climate and socio-economic change (Warszawski et al. 2014).

Large-scale model experiments, like the WATCH and ISIMIP efforts, provide a unique possibility of getting a regional overview of the state of the water cycle and the effects of changes in interrelated systems (Rosenzweig et al. 2017). As opposed to observations, models are continuous in time and scale, and generally consistent in methods for generat-

ing data (Wada et al. 2013, Bierkens 2015). Global hydrological models are often used to study the impact of climate change on the water cycle ad its extremes (e.g. Arnell 1999, Milly et al. 2002, Stagge et al. 2017). Due to uncertainties inherited in both climate and hydrological models, it is increasingly common to include several climate and/or hydrological models in such studies to capture the sensitivity of the results to the model choices (e.g. Haddeland et al. 2011, Gudmundsson et al. 2012, Hagemann et al. 2013, Prudhomme et al. 2014).

Recently, human-water interactions have been implemented in several large scale hydrological models, like WaterGAP (Water Global Assessment and Prognosis; Alcamo et al. 2003) and PCR-GLOBWB (PCRaster GLOBal Water Balance model; Wada et al. 2014), allowing for global assessments of the impact of human activities on the hydrological system. They observe large changes in drought (e.g. Wada et al. 2013, Wanders & Wada 2015) and flood (e.g. Winsemius et al. 2016). Traditionally, these assessments have focused on either one of the two hydrological extremes. Research including both extremes is sparse, especially, when taking into account the impacts of human interventions on the hydrological cycle.

This study contributes to the knowledge and understanding of the impact of different types of human interventions (HI) on the water cycle, including both hydrological extremes, at the European scale. By assessing the impacts on both extremes in addition to the general water flow, possible changes and their associated interventions can be detected in a symmetric manner. Because droughts and floods are very different in the spatial and temporal scale over which they develop, the empirical flow duration curve was used to investigate the variable the two extremes have in common; the extreme flow magnitudes (i.e. low flow and high flow). The global hydrological model PCR-GLOBWB 2 (Sutanudjaja et al. 2017) was used to simulate both runoff (based on water balance at the grid-cell scale) and discharge (i.e. routed runoff along the drainage networks) at a spatial resolution of 0.5◦ for the period 1901-2001. Three model scenarios were used for the simulations; natural conditions (i.e. no HI scenario), historical development of HI (i.e. transient HI scenario), and HI per 2010 used for the whole period (i.e. current HI scenario). Human interventions included water use for irrigation, livestock, domestic and industry, in addition to reservoirs and dam operations. Four different meteorological forcing data sets were used to generate the hydrological output to assess the results' sensitivity to the choice of forcing data.

The research questions were:

- Whether and in what ways do different types of human interventions affect the water cycle and its extremes in Europe?
- To what degree and in what ways are these results sensitive to the choice of forcing data set?

The thesis is structured as follows; The next chapter introduces the theory and studies that constitutes the background of this thesis work. The study area is portrayed in Chapter 3, followed by a description of the data and model applied in Chapter 4. Then, the methods used for the analysis are presented in Chapter 5. Chapter 6 and 7 include the results and discussion, respectively. Conclusions are drawn in Chapter 8, followed by the references.

# 2 Theory

This chapter describes the scientific background for the thesis work. It starts with defining the water cycle and its extremes, followed by a description of the main interrelated systems affecting the water cycle. Then an introduction to large scale hydrological modelling is provided. In the last section, these three aspects (definitions, changing systems and modelling) are reviewed in light of the recent hydrological modelling studies on changes in the water cycle and its extremes due to human interventions.

## 2.1 Defining the Water Cycle and its Extremes

Water is a natural resource that circulates, mostly driven by solar energy. Precipitation feeds the terrestrial world with water that further infiltrates, evaporates, stores temporarily in lakes, soils, groundwater, snow or glaciers, or forms surface runoff. Runoff accumulates through the drainage networks forming river discharge that drain to the ocean or endorheic lakes, of where water evaporates and together with the terrestrial evapotranspiration forms clouds and precipitation again. Globally, the mean residence time of water in unaltered rivers is approx. 20 days, whereas recharge rate in groundwater aquifers can reach up to thousands of years. Annually, a water total of 45 500 $km^3$ flows through the river networks around the globe of which about 3800 $km^3$ is withdrawn by humans (Oki & Kanae 2006).

Global numbers do however not reflect the large temporal and spatial variability in runoff and discharge. Flow varies both in space and time due to the varying climate regimes and catchment characteristics (Krasovskaia et al. 1994). Extremes in the water cycle are occurrences of below normal or above normal conditions, e.g. in streamflow. The extremes in streamflow are often termed droughts when it is below the normal situation and floods when it is above the normal situation.

### 2.1.1 Drought and Low Flow

Droughts can be defined as "a sustained and regional extensive occurrence of below average natural water availability" (Tallaksen & Van Lanen 2004). The definition is relative to an average situation. Accordingly, drought does not include aridity, i.e. "a permanent feature of a dry climate" (Tallaksen & Van Lanen 2004). Natural triggers to drought are prolonged periods of low precipitation and/or high temperatures and evapotraspiration. However, the response to a climatic water deficit condition depends on the dominant land surface properties and processes in the exposed region. Drought usually range from

catchment to regional and continental scale and are mainly considered to be seasonal to decadal temporal duration phenomena (Tallaksen & Van Lanen 2004). There are different types of drought; meteorological, soil moisture and hydrological. Hydrological drought include streamflow and groundwater drought. Numerous metrics has been used to quantify droughts. An operational definition of streamflow drought often includes both a duration characteristic component and a magnitude component. Low flow is defined as this magnitude component of streamflow drought (Tallaksen & Van Lanen 2004).

### 2.1.2 Flood and High Flow

The main types of floods are river floods and coastal floods (Smith & Ward 1998). Many different flood definitions exist, one of them being a river flood definition by Chow (1956): "A flood is a relatively high flow which overtaxes the natural channel provided for the runoff." This definition consists of two criteria; a relative high flow compared to a normal situation, and excessive demands on the river channel. Thus, equivalent to low flow, high flow can be considered the magnitude component of a streamflow flood. Floods are commonly catchment scale events (Tallaksen & Van Lanen 2004). Most river floods are caused by heavy and/or long-lasting rainfall or indirectly due to melt of snow and ice in cold-winter regions. Snow accumulation during the winter period followed by a rapid temperature increase, can often lead to spring and summer floods in these regions (Smith & Ward 1998).

## 2.2 Changes in the Water Cycle and its Extremes

Hydrological models should be able to deal with changing conditions on a large scale to account for the interdependent global and regional systems (Sood & Smakhtin 2015, Thirel et al. 2015). One aspect that has undergone several studies is the influence of a changing climate on the water cycle and its extremes (e.g. Arnell 1999, Milly et al. 2002, Hagemann et al. 2013, Stagge et al. 2017). Climate systems and hydrological systems have strong links, and changes in one system induce changes in the other system (Kundzewicz 2003). The Intergovernmental Panel on Climate Change, IPCC (2013) reports that the climate system has changed considerably. Warming of the atmosphere and the ocean globally has been observed since the mid-20th century, and it is very likely that human influence has been the dominant cause of this rapid temperature increase (IPCC 2013). Winter precipitation has generally increased in Northern parts of Europe and summer precipitation has generally decreased in the Mediterranean (EEA 2017). In recent decades, heavy precipitation events have also increased in several European regions, in particular in the Scandinavia (EEA 2017). Water temperatures in rivers and lakes have increased,

and the seasonal ice cover has shortened, impacting the freshwater ecosystems (van Vliet et al. 2013). European glaciers are retreating and the extent of snow cover have declined significantly (e.g. Maisch 2000, Rizzi et al. 2017). Changes in climate can influence the magnitude, frequency and severity of streamflow flood and drought events in most of Europe, and the changes are projected to continue in the future (Rojas et al. 2012, IPCC 2013, Prudhomme et al. 2014).

However, climatic changes may not be the largest influencer on natural systems (Tallaksen & Van Lanen 2004). According to studies by Gleick (1993) and Wada et al. (2011a), the impacts of human interventions on the terrestrial hydrological cycle can be much larger than the impact of climate change. Changes in land use, irrigation, abstraction of surface water and groundwater, return flows, reservoirs and dam regulations are human interventions that can modify the quality and quantity of streamflow (Tallaksen & Van Lanen 2004, Van Loon et al. 2016). Modifications of land cover, constructions of water management infrastructure and surface and groundwater water withdrawal change the catchment behaviour and the temporal variability in streamflow, which again may have consequences on floods, droughts and management (Thirel et al. 2015).

## 2.3 Large-Scale Hydrological Modelling

Since the 1990s, a number of global hydrological models (GHMs) have been developed to assess water resources availability and use, and lateral transfer of water (Haddeland et al. 2011, Sood & Smakhtin 2015, Bierkens 2015, Wada et al. 2017). These are gridded models that typically focus on solving the terrestrial water balance to estimate discharge by accumulating runoff in the global river networks (Wada et al. 2017). In the context of large scale modelling, it is common to separate between the variables runoff and discharge, schematically illustrated in Figure 1. Runoff refers to the flow variable stemming from the grid-cell water balance, whereas discharge, on the other hand, estimates the river flow by accumulating/routing runoff along the drainage networks (Wada et al. 2011a). Thus, discharge is a spatially dependent variable affected by upstream grid-cells, whereas the runoff variable is not.

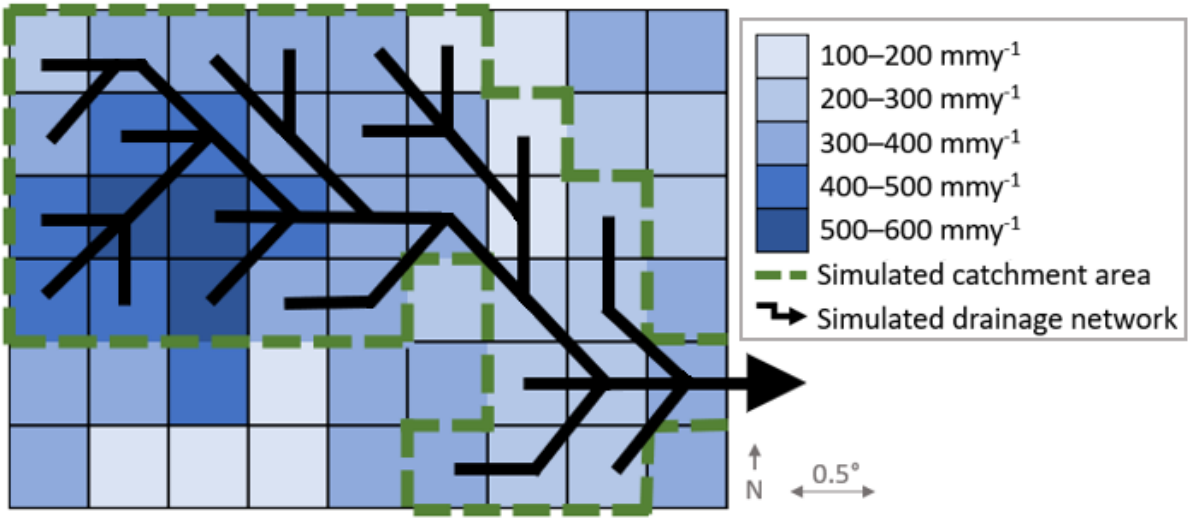


**Figure 1:** A schematic example of simulated runoff (coloured squares; based on water balance at the grid-cell scale independent of the drainage network), and a simulated drainage network (and corresponding catchment area) that controls the lateral accumulation of runoff determining discharge. Possible discharge values for the grid-cells are not given in the figure, however, will generally increase downstream along the drainage network.

GHMs were commonly developed as conceptual hydrological models that were parsimonious regarding data requirement (Harding et al. 2011a, Wada et al. 2017). However, technological advancements have expanded the computational resources, data collection and availability (Bierkens 2015), and hence the parsimonious attribute has weakened in necessity. GHMs have recently improved towards more sophisticated physically based representations of hydrological processes, using finer spatial and temporal resolutions (Wada et al. 2017). In addition to GHMs, there has also been developments in large-scale gridded hydrological modelling through land surface models (LSMs) (Nasonova & Gusev 2008, Haddeland et al. 2011, Sood & Smakhtin 2015). Originally, LSMs were the terrestrial part of global circulation models (GCMs), describing the vertical heat end water exchange processes between the land surface and the near surface atmosphere (Nasonova & Gusev 2008, Harding et al. 2011a). However, they can now work independently (i.e. be run offline) of GCMs and, as GHMs, get meteorological information as an external input (Nasonova & Gusev 2008, Wada et al. 2017). Although LSMs focus on the vertical exchange processes, some also represent lateral transfer of water (Blyth 2001, Harding et al. 2011a). Together with dynamic vegetation models (DVMs) that include land surface hydrology, GHMs and LSMs form the main fields of current large scale hydrological modelling efforts (Wada et al. 2017).

### 2.3.1 Inclusion of Human Interventions

The inclusion of human interventions in GHMs started in the early 2000s (Bierkens 2015, Wada et al. 2017). Whereas LSMs and DVMs typically have a simplistic treatment of surface hydrology and human changes on the land surface, GHMs have a detailed representation of terrestrial hydrological processes (Wada et al. 2017). GHMs may therefore enable a more sophisticated treatment of impacts of human interventions on the water cycle compared to LSMs and DVMs. Some of the GHMs that do include these interventions are versions of WaterGAP (Alcamo et al. 1997, 2003, Verzano et al. 2012), WBM (Vörösmarty et al. 1998, Wisser et al. 2010), H08 (Hanasaki et al. 2008) and PCR-BLOBWB (Van Beek & Bierkens 2009, Van Beek et al. 2011, Wada et al. 2014, Sutanudjaja et al. 2017). A paper by Wada et al. (2017) provides a synthesis of the development of human impact modelling in large scale hydrological models. They summarize that more sophisticated schemes have been implemented to account for the seasonal changes in human water use, and that water use is subdivided among the different sources into different sectors (i.e. domestic, industry, agriculture). Human representations that can typically be found in large scale hydrological models include lake and dam regulations, irrigation, livestock and thermal power cooling among others. However, Wada et al. (2017) argues that "human representations in hydrological models are still rather simplistic". For example, the dynamical interactions and feedbacks between terrestrial water fluxes and human water demands are rarely taken into account (Wada et al. 2014).

### 2.3.2 Uncertainties in Large-Scale Hydrological Modelling Results

Several studies have investigated how well large scale models reproduce regional hydrological extremes in Europe, and notable differences are commonly found in the results when a set of GHMs are applied (e.g. Prudhomme et al. 2011, Stahl et al. 2012, Tallaksen & Stahl 2014, Veldkamp et al. 2018). Prudhomme et al. (2011) found that GHMs can broadly reproduce the spatiotemporal evolution of hydrological extremes. In a study by Tallaksen & Stahl (2014), the large scale models applied had a general tendency to overestimate the number of drought events and underestimate drought duration. Gudmundsson et al. (2012) investigated the ability of nine GHMs to simulate both low flow and high flow percentiles, and found that model performance were notably lower for low flows compared to high flows. Consistency in trends in annual maximum, minimum and monthly mean flow from a set of GHMs was investigated by Stahl et al. (2012). They found agreement among models for the predominant continental-scale pattern of trends, and disagreement among models in magnitude and direction of trends in areas between regions with increasing and decreasing trends. In a recent validation study of GHMs with

human intervention parameterization, Veldkamp et al. (2018) found that the performance of all GHMs in simulating monthly discharge and hydrological extremes improves when human interventions were included.

Recent intercomparison efforts evaluating different large scale hydrological models revealed that large model uncertainties stem from both the meteorological forcing and the hydrological model applied (e.g. Haddeland et al. 2011, Hagemann et al. 2013, Prudhomme et al. 2014, Gosling & Arnell 2016, Gosling et al. 2017). To try to grasp the uncertainty, it has been recommended to use ensembles when analysing large scale hydrological model output, preferably by both using different meteorological data sets and different large scale hydrological models (Haddeland et al. 2011, Gudmundsson et al. 2012, Hagemann et al. 2013). However, it must be noted that such ensembles may underestimate the uncertainty because interactions between researchers tend to increase the consistency between model set ups and thus reducing the range of possible outcomes (Rosenzweig et al. 2017).

## 2.4 Large Scale Modelling Studies of Human Impacts on...

### 2.4.1 Average Flow and Flow Variability

In the first global assessment of the anthropogenic alteration of river flow regimes by Döll et al. (2009), the flow variability was assessed using monthly discharge time series simulated by WaterGAP with different human intervention scenarios over the period 1961-1990. They found that irrigation caused decreases in long-term average river discharge and low flow, and increases in the inter-annual variability. The few places globally where low flow had increased due to human alterations were downstream of reservoirs. Reservoirs and water withdrawals caused decreases in flow amplitude. Wada et al. (2014) investigated the impact of human water use and reservoir regulations on terrestrial water resources globally for the period 1979–2010 using the version of PCR-GLOBWB that includes dynamical feedback between supply and demand. An increase by more than 60% of surface water and groundwater use were found. Agriculture accounted for 80% of the total water withdrawal. They also found that water withdrawal and upstream reservoirs affected the water availability downstream, with an accumulated effect along the river network. In a study by Haddeland et al. (2014), the effect of both climate change and direct human interventions on the global terrestrial water cycle were assessed using seven different models forced with eight different climate projections. They found that the impact of anthropogenic interventions was significant for several large river basins, despite a considerable spread in individual results. For the historical period 1971–2000, they found

decreases of down to -5% in basin discharge due to human interventions in southern and south-eastern Europe. Historical changes in long term average river discharge (1901–2010 divided into four 30-years periods) using the WaterGAP model and four different forcing data sets, were analysed globally by Müller Schmied et al. (2016). They found that human water use and dam constructions were the dominant drivers over precipitation for changes in long term average discharge in about a tenth of the land area, including areas in the Iberian Peninsula, and drainage systems close to the Black sea in the south, west and north.

### 2.4.2 Water Scarcity

Several of the large-scale modelling research on impacts on the water cycle due to human interventions has focused on water scarcity, a topic that also was a main reason for the first generation of GHMs (Wada et al. 2017). Water scarcity is distinct from drought by being caused by high human consumption relative to the natural renewable availability (Loon & Lanen 2013). In a study by Veldkamp et al. (2015), water scarcity from 1960–2000 was investigated globally using three GHMs, for the first time by accounting for both temporal changes in socioeconomic conditions and hydro-climatic variability over the period. Their finding revealed that hydro-climatic variability and socioeconomic changes interact and can both strengthen or attenuate each other. Annual changes in water scarcity result mainly from hydro-climatic variability, although the relative contribution of socioeconomic developments has increased throughout the period. Of irrigation, industrial, domestic and livestock water use, they found that industrial water use had the largest relative impact on water stress conditions in Western Europe. In a multi-model assessment of water availability and water scarcity in the period 1971-2010, Veldkamp et al. (2017) found that human interventions caused water scarcity to propagate downstream, and that positive impacts of human interventions mostly occur upstream. They also found differences among the models in the attribution of water scarcity changes to different types of human interventions, and substantial variation in the seasonal impact and dominant intervention type.

### 2.4.3 Streamflow Droughts

Drought are often studied at regional to global scale, as they have larger spatial extents and longer durations than other hydrological extremes. This makes large scale hydrological modelling studies particularly well suited to study droughts. Some recent studies also take advantages of the recent development in large-scale hydrology by looking at the interaction between drought and human interventions in their investigations. Impacts of human interventions on the intensity and frequency of streamflow droughts (by specific

deficit volume and occurrences below the $20^{th}$ percentile, respectively) over the period 1960-2010 were investigated by Wada et al. (2013) using monthly time series simulated by PCR-GLOBWB. In Europe, they found that human water consumption substantially reduced local and downstream monthly streamflow, and increased drought frequency by approximately 20%. Also, an intensification of the drought intensity by 10–500% was found globally, causing persistent low flow conditions. In southern Europe, this is mainly attributable to irrigation where water use during the cropping period reduces the downstream streamflow, whereas the impact of industrial and household water consumption is larger for central and western Europe. Using daily discharge data simulated by PCR-BLOBWB over California 1979–2014, He et al. (2017) analysed the contribution of human water management to the intensification and mitigation of streamflow drought. The inclusion of human interventions improved the performance of simulated discharge to the observations. They found that the severe 2014 drought deficit (volume below $10^{th}$ percentile) was alleviated in Southern California by reservoir operation during low flow periods. On the contrary, the drought deficit and duration (of streamflow below $10^{th}$ percentile) was increased due to water consumption in the densely irrigated region of Central Valley.

In addition to historical simulations, several studies incorporate human interventions in future scenarios. For example, Forzieri et al. (2014) investigated the effect of climate change and water consumption on future streamflow droughts in Europe using 7-day moving averages of simulated discharge from the large scale model LISFLOOD (Van Der Knijff et al. 2010). Climate driven changes included more severe (based on return periods from an extreme value distribution fitted to annual minima) and persistent (deficit volume below $20^{th}$ percentile) streamflow droughts in many parts of Europe, except in the north and north-east. Human water use aggravates this situation in southern Europe. In some areas in western, central and eastern Europe, water use can reverse the climate induced reduction in droughts. However, reservoir and flow regulations were not implemented in these analyses. In another study of human and climate impacts on future streamflow droughts, Wanders & Wada (2015) investigated impacts on deficit volume and duration (below variable $90^{th}$ percentile), as well as severity defined as the ratio of deficit volume over duration, of drought based on daily data simulated by PCR-GLOBWB. They found that reservoirs tend to reduce the impact of drought because water retention during wet seasons leads to more water during the dry seasons. They found high impacts of human interventions in Europe during summer and fall; with more severe drought in southern Europe, and a decrease in drought severity in eastern and parts of northern Europe.

### 2.4.4 Floods

To the author's knowledge, large scale modelling research of impacts of human interventions on floods or high flows are sparse. This is presumably because floods are often smaller in their spatial extent, and their hazards dependent on local characteristics, e.g. the geometry of the specific river channel. However, there are recent studies aiming at modelling the flood risk including human aspects other than what is considered in the present study, such as cost-benefit assessments of flood management in urban areas (Ward et al. 2017) and socio-economic development (Winsemius et al. 2016). On local scale, several studies assessing human-flood interactions in settled flood plains have been undertaken (e.g. Remo et al. 2012, Di Baldassarre et al. 2013). In a study of the Middle Mississippi River, Remo et al. (2012) found that a removal of all the flood-control structures would cause a reduction in average flood stages, however, increase the potential flood losses. By a dynamical human-flood model, Di Baldassarre et al. (2013) were able to simulate the emergence of real-case patterns, such as shifts from frequent, small flooding events to the occurrence of rare, catastrophic flood disasters.

## 2.5 The Contribution of This Study

The present study is novel in its use of flow duration curve based symmetric metrics in the assessment of human interventions on hydrological extremes. In addition to simulating the natural and historical human intervention scenarios, the present study also investigate the impacts current human interventions would have implied given the meteorological conditions of the 20th century. Further, it is one of the first studies revealing continental impact patterns of current human interventions on high flows. The historical meteorological time series used were longer than what is used in most studies on this topic. Finally, it contributes to the knowledge of impacts of human interventions on both runoff (vertical water balance) and discharge (routed water down the drainage system), and by that highlighting the different pros and cons of these two flow variables when analysing the human-water interface.

# 3 Study Area

The study area of the thesis is the European domain (from now on called Europe) defined as the terrestrial part of the box from -12°–47°E longitude and 33°–72°N latitude, excluding regions of Northern Africa (exact grids and coverage is visualized in Figure 12 in Chapter 4). A map of Europe with names of several countries, rivers and seas is given in Figure 2. Note that maps used in this chapter are not always in line with the domain defined for the analyses, due to the various projections and definitions of Europe that exist.

Europe is situated in the northern hemisphere and have a large variety in topography (top left map of Figure 3). The elevation ranges from below sea level (e.g. in the Netherlands) to high altitudes found in mountainous regions such as the Alps (North of Italy), Carpathian Mountains (between the Alps and the Black Sea) and (outside of the coverage of the Figure) the Caucasus Mountains (East of the Black Sea) where the highest peak of the study area, Mount Elbrus at 5642 [m.a.s.l.], is situated. Europe has a large diversity in both natural characteristics and human influences. In the following sections, an overview of the climate, hydrology and human interventions in Europe is presented.

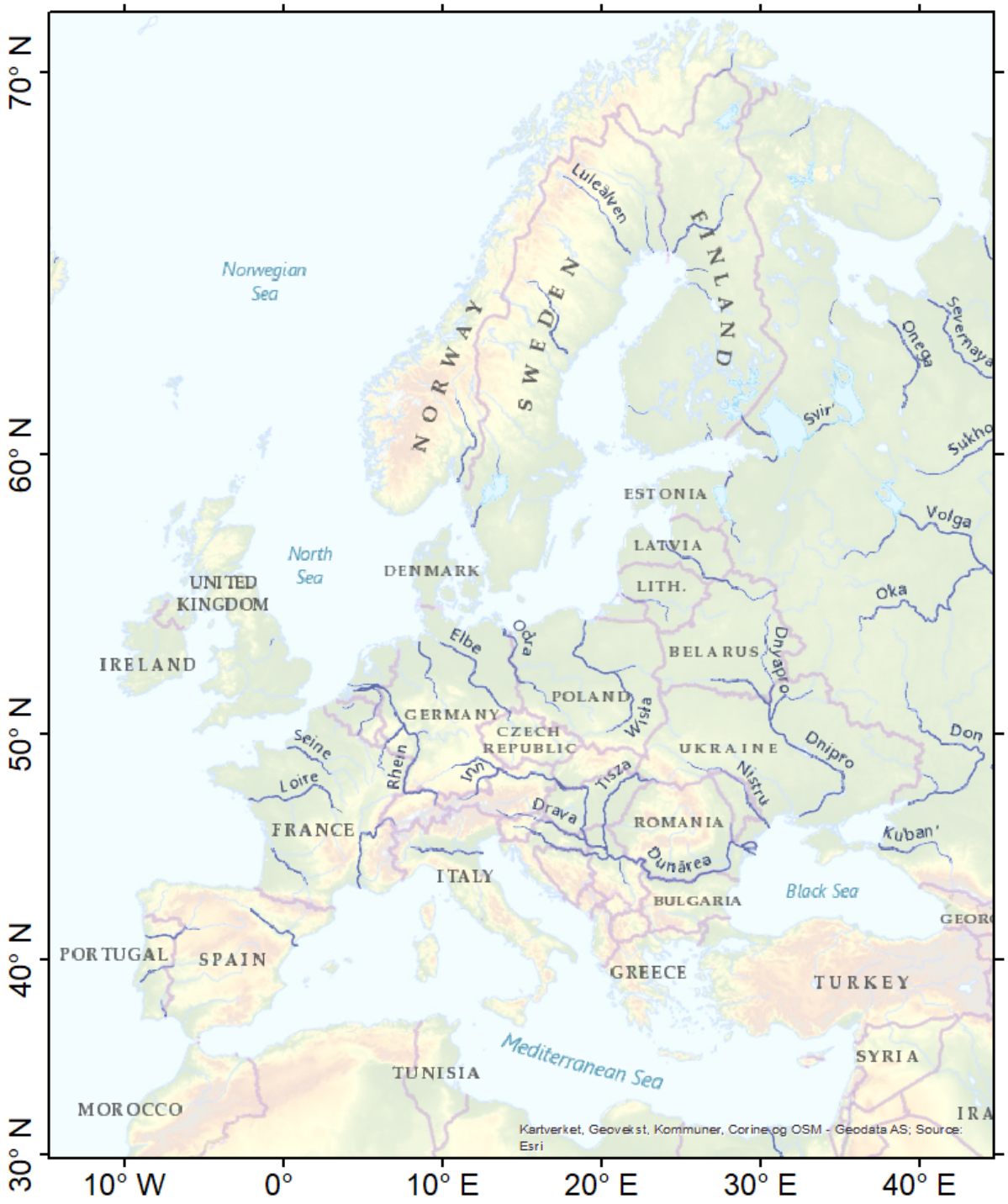


**Figure 2:** Map of Europe including names of the largest rivers (credit: Kartverket, Geovekst, Kommuner, Corine og OSM - Geodata AS; Source ESRI). The rivers Rhein, Dunărea and Dnipro will be referred to with their English names Rhine, Donau and Dnieper, respectively. Two large rivers, Euphrates and Tigris, are not named in the map. They are visible as lines in light blue moving southward from their origin in eastern Turkey. The Iberian Peninsula will be referred to in this study, and is the peninsula that mainly consists of Portugal and Spain.

## 3.1 Climate in Europe

Long term precipitation (P), temperature (T) and actual evapotranspiration (AET) in Europe for the period 1975-2005 are shown in Figure 3. Because these maps do not cover the whole domain (or period) used in the thesis, additional maps of P and T (AET data was unavailable) from the Water and global change project's newest meteorological Forcing Data set (WFDEI: Weedon et al. 2014, explained more in detail in Section 4.4.4) over the period 1901-2001, are shown in Appendix A as Figure 27 and 28, respectively.

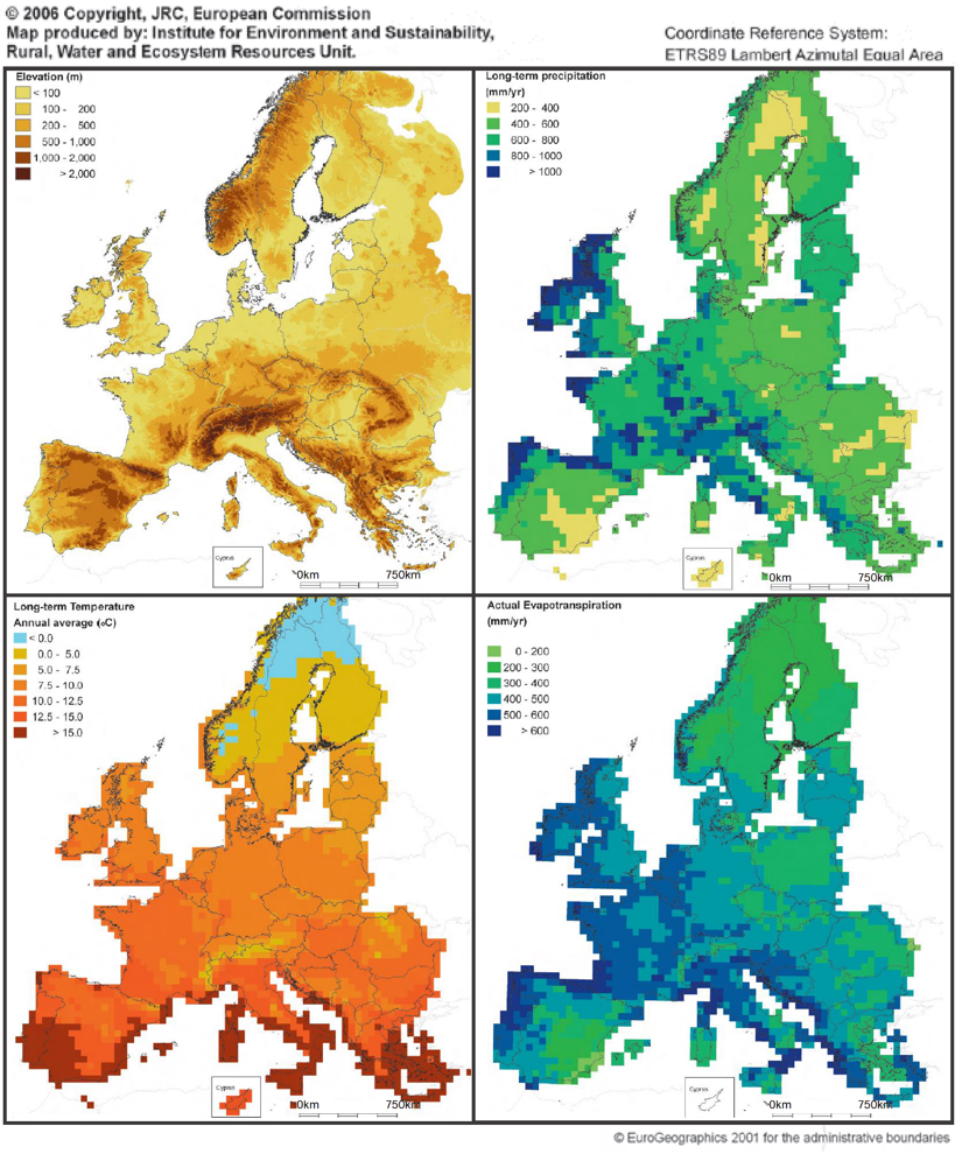


**Figure 3:** Digital elevation map (DEM; top left) and long-term precipitation (P; top right), temperature (T; bottom left) and actual evapotranspiration (AET; bottom right). P and T are interpolated observational data covering the period 1975-2005, and AET is calculated based on P and T. Maps are produced by the Joint Research Centre, European Commission (Mulligan et al. 2006), and edited by author for easier readability. Note that the domain used in this study is not fully covered.

The influence of latitude, topography and distance to the sea results in high variability in precipitation in Europe (EEA 2009). The highest amounts of precipitation are more than a meters per year, and found in regions along western coastlines and the mountain ranges. Eastern Europe, Sweden and Spain hold the lowest precipitation amounts (around 200 $mmy^{-1}$). Europe spans over approximately 40 degrees in latitude, and there is a temperature gradient following the latitudes northward from the hottest areas in southern Europe with annual means of more than 15°C to below zero temperatures found in northern Europe. Altitude also affects the temperature, and low temperatures compared to the surroundings are found in high altitude regions such as the Alps. Due to high AET, most of Europe have no more than 250 $mmy^{-1}$ excess rainfall, and lower than 50 $mmy^{-1}$ in parts of southern Europe (Mulligan et al. 2006).

Regional climate classification is a nice tool to divide continents into regions with similar climatic characteristics, and such regionalizations are commonly used in large scale studies of climate and hydrology. The first quantitative climate classification was developed by Köppen (1900), and despite its age it is still commonly used. According to this classification, most of Europe is characterized by warm temperate climate, is fully humid and have warm summers. North-eastern Europe and high altitudes have snow dominated climate instead of warm temperate climate, and southern Europe have dry and hot summers instead of the fully humid climate characterizing the rest of the continent (Kottek et al. 2006). A more recently developed climate classification of Europe is used in the European chapter of the IPCC Fifth Assessment Report (Kovats et al. 2014), and was derived from environmental zones made by Metzger et al. (2005) based on principal component analysis using different variables of temperature, precipitation and proportion of sunshine, in addition to altitude, slope, latitude and oceanicity. The classification divides Europe into a Continental, Northern, Southern, Atlantic and Alpine region (Figure 4). Relating the regions to the climatic information in Figure 3, the Alpine region is characterized by cold and wet conditions, the Southern by warm and dry conditions, the Atlantic by wet conditions and intermediate temperatures, and the Southern and Northern regions by dry conditions and intermediate and low temperatures, respectively. However, there are naturally large variabilities within each region. This classification (as defined in Figure 4) was used in this study to look at regional impacts of human interventions on hydrology.

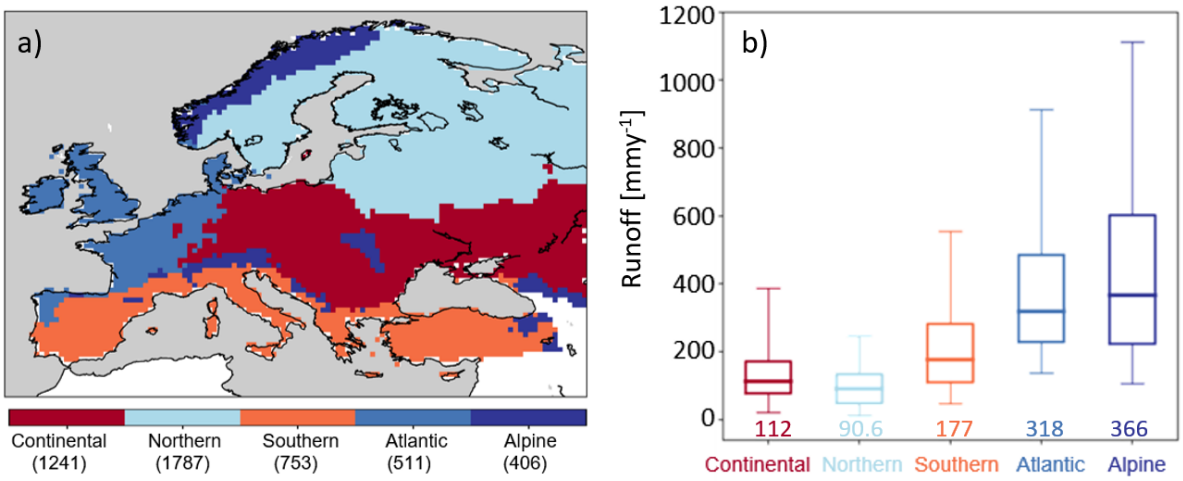


**Figure 4:** A climate region classification based on Metzger et al. (2005), and used in the European chapter of the IPCC Fifth Assessment Report (Kovats et al. 2014): a) the classification plotted at 0.5° resolution with the number of 0.5° x 0.5° cells included in each region given in brackets, and b) boxplot of the spread of median runoff within each region corresponding to simulated runoff given in Figure 5a). The boxes and whiskers give the range of the mid half and mid 90% of the medians, respectively, whereas the regional medians are given as lines in the boxes, and as numbers below each boxplot.

## 3.2 Hydrology in Europe

The hydrological variability in Europe is large. Figure 5 shows simulated natural median runoff (local water balance) and discharge (routed runoff) under natural conditions. The runoff pattern (Figure 5a)) has distinct similarities to the meteorological patterns, in particular precipitation. The consistency in median runoff within each climate region is shown in Figure 4b). Eastern Europe, Sweden and the southern most areas of the study area are dry regions with runoff values generally less than 200 $mmy^{-1}$, and many places less than 100 $mmy^{-1}$. Runoff is largest in western Norway, United Kingdom, Ireland, the Alps and in the Caucasus Mountains, with values exceeding 1000 $mmy^{-1}$. In the map of natural discharge (Figure 5b)), the river network emerges, and the highest flows are found downstream in long rivers, such as Donau, Volga, Rhine and Dnieper (see Figure 2). Regions like western Norway have lower discharge values despite the high runoff, as a result of the smaller river basins.

The distribution of river flow throughout the year (i.e. flow regime) varies across Europe, and reflect two main controlling factors; the climate regime and the storage capacity of the basin (Krasovskaia et al. 1994). The climate regime determine the seasonal distribution of rain and snowfall, evaporation and snowmelt that controls the timing of low and high flow

periods, whereas the storage capacity reflect the presence of aquifers, lakes and marshes that influence the range between low and high flows (Krasovskaia et al. 1994). A high storage capacity in a basin generally causes a slower and more persistent response to water input, and thus have a smaller variability in flow throughout the year compared to a basin with low storage capacity.

In northern and north-eastern Europe, as well as in mountainous regions, much of the precipitation during winter falls as snow, and a large proportion of the discharge therefore occurs during melt-season in spring/summer EEA (2009). Such regions are therefore commonly characterized by a flow minimum in winter and a distinct flow maximum in spring/summer (Krasovskaia et al. 1994). For inland regions further south it is common with an additional rain caused flow maximum during autumn and/or flow minimum during summer due to evaporation losses (Krasovskaia et al. 1994). Atlantic and southern regions have rain as the main generic source in flow formation. High flows are found in winter and low flows in summer because rainfall is highest during winter months in these regions (Krasovskaia et al. 1994). Due to high evaporation and low precipitation river flow may be very low during summer in southern Europe, with some intense rainfall events causing sudden and short-lasting dramatic rises in discharge (EEA 2009).

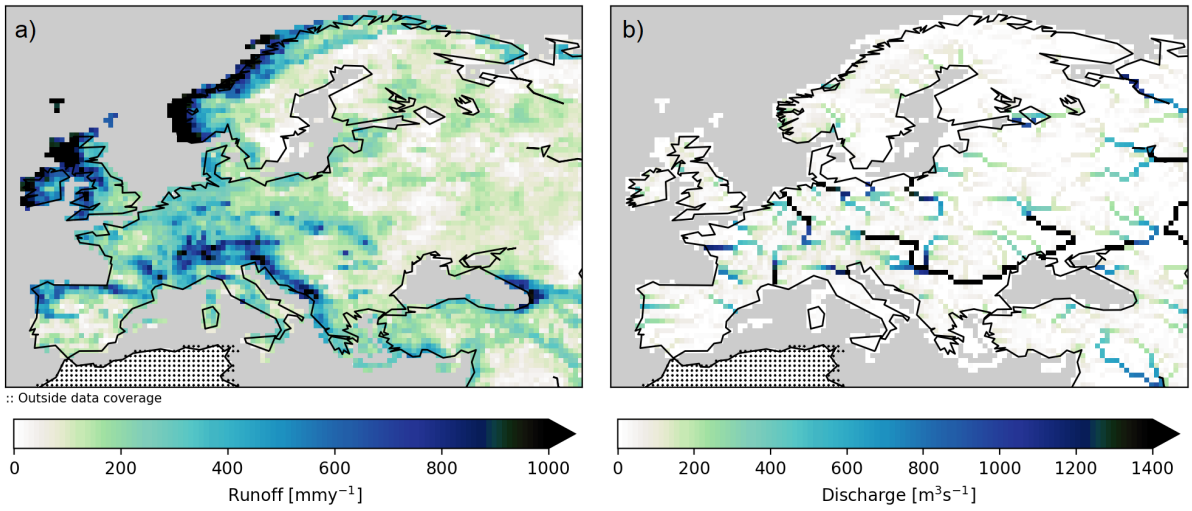


**Figure 5:** a) Median runoff (local water balance) and b) median discharge (routed runoff) over the period 1901–2001 given natural conditions simulated by the hydrological model PCR-GLOBWB 2 using WFDEI meteorological forcing data.

## 3.3 Human Interventions in Europe

The total annual abstraction of freshwater in Europe is approx. 288 km$^3$ (EEA 2009). Of this volume, 44% is for energy production, 24% for agriculture, 21% for public water

supply and 11% for industry. For eastern and northern countries, energy production account for over half of the water abstracted. On the contrary, countries in southern Europe use most of the abstracted water for agriculture, where approx. 60% of the water is used for irrigation alone (EEA 2009).

Figure 6–9 show the irrigated areas, and (gross) water demand for industry, domestic and livestock in Europe. The spatial pattern in 2010 is shown in the left plot, and the regional development since 1960 (data pre-1960 is unavailable) in the right plot of each figure. The most densely irrigated areas are found in southern Europe, around the Black Sea and along the western coast up to Denmark (Figure 6). Northern Europe have the least irrigation. Water demand for industry (Figure 7) and domestic use (Figure 8) are commonly found in densely populated regions, with domestic use generally demanding the most water. Livestock water demands are mostly found in the United Kingdom and surrounding regions (Figure 9). Generally, water demands and irrigated areas have increased since 1960. However, clear exceptions are found in the Continental and Northern regions for irrigation and livestock where there have been decreases from around 1990 following the collapse of the Soviet Union. From around year 2000 there has been a notable change to higher increases in industry and domestic water demand in the same regions. In general, irrigation, industry and domestic water demand follow the increasing population and its societal developments.

Surface water is the dominant source from which water is abstracted in Europe, accounting for nearly all water for energy production and three quarters of the water for industry. Surface water is also, to a smaller extent, the major source for agricultural use, however, the numbers are uncertain due to unreported illegal groundwater abstractions. Just over half of the water abstracted for public water supply originates from groundwater. In some countries, groundwater aquifers are artificially recharged with water from excess storm water, river water or treated wastewater. Desalinated water is a freshwater source primarily used in arid regions. In Europe, Spain is the leading user of desalination technology, followed by other Mediterranean countries, such as Greece, Italy and Portugal (EEA 2009).

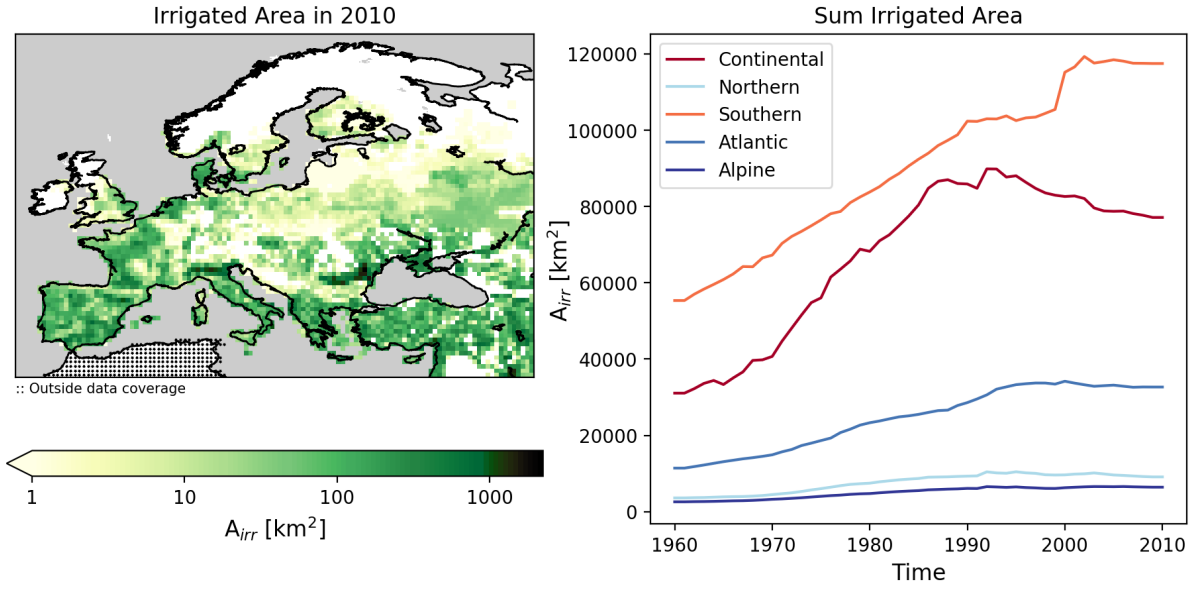


**Figure 6:** Irrigated area ($A_{irr}$ [km$^2$]) per cell in 2010 (left; given in $Log_{10}$ scale), and annual $A_{irr}$ in each region in the period 1960–2010 (right). Data are based on FAOSTAT (Food and Agriculture Organization of the United Nations 2012).

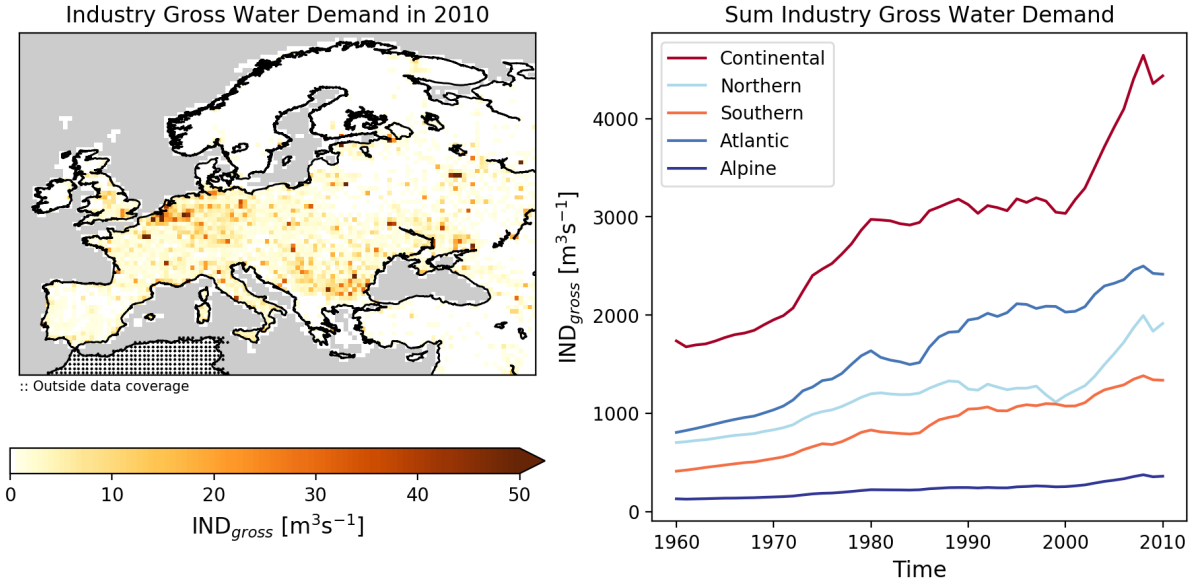


**Figure 7:** Industry gross water demand ($IND_{gross}$ [m$^3$s$^{-1}$]) per cell in 2010 (left), and annual $IND_{gross}$ in each region in the period 1960–2010 (right). Data were calculated following methods by Wada et al. (2014).

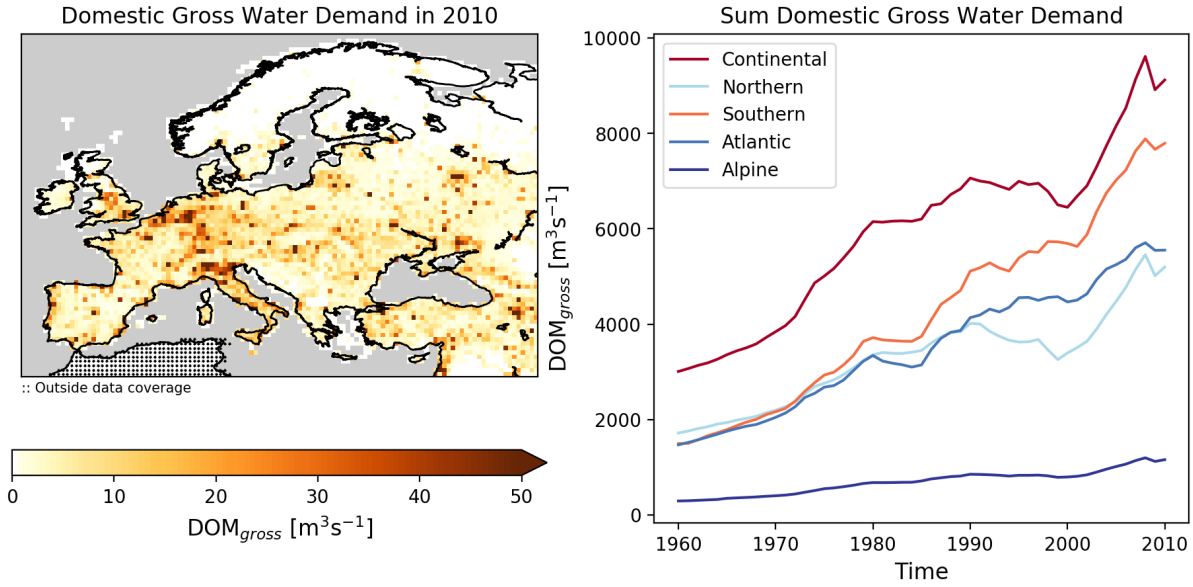


**Figure 8:** Domestic gross water demand (DOM$_{gross}$ [m$^3$s$^{-1}$]) per cell in 2010 (left), and annual DOM$_{gross}$ in each region in the period 1960–2010 (right). Data were calculated following methods by Wada et al. (2014).

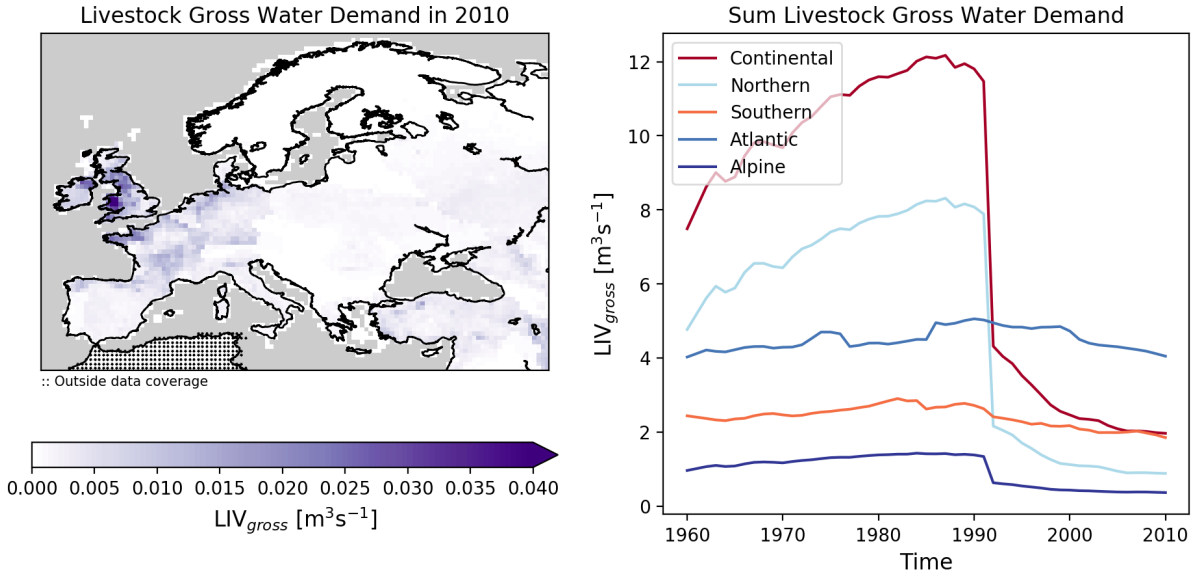


**Figure 9:** Livestock gross water demand (LIV$_{gross}$ [m$^3$s$^{-1}$]) per cell in 2010 (left), and annual LIV$_{gross}$ in each region in the period 1960–2010 (right). Data were calculated following methods by Wada et al. (2014).

Because streamflow varies over the year, water storage systems are needed to be able to use water from the high flow season during low flow season (Oki & Kanae 2006). Reservoirs across Europe have a total storage capacity equivalent to approx. 20% of the total available freshwater resources (EEA 2007). The capacity volume increased significantly

throughout the 20th century for many European countries, a trend that recently has flattened out due to both depletion of suitable reservoir construction locations and an increasing concern regarding the environmental impacts.

Figure 10 and 11 show the 2010 situation (left plot of both figures) and the region-wise development from 1901 (right plot of both figures) in reservoir capacity and upstream reservoir capacity, respectively. There was a sharp increase in construction of reservoirs in the 1950s and 60s in the Northern and Continental region, whereas the Southern region had the largest increase during the 1990s. The very low reservoir capacity in the Atlantic region reflects densely populated areas with very little variations in topography. Most of the largest reservoirs (i.e. storage capacity exceeding 3 mill m3) are found in Spain (approx. 1200), Turkey (approx. 610), Italy (approx. 570), France (approx. 550), UK (approx. 500), Norway (approx. 360) and Sweden (approx. 190) (EEA 2009).

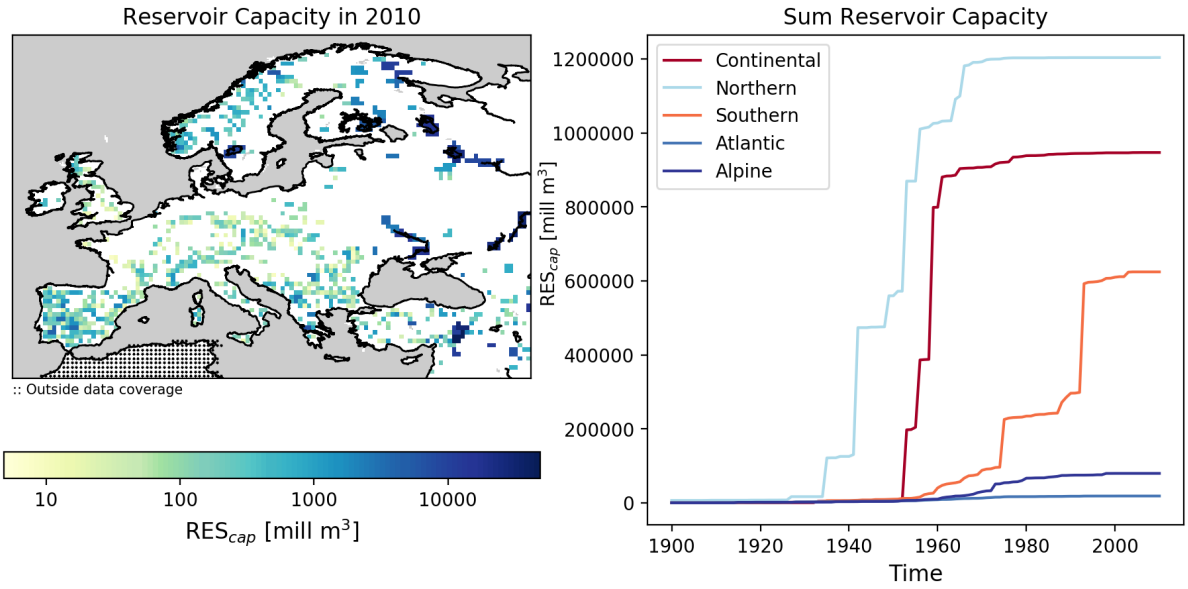


**Figure 10:** Reservoir capacity ($RES_{cap}$) per cell in 2010 (left; given in $Log_{10}$ scale), and annual $RES_{cap}$ in each region in the period 1900–2010 (right). Reservoir data are obtained from GranD (Lehner et al. 2011).

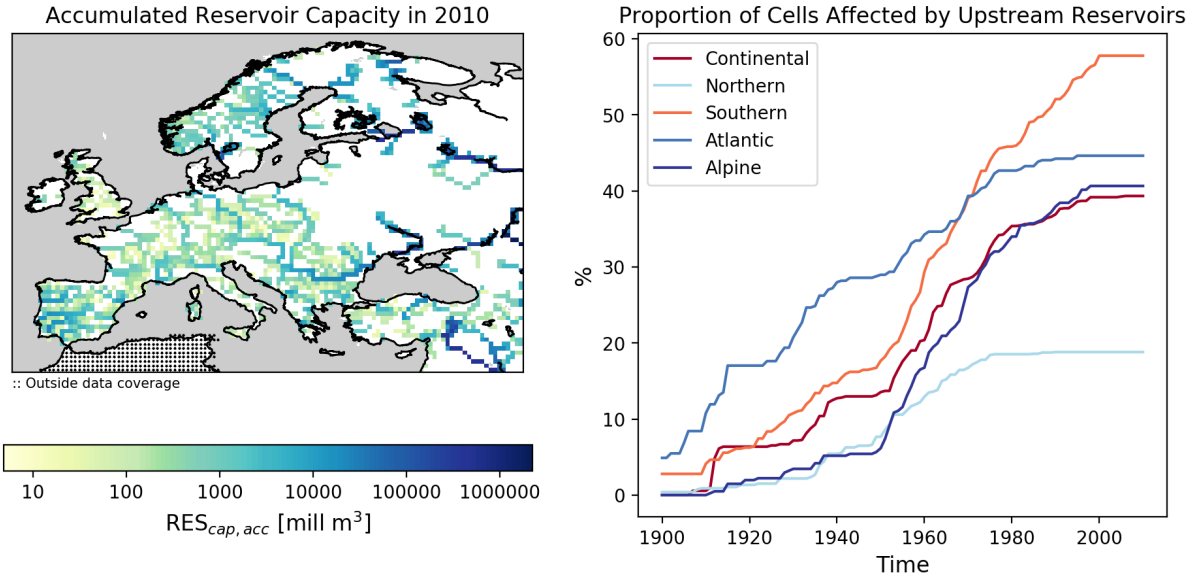


**Figure 11:** Accumulated reservoir capacity of upstream reservoirs ($RES_{cap,acc}$) of each cell in 2010 (left; given in $Log_{10}$ scale), and annual proportion [%] of cells in each region with upstream reservoirs in the period 1900–2010 (right).Reservoir data are obtained from GranD (Lehner et al. 2011), and the drainage networks are based on HydroSHEDS (Lehner et al. 2008), GTOPO30 (Gesch et al. 1999) and Hydro 1k (Verdin & Greenlee 1996, USGS EROS Data Center 2006).

# 4 Data and Model

## 4.1 Data

Data used for analysis were runoff [$mmd^{-1}$] and discharge [$m^3s^{-1}$] simulated at a daily time step by the gridded global hydrological model PCRaster GLOBal Water Balance model version 2.0 (PCR-GLOBWB 2; Sutanudjaja et al. 2017). Whereas runoff stems from the vertical water balance at the grid-cell scale, discharge is the accumulated water flow through the drainage network (explained in more detail in Section 4.2, see also Figure 5). Hence, the two flow variables provide different types of information; the impact of the local human intervention (HI) in case of runoff and the additional accumulated impacts of the upstream HI in case of discharge.

The model was run with a spatial resolution of 0.5x0.5 arc-degrees (approx. 55x55 km at equator). The focus was the pan-European domain as shown in Figure 12. Meteorological forcing data for the historical period of 101 years from 1901-2001 were used for the model runs. Four different meteorological forcing data sets were applied to allow for an assessment of the meteorological uncertainty in the model simulations.

Three model scenarios were included in the simulations; no HI (i.e. natural scenario), transient HI (i.e. historical HI introduced on an annual basis) and current HI (i.e. whole period simulated with the HI of 2010). Impacts of HI could therefore be investigated by comparing the transient and current HI scenarios with the natural (no HI) scenario. Whereas the transient HI scenario attempts to represent the actual developments of HI during the $20^{th}$ century, the current HI simulates how HI as present in 2010 will impact the water cycle given meteorological conditions as we had we had the last century. Seven-day moving averages were calculated from the original output of daily data, and used as temporal resolutions for the analysis. This allows for quantification of low and high flows at a high temporal resolution, and also reduces the influence of one day event outliers.

Specifications of the data are summarized in Table 1. All simulations were run at Utrecht University and model outputs made available for the author to utilize. In the subsequent sections, PCR-GLOBWB 2 will be presented, followed by an introduction to the human interventions simulations and the meteorological forcing data used.

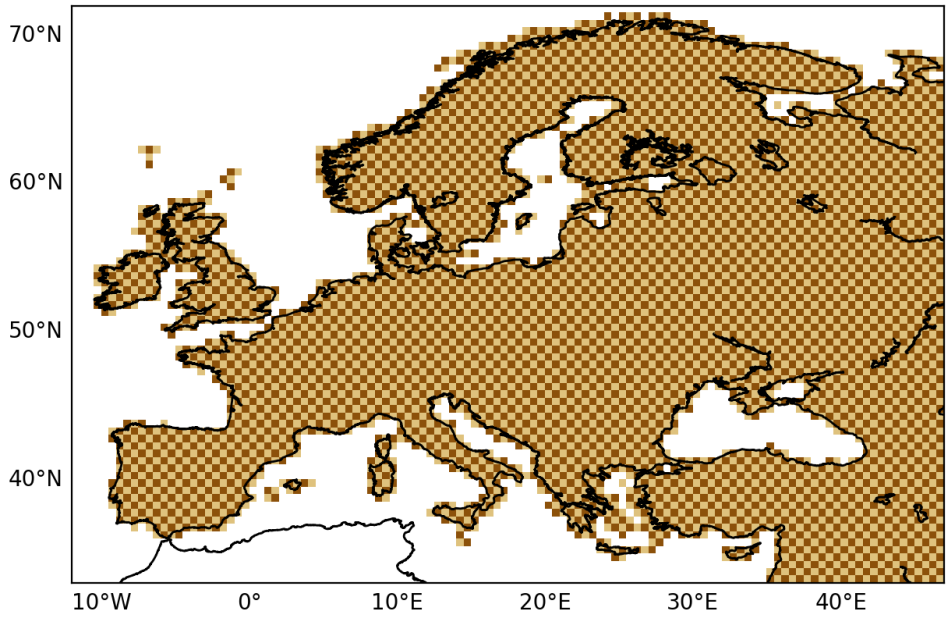


**Figure 12:** Spatial coverage (coloured area) and spatial resolution (coloured squares) used for the analysis. Main coastlines are outlined in black (retrieved from the python package *mpl_ toolkits.basemap).*

**Table 1:** Specifications of the PCR-GLOBWB 2 model output, and the data used for the analysis.

| | **Model choices** | **Data for the analysis** |
|---|---|---|
| Flow variables | Runoff [$md^{-1}$], Discharge [$m^3s^{-1}$] | Runoff [$mmd^{-1}$], Discharge [$m^3s^{-1}$] |
| Spatial resolution | 0.5 arc-degree | 0.5 arc-degree |
| Spatial coverage | All continents | Europe |
| Temporal resolution | Daily | 7-day moving average |
| Time period | Period of each forcing data set | 01.01.1901-31.12.2001 |

## 4.2 PCR-GLOBWB 2

The PCRaster GLOBal Water Balance model version 2.0 (PCR-GLOBWB 2) was developed at the Department of Physical Geography, Faculty of Geosciences, Utrecht University, the Netherlands, and is freely available at github `https://github.com/UU-Hydro/PCR-GLOBWB_model` (Sutanudjaja et al. 2017). Its subsequent description is based on the model presentation by Sutanudjaja et al. (2017), if no other references are given.

PCR-GLOBWB 2 is an uncalibrated gridded global hydrological model (GHM), covering all continents except for Greenland and Antarctica. It has been implemented at two spatial

resolutions; 5x5 arc-minute and 0.5x0.5 arc-degree grid-cells. The coarse resolution was used in this study to reduce the computational demand. Since the first version (Van Beek & Bierkens 2009, Van Beek et al. 2011), it has been developed to include several new as well as more sophisticated, model features. For instance, from treating water demand and water availability independently, the model now includes a two-way interaction between water demand, water withdrawal, water consumption and water availability (Wada et al. 2011a, 2014, De Graaf et al. 2014).

PCR-GLOBWB 2 has a modular structure. In the following, the five modules constituting the model will be presented; irrigation and water use, meteorological forcing, land surface, groundwater and surface water routing module. Figure 13 shows a schematic overview of the modelled states and fluxes. Following the model structure is a high degree of flexibility, and many choices regarding the model setup are available. The following description will focus on the setup chosen for the simulations used in this study.

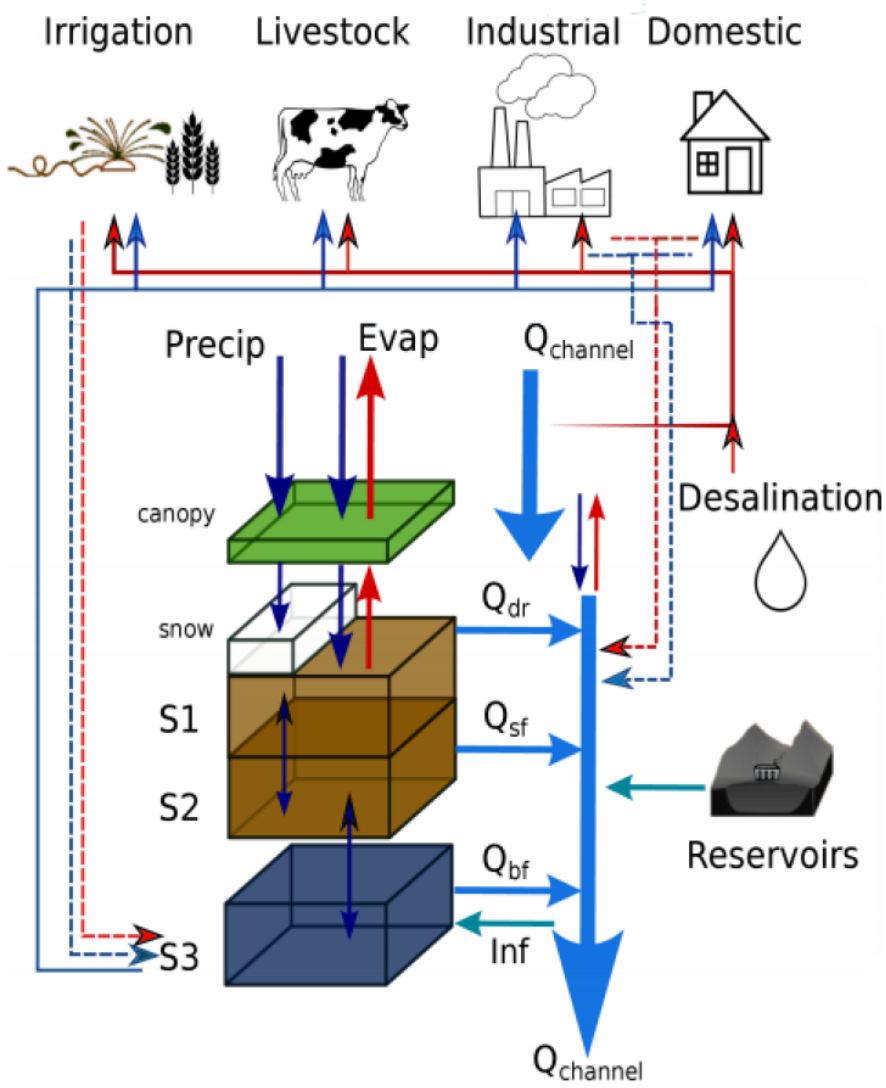


**Figure 13:** A schematic overview of one cell in PCR-GLOBWB 2 affected by human interventions. S1, S2 and S3 are the upper and lower soil moisture storage and ground water storage, respectively. Total runoff is the sum of direct surface runoff ($Q_{dr}$), interflow ($Q_{sf}$) and baseflow ($Q_{bf}$), as well as return flow from domestic and industry. Runoff (minus infiltration; Inf) together with discharge from neighboring upstream cells constitutes the discharge of the cell ($Q_{channel}$). The thin red line indicate withdrawal (continuous line) and return flow (dashed line) from surface water, and the thin blue line indicate withdrawal (continuous line) and return flow (dashed line) from groundwater. The figure is used with permission from Sutanudjaja et al. (2017).

### 4.2.1 Meteorological Forcing

In PCR-GLOBWB 2, the meteorological data required for a model simulation are daily spatially gridded time series of temperature (T), precipitation (P) and potential evapotranspiration (PET). T and P are extracted from a meteorological forcing data set. Precipitation is partitioned into rain and snow based on the temperature data. Temperature

is also used to drive snow melt. Both the rain/snow partitioning threshold and the onset of snow melt is set at 0°C. The amount of snow melt is determined by a simple degree day equation. PET is calculated based on mean temperatures and day lengths, using the Hamon equation (Hamon 1960).

### 4.2.2 Land Surface

The land surface scheme covers the vertical exchanges between the surface and the atmosphere, between the surface and the soil, and between the soil and groundwater. PCR-GLOBWB 2 has sub-grid variability of land cover types, and all calculations in this module are done per land cover type and weighted by the fraction it occupies within each cell. The land-atmosphere exchanges include precipitation (rain and snow), vegetation-specific transpiration and evaporation from intercepted water, soil, snow and open water. Snow accumulation and snow melt is also simulated in this module. Topography, in addition to the land cover type, influence which proportion of the water on the surface that infiltrates. Subsurface exchange of water is simulated between two vertically stacked upper soil layers, and between the lower soil layer and the underlying groundwater reservoir in terms of recharge and capillary rise. The runoff generated from this module is the sum over the surface runoff (including snow melt) and the interflow from the soil.

The standard land cover types used in PCR-GLOBWB 2 are open water, tall natural vegetation, short natural vegetation, non-paddy irrigation and paddy irrigation (i.e. wet rice). The non-irrigation land cover classification stems from the Global ecosystem framework papers by (Olson 1994*a*,*b*). The fraction each type occupies within each cell are based on the Global Land Cover Characteristics Data Base Version 2.0 (Loveland et al. 2000), whereas the vegetation parameters are based upon Hagemann et al. (1999) and Hagemann (2002). Parameterization of the non-paddy and paddy irrigation type are based on MIRCA2000 dataset by Portmann et al. (2010) and the Global Crop Water Model by Siebert & Döll (2010). Calculation of irrigation water are covered by the irrigation and water use scheme. Soil and vegetation properties can be specified and are fully spatially distributed. Thus, the properties can vary both between land cover types and between cells for one land cover type. Vegetation properties also vary over time following a monthly climatology of crop factor and leaf area index.

### 4.2.3 Groundwater

The groundwater storage is updated based on withdrawal of water (calculated in the irrigation and water use scheme), exchange with the overlying soil layer (i.e. recharge and capillary rise calculated in the land surface module), and exchange with the river bed

consisting of groundwater discharge (defined as baseflow) and river bed infiltration. The groundwater storage is allowed to become negative if the withdrawal exceeds the input. In case of negative storage, groundwater discharge stops, and riverbed infiltration can take place. Groundwater generates baseflow that is part of the total runoff generated by the model.

### 4.2.4 Surface Water Routing

Discharge is simulated by routing the runoff originating from surface runoff (including return flow), interflow and baseflow down the drainage network ending in the ocean or in endorheic lakes. The drainage networks are based on HydroSHEDS (Lehner et al. 2008), GTOPO30 (Gesch et al. 1999) and Hydro 1k (Verdin & Greenlee 1996, USGS EROS Data Center 2006). For the data used in this thesis, a simple accumulation routing scheme was used. The river channels are subject to open water evaporation and withdrawal of water. Reservoirs and unregulated lakes are incorporated in the river network, and obtained from GranD (Lehner et al. 2011) and GLWD1 (Lehner & Döll 2004), respectively. The water bodies can consist of several cells, and they are updated in storage and surface area at a daily time step. The water body storage is calculated based in inflow, outflow, open water evaporation and withdrawal of water. The outflow is determined by a storage-outflow relationship in case of lakes, and release strategies that mimic real observed release policies for water supply reservoirs (Hanasaki et al. 2006). The withdrawal of water from river channels, lakes and reservoirs is calculated in the irrigation and water use scheme.

### 4.2.5 Irrigation and Water Use

The irrigation and water use scheme covers the fully integrated computations of net and gross water demand, water withdrawal and return flow for irrigation, industry, households and livestock. Together with reservoir regulations, these irrigation and water use schemes comprise the human interventions used in this study. Irrigation water demand follow the Food and Agriculture Organization of the United States (FAO) guidelines (Doorenbos & Pruitt 1977, Allen et al. 1998). For paddy irrigation, the water level is kept constant at 5 cm above surface until approx. 20 days before harvest after which no water is added. In the case of non-paddy irrigation, the soil column is filled up to field capacity each time the soil moisture drops below a pre-set level. To allow for reduced irrigation efficiency, the net water demand is in each case increased by a country specific irrigation efficiency (ranging from 10 to 50%, depending on the country's economic development level), defining the gross irrigation water demand. The irrigation efficiency accounts for losses via evapotranspiration, whereas the remaining water (i.e. return flow) percolates and contributes to groundwater recharge. The irrigated area within one cell can change

over time on an annual basis based on FAOSTAT (Food and Agriculture Organization of the United Nations 2012). However, the fraction of paddy and non-paddy irrigation and the monthly crop composition calendar stay fixed. They are obtained from the the MIRCA2000 data set (Portmann et al. 2010) and the Global Crop Water Model (Siebert & Döll 2010).

Net and gross water demand for industry, households and livestock are calculated independent of the current hydrological conditions, following methods by Wada et al. (2014). The demand changes over time on an annual basis following changes in population, electricity demand and gross domestic product per capita. PCR-GLOBWB 2 also includes a temperature based seasonal variation in domestic water demand. The gross demand is computed based on a country-specific recycling ratio (gross=net/[1-recycling ratio]) to account for the proportion of water that is returned as surface water. Thus, return flow equals withdrawal*recycling ratio, and the remaining water is consumed. For livestock, all water is assumed consumed (i.e. gross=net). The return flow from irrigation goes via percolation to recharge the groundwater and eventually returns as runoff, whereas the return flow from industry and household is returned as runoff within a day.

The computation of water withdrawal is based on De Graaf et al. (2014) and Wada et al. (2014). Within each cell, the withdrawal of water is set equal to the total gross water demand if the water availability exceeds the demand, and set equal to the available water otherwise. In case of the latter, the water is assigned such that each sector acquires the same percentage of its gross water demand. The water is abstracted from three sources; surface water, groundwater and desalinated water. Desalinated water abstraction is prescribed following Wada et al. (2011b). The relative availability of surface and groundwater governs the fraction of water abstracted from each. This relative availability is determined on a monthly basis by two-year running means of groundwater recharge and river discharge for groundwater and surface water, respectively. The groundwater abstraction is restricted by the pumping capacity based on the database of global groundwater resources (Global Groundwater Information System, GGIS) by the International Groundwater Resources Assessment Centre (IGRAC; `https://www.un-igrac.org/global-groundwater-information-system-ggis`), whereas the surface water withdrawal stops when the river discharge falls below 10% of the long-term yearly natural (no human interventions) discharge. There are some exceptions to this procedure. In urban areas with a surface water distribution infrastructure according to the data set by McDonald et al. (2014) water for households and industry is mainly abstracted from surface water before abstracting groundwater. For urban areas with limited

surface infrastructure according to the same data set, groundwater abstractions are set as the main source. In irrigated areas, the ratios from Siebert et al. (2010) or an average between the ratio and the estimate from the above procedure are used for reliable and medium reliable ratios, respectively.

## 4.3 Natural and Human Interventions Scenarios

Three different model scenarios were used to investigate impacts of human interventions (HI) on the water cycle; no HI, transient HI, and current HI (Table 2). HI included reservoirs and dam operations, as well as water use for irrigation, livestock, domestic and industry. All scenarios used a spin-up period of 50 years using the meteorological data of the year 1901 to ensure no drifts in groundwater levels and other hydrological state variables. In the no HI scenario, both the spin-up period and the period of analysis were run under natural conditions, i.e. with all HI excluded. This scenario of natural conditions was used as a baseline to quantify the effect of human activities. In the transient HI scenario, each HI component (e.g. a specific reservoir or the irrigated area within a cell) was introduced on the 1st of January of the year it appeared according to the data available (introduced in Section 4.2.4 and 4.2.5). Thus, the transient HI scenario represented the actual evolution of HI on an annual basis throughout the period of analysis. The current HI scenario used the HI in 2010 for every year throughout the period. Also in the spin-up period, the HI from 2010 were used. This scenario was used to investigate how present HI affect the hydrological behaviour given the meteorological conditions throughout the $20^{th}$ century.

**Table 2:** The choices of no or various human interventions (HI) model scenarios. The spin-up period consisted of 50 years with the meteorological data for 1901 for all model scenarios.

| **Model scenario** | **Specification** | **Spin-up period conditions** |
|---|---|---|
| No HI | Natural conditions | No HI |
| Transient HI | Annually introduced HI | No HI |
| Current HI | HI of 2010 | HI of 2010 |

## 4.4 Meteorological Forcing Data

Like many other large scale hydrological models, PCR-GLOBWB 2 requires full terrestrial coverage of meteorological data at a fine temporal resolution without gaps in time or space. Atmospheric reanalysis data meets the requirement of continuity in time and space, how-

ever contains systematic errors and biases. Surface observation datasets, usually have the better quality of the data, but lack the spatial temporal consistency (Dirmeyer et al. 2006). As a consequence, meteorological forcing data sets are developed as hybrids profiting from the advantages from each source of data. Such forcing data sets vary in the methods they use, as well as the reanalysis and observational data sets they are based upon. Because hydrological behaviour is highly dependent on precipitation,temperature, evapotranspiration and snow processes, modelled runoff and discharge can be highly sensitive to the choice of meteorological data.

To investigate the effect of the forcing data set on the outcome of the study, four forcing data sets were used to drive the PCR-GLOBWB 2 model. The forcing data sets are GSWP3 (meteorological forcing data set from the Global Soil Wetness Project Phase 3), PGMFDv2 (Princeton Global Meteorological Forcing Dataset for land surface modeling version 2), WFD (the Water and global change project's meteorological Forcing Data set based on reanalysis ERA-40) and WFDEI (the Water and global change project's meteorological Forcing Data set based on reanalysis ERA-Interim from 1979, and ERA-40 before 1979), and they are all available within the ISI-MIP project phase 2a (Müller Schmied et al. 2016). Specifications of the forcing data sets are summarized in Table 3. European median time series (across grid-cells) of the meteorological components used in PCR-GLOBWB 2, are shown in Figure 14, whereas regional specific time series are given in Appendix B. There are clear differences in temperature and precipitation between the forcing data sets, most notably in the upper quartile of precipitation for PGMFDv2 compared to the others. In the next subsections a short introduction to each data sets is provided.

### 4.4.1 GSWP3

The Global Soil Wetness Project (GSWP) is a research activity focusing on analysis of the terrestrial water and energy budgets (Dirmeyer et al. 1999, 2006). GSWP is currently in its third phase, using a forcing data set, accordingly named GSWP3, that provides daily data from 1901 to 2010 on the 0.5 arc-degree grid (`http://hydro.iis.u-tokyo.ac.jp/GSWP3/`; Kim 2014). It is based on the $20^{th}$ century reanalysis dataset (20CR; Compo et al. 2011) which is dynamically downscaled to approx. 0.5° spatial resolution. Bias correction is performed using the Global Precipitation Climatology Centre (GPCC; `https://www.dwd.de/EN/ourservices/gpcc/gpcc.html`) dataset version 6 for precipitation, the Climate Research Unit (CRU) TS3.21 (Harris et al. 2014) for temperature and the Surface Radiation Budget project (SRB; Cox et al. 2017) data set for short and long wave downward radiation. Wind-induced under-catch correction for precipitation is

applied following the description of Hirabayashi et al. (2008).

### 4.4.2 PGMFDv2

PGMFDv2 is an updated version of the Global Meteorological Forcing Dataset for land surface modeling developed at the Terrestrial Hydrology Group at Princeton University (Sheffield et al. 2006) covering the period 1901-2012 (`http://hydrology.princeton.edu/data.pgf.php`; see also description in Müller Schmied et al. (2016)). It is available at different spatial resolutions, 0.5 arc-degrees being the one applied in this thesis. PGMFDv2 is constructed using reanalysis data from the National Centers for Environmental Prediction – National Center for Atmospheric Research (NCEP/NCAR) (Kalnay et al. 1996, Kistler et al. 2001) together with observation-based station and satellite data. Bias-correction is done for precipitation, temperature and trends in shortwave downward radiation (through cloud-cover data) using CRU TS3.21 data (Harris et al. 2014), and short and long wave radiation are adjusted using products from the University of Maryland. Precipitation has not undergone any under-catch corrections.

### 4.4.3 WFD

The WATer and global CHange (WATCH) project was a project aiming at bringing together hydrological, water resources and climate communities to evaluate and predict the terrestrial water cycle components (Harding et al. 2011a,b). Part of this work involved comparing different large scale models (Haddeland et al. 2011), and the necessity of meteorological input data lead to the creation of a WATCH Forcing Data Set (WFD) (Weedon et al. 2010, 2011). WFD is based on the 40-yr European Centre for Medium-Range Weather Forecasts (ECMWF) reanalysis (ERA-40) for the period 1958-2001 (Uppala et al. 2005), and reordered ERA-40 for the period 1901-1957. The creation of WDF included a bilinear interpolation of all variables to get from the 1 arc-degree resolution of ERA-40 to the 0.5 arc-degree resolution. Precipitation is bias-corrected based on GPCC version 4 (Schneider et al. 2011a), and temperature and short wave downward radiation based on CRU TS2.1 (Mitchell & Jones 2005). Long wave downward radiation is not bias-corrected. The description in Adam & Lettenmaier (2003) is used for wind-induced under-catch correction of precipitation.

### 4.4.4 WFDEI

Following a relatively new reanalysis data product, ERA-Interim (Dee et al. 2011), a new WATCH Forcing Data Set was generated know as the WATCH Forcing Data methodology applied to ERA-Interim data (WFDEI) (Weedon et al. 2014). As the name implies, the WFD methodology was used in the creation of WFDEI. Precipitation is bias-corrected

based on GPCC version 5 and 6 (Schneider et al. 2011b), and under-catch corrected according to Adam & Lettenmaier (2003). CRU TS3.1 and TS3.21 (Harris et al. 2014) was used for bias-correction of temperature and short wave downward radiation. Following the period covered by ERA-Interim, WFDEI alone covers 1979-2012. Therefore, WFDEI is merged with data before 1979 from WFD to cover an overall period of 1901-2012. The combined WFD and WFDEI dataset is in this study referred to as WFDEI, to distinguish it from the forcing data set solely made up by WFD (Section 4.4.3). A simple coupling was problematic due to offsets in short wave downward radiation in WFDEI relative to WFD, affecting the estimation of actual evapotranspiration and accordingly, water storages and other water balance components (Müller Schmied et al. 2014, Stagge et al. 2017). A homogenized forcing data set combining WFD and WFDEI has therefore been created as an alternative (Müller Schmied et al. 2016). However, the offset problem is not an issue in this study because PCR-GLOBWB 2 was forced with only precipitation and temperature, estimating the evapotranspiration variables itself (ref. 4.2.1). To be true to the forcing data set versions used within the ISI-MIP 2a framework, the original WFDEI combination with WFD (i.e. simple merging) was applied.

**Table 3:** Specifications of the forcing data sets used for the different model runs.

| **Forcing** | **Time span** | **Reanalysis basis** | **Bias-corrected to** | **Precipitation under-catch correction** |
|---|---|---|---|---|
| GSWP3 | 1901-2010 | 20CR | GPCC v6, CRU TS3.21 | Yes |
| PGMFDv2 | 1901-2012 | NCEP/NCAR | CRU TS3.21, University of Maryland | No |
| WFD | 1901-2001 | ERA-40 | GPCC v4, CRU TS2.1 | Yes |
| WFDEI | 1901-2010 | ERA-Interim (and ERA-40 before 1979) | GPCC v5/6, CRU TS3.1/3.21 | Yes |

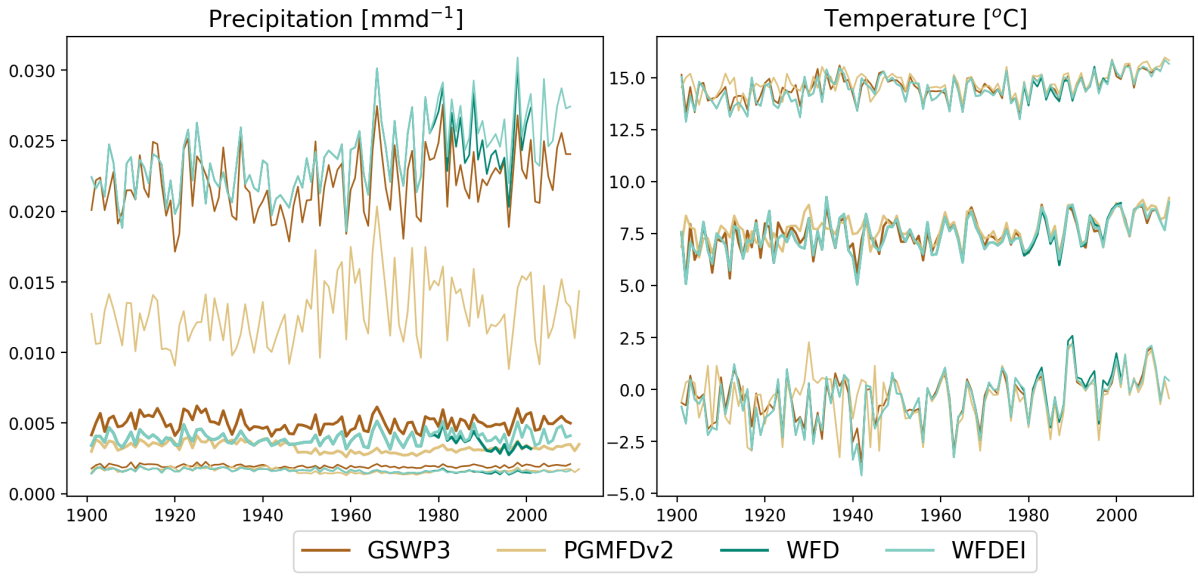


**Figure 14:** European annual medians of $1^{st}$, $2^{nd}$ and $3^{rd}$ quartile of temperature (left) and precipitation (right) derived from the four forcing data sets GSWP3, PGMFDv2, WFD and WFDEI.

# 5 Methods

## 5.1 Discharge Validation Metrics

To evaluate the performance of PCR-GLOBWB 2, time series of simulated discharge from the transient human intervention run using each forcing data set were validated against observed discharge time series in the period 1976-2001, obtained from the Global Runoff Data Centre (GRDC, 2014). Monthly discharge data was used for the validation because the observation data was available at this temporal resolution. A subset of the GRDC stations was chosen for the validation based on three criteria: i) the stations are not more than one cell distance from a main river in PCR-GLOBWB 2, ii) the station had a reported catchment area which differentiates less than ten percent from the catchment area of the corresponding location in PCR-GLOBWB 2, and iii) the station had at least five years of data. This resulted in a final selection of 316 GRDC stations. The validation metric was the correlation coefficient ($corr(X, Y)$) between the simulated series $X$ and the observation series $Y$ at each location:

$$corr(X, Y) = \frac{\Sigma_{t=1}^{n}(x_t - \hat{x})(y_t - \hat{y})}{\sqrt{\Sigma_{t=1}^{n}(x_t - \hat{x})^2}\sqrt{\Sigma_{t=1}^{n}(y_t - \hat{y})^2}} \quad (1)$$

Here, $x_t$ and $y_t$ are the values of each time step $t = 1, 2, \ldots, n$, for the simulated and observed discharge, respectively. The $\hat{x}$ and $\hat{y}$ are the average simulated and observed discharge value, respectively.

## 5.2 Human Impact Indicators

To assess the impact of human interventions (HI) on the water cycle and its extremes, deviations from the natural scenario (i.e. no HI) were investigated for the transient and current HI scenario by using the Flow Duration Curve (FDC). The FDC is a century-old tool that provide an easy-to-use graphical and computational format that can be used to show the effect of alterations in the hydrological system, e.g. HI on all flows, or high and low flows in particular (McKay & Fischenich 2016). However, the FDC is not suitable for time-dependent flow characteristic (e.g. low flow duration) because it breaks the temporal component of the time series. The investigations were based on the empirical non-exceedance FDC consisting of the $P^{th}$ non-exceedance percentile values for a given runoff time series, where $P = 0, 1, 2, ..., 100$. Thus, the lowest percentiles correspond to the lowest flows. Figure 15 illustrates two different FDCs; one for flow with high, and one for flow with low natural storage capacity upstream. The non-exceedance FDC were used

instead of exceedance FDC to be true to the statistical definition of percentiles, and must not be mixed up with the term "quantiles" often defined as exceedance probabilities in hydrological contexts. For example, the $10^{th}$ percentile is the flow value below which 10% of the data is found. Three metrics stemming from the FDC were applied, and presented in the following subsections. All metrics were calculated for each of the four forcing data sets.

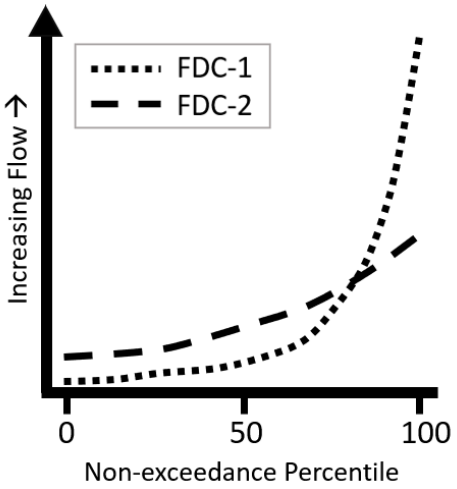


**Figure 15:** Schematic example of two Flow Duration Curves (FDCs); FDC of a flow time series with low storage capacity in its catchment (FDC-1), and FDC of a flow time series with high storage capacity in its catchment (FDC-2). FDC-2 have larger flow values in the low range of percentiles and smaller flow values in the high range of percentiles compared to FDC-1, reflecting the effect of storage capacity upstream in the case of FDC-2 causing a lower variability in flows.

### 5.2.1 Metric of Impacts on Low, Mid and High Flow

To evaluate possible impacts of HI on low, mid and high flow, time series for each grid-cell were computed for runoff percentile $P = 10, 50, 90$, respectively. This was done for all model scenarios (i.e. natural, transient HI and current HI). Time series allow for assessing the impacts of HI for variable meteorological conditions over time, as well as the impacts of the historical development of HI represented by the transient HI scenario. The time series for each cell were created by computing percentile values from 30-years sub-periods, moving one year at a time, resulting in 72 analysis windows over the 101 year period. A time period of 30 years was used because it is the standard climate reference period length (e.g. WMO, Fleig et al. 2013). This reduced the sensitivity of the FDC to single underlying data points and thus better represent the range of flows characterizing the site (McKay & Fischenich 2016). To reduce the amount of spatiotemporal data, regional medians of the runoff results were computed for each of the five climate regions, i.e. the Continental, Northern, Southern, Atlantic and Alpine regions (introduced in Figure 4 in

Chapter 3).

### 5.2.2 Metric of Impacts on the Flow Variability

Possible impacts of HI on the flow variability were investigated by computing time series of the ratio of the $20^{th}$ over the $80^{th}$ runoff percentile ($\Delta$FDC) for each grid-cell and each model scenario. The $\Delta$FDC is a dimensionless metric [0,1] that represents the gradient of difference in high and low flow. The closer $\Delta$FDC is to 1 [-], the smaller the flow variability is, because the more similar the $20^{th}$ and $80^{th}$ percentile values are. The $20^{th}$ and $80^{th}$ percentiles were preferred to the $10^{th}$ and $90^{th}$ percentiles to reduce the high sensitivity of the metric to the high end compared to the low end of the FDC. The same time steps and regions as described in Section 5.2.1 were use for this metric.

### 5.2.3 Metric of Impacts on Overall, Low and High Flows

Impacts of current HI on overall, low and high flow water gain and loss were investigated based on whole period (1901-2001) FDCs for both runoff and discharge. For this purpose, two metrics were used, namely ecosurplus and ecodeficit. These ecometrics were first introduced by Vogel et al. (2007) in an attempt to evaluate the overall gain and loss, respectively, in streamflow due to reservoir regulation. In a study investigating different indicators of hydrological alteration, Gao et al. (2009) found that ecosurplus and ecodeficit could provide a good measures of the degree of hydrologic alteration. Although investigation of the impact on ecological flow regimes given rise to the "eco"-prefix in the metric names (Vogel et al. 2007) were not in focus in this study, the prefixes were kept to stay true to the terminology used in the existing literature.

The computation of ecosurplus and ecodeficit follow Vogel et al. (2007) and Gao et al. (2009). A visual explanation of the FDC basis of the computations is given in Figure 16. Given a natural (no HI) FDC, and a current HI FDC, the area below the current HI FDC and above the natural FDC is defined as the ecosurplus area ($A_s$). Conversely, the area above the current HI FDC and below the natural FDC is defined as the ecodeficit area ($A_d$). The transient HI scenario was excluded from this part of the analysis because the HI conditions and thus also their impacts, are not constant over the period for this scenario. For percentiles in a given range [Pmin, Pmax], $A_s$ and $A_d$ for a given flow variable (i.e. either runoff or discharge) were estimated by:

$$A_s = \sum_{P=Pmin}^{Pmax} \max(cur_P - nat_P, 0) \tag{2}$$

and

$$A_d = \sum_{P=Pmin}^{Pmax} |\min(cur_P - nat_P, 0)| \tag{3}$$

where $cur_P$ and $nat_P$ are the percentile value P from the current and natural FDC, respectively. The area under the natural FDC ($A_n$) in a given percentile range, were computed by:

$$A_n = \sum_{P=Pmin}^{Pmax} nat_P \tag{4}$$

Ecosuplus and ecodeficit were then defined as:

$$ecosurplus = \frac{A_s}{A_n} \tag{5}$$

and

$$ecodeficit = \frac{A_d}{A_n} \tag{6}$$

Thereby, ecosurplus and ecodeficit provide non-dimensional metrics of the overall water gains and losses, respectively, due to HI. For this thesis, the ecometric results are expressed as percentages to emphasize that the they represent changes relative to a natural condition. Figure 16 shows an example of $A_s$, $A_d$ and $A_n$ for the percentile range [0,100] (i.e. the whole FDC) for one cell. As long as $A_s$ and $A_d$ are smaller than $A_n$, the absolute values of the resulting estimates are in the range $[0, 1]$, where 0 indicate no impact. Ecosurplus and ecodeficit were computed over three percentile ranges; the water cycle in general (i.e. the whole FDC; $0^{th}$–$100^{th}$ percentile), as well as the low flow end FDC ($0^{th}$–$10^{th}$ percentile) and the high flow end FDC ($90^{th}$–$100^{th}$ percentile).

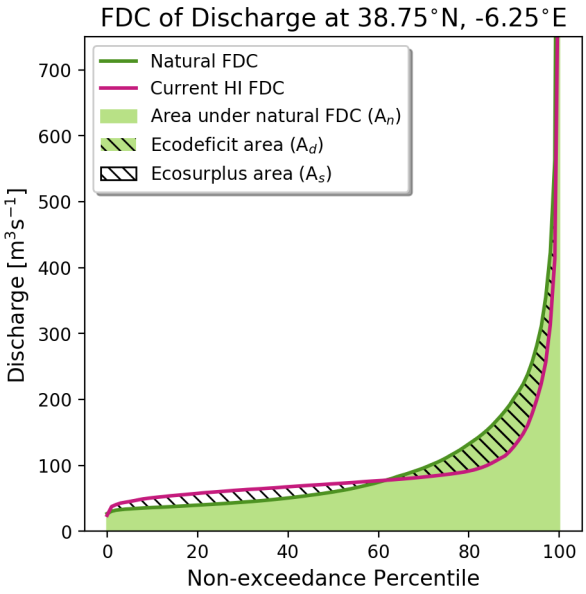


**Figure 16:** Flow Duration Curve (FDC) of the no human interventions scenario (i.e. natural FDC; green line) and current human intervention scenario (i.e. current HI; pink line) for 7-day moving average discharge over the period 1901–2001 at grid 38.75$^o$N, -6.25°E (Midwestern Spain) simulated by the hydrological model PCR-GLOBWB 2 using forcing data WFDEI. Shown are the area under the natural FDC ($A_n$), ecodeficit area ($A_d$) and ecosurplus area ($A_s$) for the percentile range [0,100].

# 6 Results

## 6.1 PCR-GLOBWB 2 Performance

Correlation coefficients between the observed GRDC discharge (GRDC, 2014) and the simulated discharge for the transient human intervention scenario and the four different forcing data sets are shown for different catchment sizes in Figure 17. For all forcing data sets, less than 5% of the discharge time series had a negative correlation. Simulation with PGMFDv2 generally showed a lower correlation with observations compared to simulations using any of the other three forcing data sets. Median correlation was 0.56 [-] for PGMFDv2, 0.65 [-] for WFD and WFDEI, and 0.67 [-] for GSWP3. GSWP3, WFD and WFDEI had similar spatial distributions of correlation coefficients across Europe, however WFD and WFDEI had slightly lower coefficients for the larger catchments. All three had the highest number of correlation coefficients in the interval 0.8–0.9 [-], followed by 0.7–0.8 [-] and 0.6–0.7 [-].

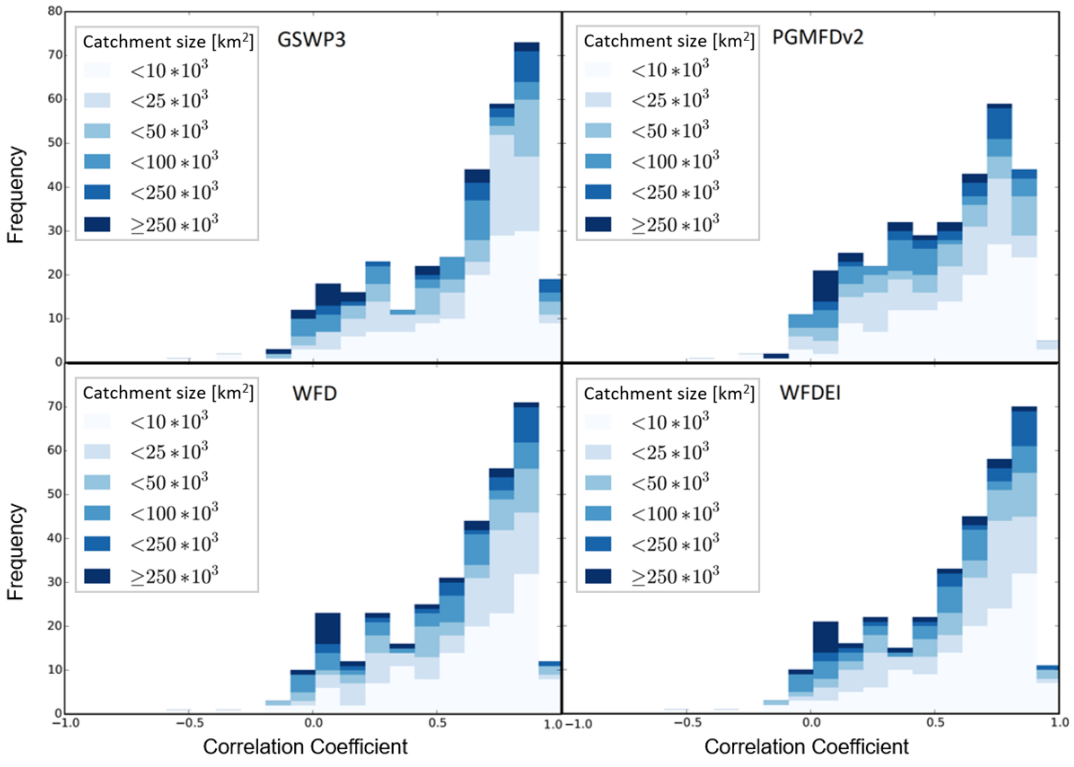


**Figure 17:** Histograms of the correlation coefficients between GRDC monthly discharge observations and monthly discharge simulated by PCR-GLOBWB 2 using the transient human intervention scenario and the four different forcing data sets: GSWP3 (top left), PGMFDv2 (top right), WFD (bottom left) and WFDEI (bottom right). Different catchment sizes are represented by different shades of blue.

A map of the discharge stations and their correlation coefficients based on the WFDEI forcing data is shown in Figure 18. In the remained of the thesis, WFDEI is used to present the results to avoid a redundancy in figures throughout the thesis. The results of the other forcing data sets are given in Appendix C–E. WFDEI was chosen because it is based on the most recent developed reanalysis of the three forcing data sets giving the best correlation scores and showed very similar spatial patterns compared to the other forcing data sets. The discharge station density is highest in central Europe, and sparse in eastern and southernmost parts of the spatial domain. There is no clear spatial pattern in model performance, i.e. in the spatial distribution of the stations with high correlation or the fewer uncorrelated stations. Two locations had clear negative correlation scores, one in Ireland and one in northern Russia.

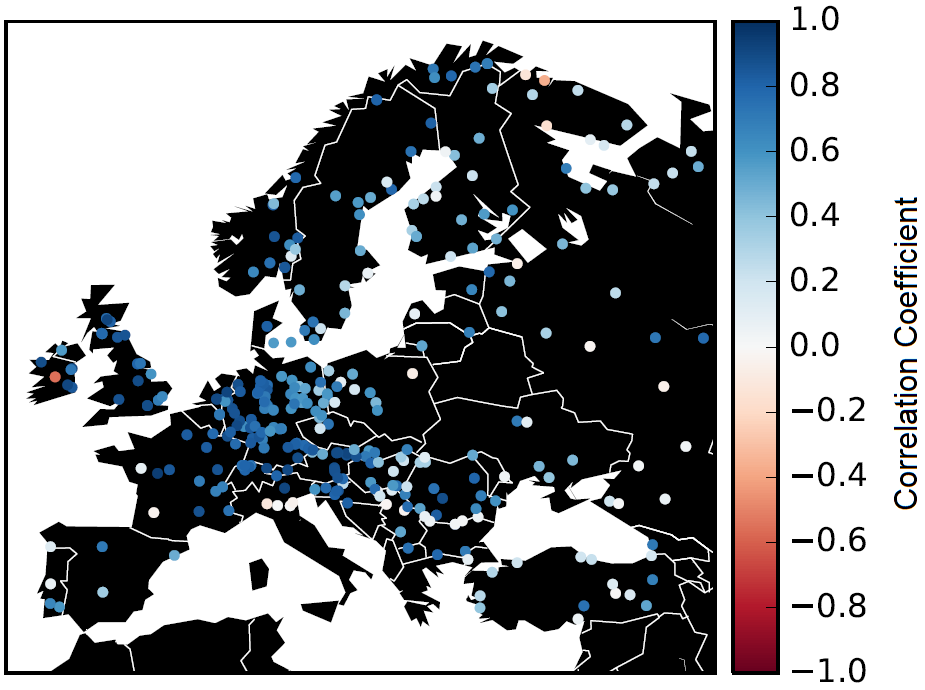


**Figure 18:** Map of correlation coefficients between GRDC monthly discharge observations and monthly discharge simulated by PCR-GLOBWB 2 using the transient human intervention scenario and the forcing data set WFDEI.

## 6.2 Human Impacts on Regional Low, Mid and High Flow

Regional median 30-years moving $10^{th}$, $50^{th}$ and $90^{th}$ percentile runoff for each model scenario (i.e. no HI/natural, transient HI and current HI scenario; HI abbreviates human interventions) using WFDEI forcing data are shown in Figure 19, 20 and 21, respectively. Results for each percentile is plotted with the same increment for all regions to easily compare differences in model scenarios between regions. However, the ranges differ, and

a sixth plot showing all results together is therefore included in each figure. Results based on all four forcing data sets are given in Appendix C (Figure 30–41). For all results the differences between regions were noticeably larger than the variability over time within each region, and the variability over time were larger than the differences between the three model scenarios.

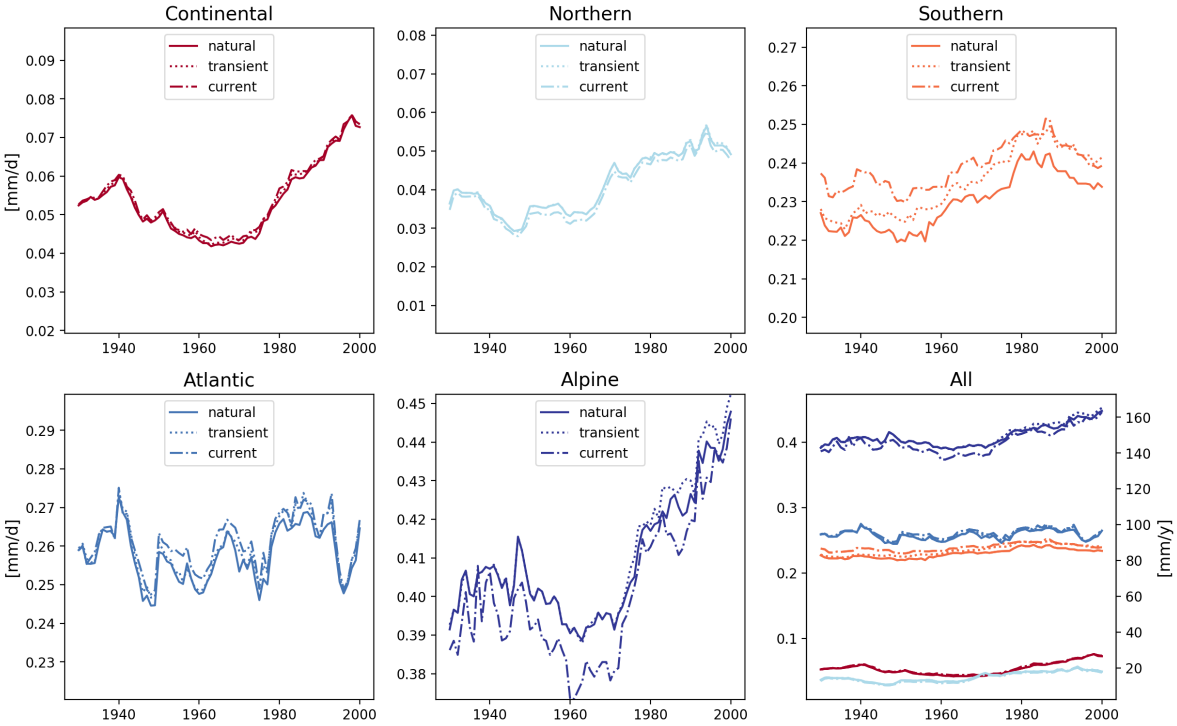


**Figure 19:** Regional median 30-years moving $10^{th}$ percentile runoff (i.e. low flow) for five climatic regions in Europe over the period 1901–2001 using WFDEI forcing data. The lower right plot shows all regions' results together. Note the different scales on the Y-axes.

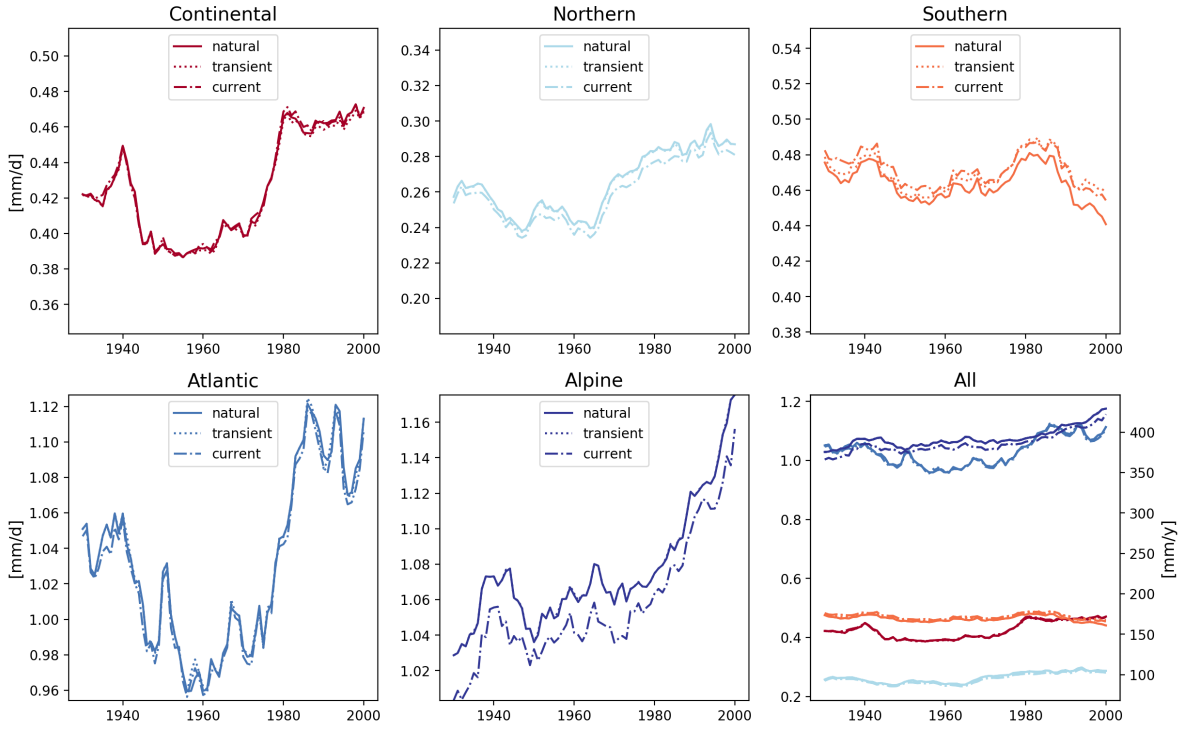


**Figure 20:** Regional median 30-years moving $50^{th}$ percentile runoff (i.e. mid flow) for five climatic regions in Europe over the period 1901–2001 using WFDEI forcing data. The lower right plot shows all regions' results together. Note the different scales on the Y-axes.

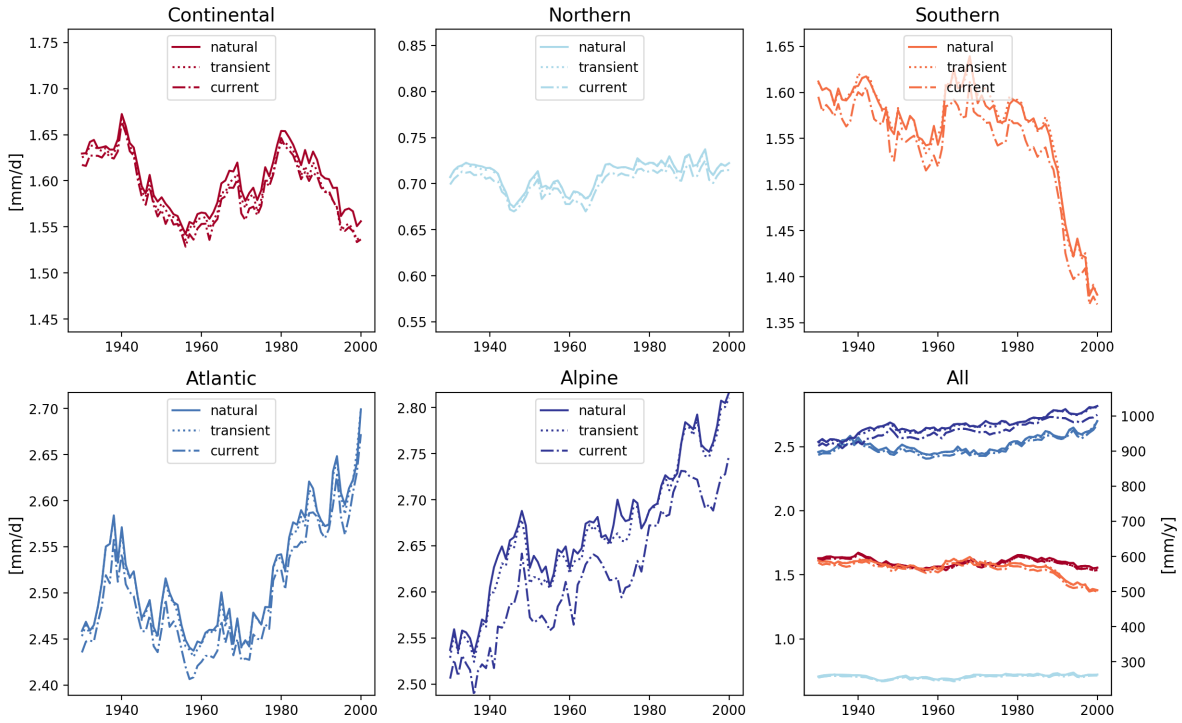


**Figure 21:** Regional median 30-years moving $90^{th}$ percentile runoff (i.e. high flow) for five climatic regions in Europe over the period 1901–2001 using WFDEI forcing data. The lower right plot shows all regions' results together. Note the different scales on the Y-axes.

Regional median low flows (i.e. $10^{th}$ percentile; Figure 19) over the period 1901–2001 spanned from 0.28 to 0.45 $mmd^{-1}$, where the Continental and Northern regions had low flows $\leq 0.076 mmd^{-1}$, the Southern and Atlantic regions had low flows in the range 0.22 to 0.28 $mmd^{-1}$, whereas the Alpine region had the largest low flows ranging from 0.37 to 0.45 $mmd^{-1}$. The Alpine region had also the largest range of low flows. The region showed a decrease in the 30-year periods until about 1960 for all scenarios, followed by a steep increase the rest of the period. A similar, however less pronounced, pattern was found for the Continental region. The Atlantic region showed a large variability in runoff throughout the period for all scenarios. The absolute differences in scenarios within each region were largest in the Southern and Alpine regions, where the runoff values from the current HI scenario were on average 0.0092 $mmd^{-1}$ and -0.0082 $mmd^{-1}$ compared to the natural scenario runoff, respectively. In addition to the Southern region, the current HI scenario resulted in an increase in percentile values in the Continental and Atlantic regions. The Northern and Alpine regions showed a reduction in low flow with the current HI scenario. The Northern region had in general the lowest low flows, and the largest percentage difference (of -3.6% on average) between current and no HI scenario results. The low flows resulting from the transient HI scenario were generally closer to the natural scenario results compared to the current HI scenario results throughout the period. An exception was the Southern region were the transient runoff results moved from the natural to the current HI scenario time series.

Regional median mid flows (i.e. $50^{th}$ percentile; Figure 20) were smallest in the Northern, Continental and Southern regions with values ranging from 0.23 to 0.49 $mmd^{-1}$. The Atlantic and Alpine regions had notably larger median runoff values (between 0.96–1.2 $mmd^{-1}$). As for the low flows, the largest impacts of HI were found in the Southern and Alpine regions, with a change of 0.0078 and -0.019 $mmd^{-1}$, respectively. The largest average percentage change from the natural to the current HI scenario was a reduction of 2.0% that found in the Northern Region. The smallest percentage changes in mid flows were found in the Continental and Atlantic regions. The transient shows a similar behaviour for the mid flow results as the low flow results.

The results for the regional median high flows (i.e. $90^{th}$ percentile; Figure 21) showed that there had been an increase in high flow over time in the Atlantic and Alpine regions, whereas the Southern region experienced a decrease in high flow since the second half of the period. These finding were independent of the model scenario. All regions showed a reduction in median high flow in the current HI scenario compared to the natural scenario. Averaged over the period, the highest reduction of 0.052 $mmd^{-1}$ (2.0%) was found in the

Alpine region. Except for the Continental region, the transient HI scenario gave high flows more similar to the natural scenario than the current HI scenario. As for the regional median low and mid flow results, the Northern region held the smallest high flows, and the Alpine and Atlantic held the largest high flows.

The four forcing data sets had similar shift in the current HI relative to no HI scenario for low, mid and high flow (Figure 30–41 in Appendix C). However, they differed in the magnitude of the percentiles. Results from GSWP3 in the Alpine, Atlantic and Northern regions were notably higher for all scenarios compared to the other forcing data sets. The Continental and Northern regions were lower in percentile values for all model scenarios by PGMFDv2 and GSWP3 compared to WFD and WFDEI.

## 6.3 Human Impacts on Regional Flow Variability

Figure 22 shows the results of the ratio of the $20^{th}$ percentile over the $80^{th}$ percentile (i.e. $\Delta$FDC) for each of the three model scenarios (i.e. no HI/natural, transient HI and current HI scenario; HI abbreviates human interventions) using WFDEI forcing data. Results for all four forcing data sets are given in Figure 42–45 in Appendix D. The $\Delta$FDC values are all in the range [0,1], and the flow variability decreases when $\Delta$FDC value increases and vice versa.

The highest flow variability (lowest $\Delta$FDC values) throughout the period was found in the Continental region with values in the range 0.10 to 0.15 [-] (Figure 22). The Alpine region held the least variable flow throughout the period, with $20^{th}$ percentile values between 29 and 32% of the $80^{th}$ percentile values. In the second half of the time steps, a general decrease in flow variability (i.e. increase in the ratio) were found in all regions except for the Atlantic region where the variability generally increased. The current HI scenario had a decrease in variability in all regions except in the Northern region. The largest difference between model scenarios was observed in the Southern region, with approx. 7.5% (i.e. 2 percentage points) decrease in flow variability for the current HI scenario compared to the natural scenario, and the transient HI scenario moving from being closest to the natural scenario, and over to the current HI scenario time series.

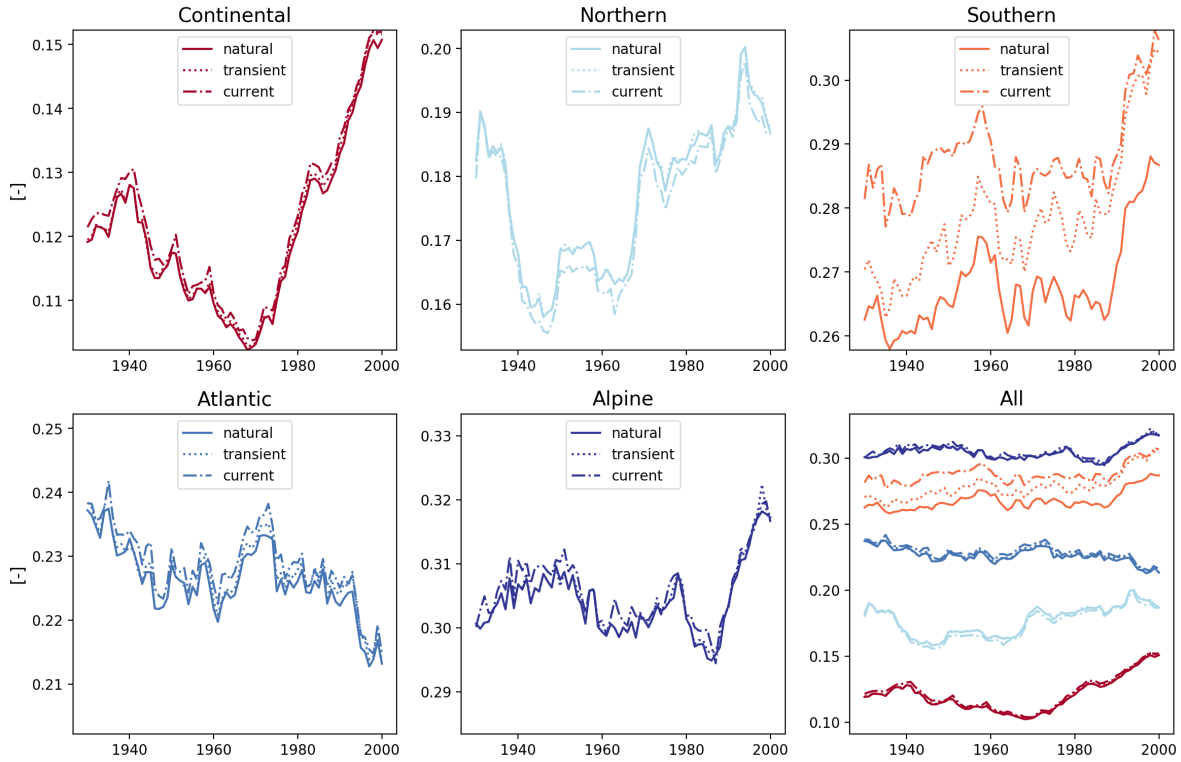


**Figure 22:** Regional median 30-years moving $20^{th}/80^{th}$ percentile runoff ($\Delta$FDC) for five climate regions in Europe over the period 1901–2001 using WFDEI forcing data and three model scenarios; no human interventions, transient human interventions and current human interventions. The lower right plot shows all regions' results together. The flow variability increases when $\Delta$FDC decreases, because a decrease in the ratio corresponds to a larger difference between the $20^{th}$ and $80^{th}$ percentile. Note the different scales on the Y-axes.

The differences between model scenarios were similar for all forcing data sets (Figure 42–45 in Appendix D). The $\Delta$FDC values for the Southern region were lower than for the Alpine region when using PGMFDv2, and opposite for the others. The Northern and Continental region had notably larger interannual variability in $\Delta$FDC for the GSWP3 results compared to the others.

## 6.4 Human Impacts on Water Gain and Loss for the Whole Period

The WFDEI results for ecosurplus and ecodeficit (i.e. ecometrics) comparing the natural scenario with the current human interventions (i.e. current HI) scenario for the whole FDC, and the low and high flow end of the FDC, are shown in Figure 23 for runoff and Figure 24 for discharge. Europewide and regional distributions of ecometric values are provided in Figure 25 and 26 for runoff and discharge, respectively. Appendix E provide the results for all forcing data sets; Figure 46–49 for runoff and Figure 50–53 for discharge.

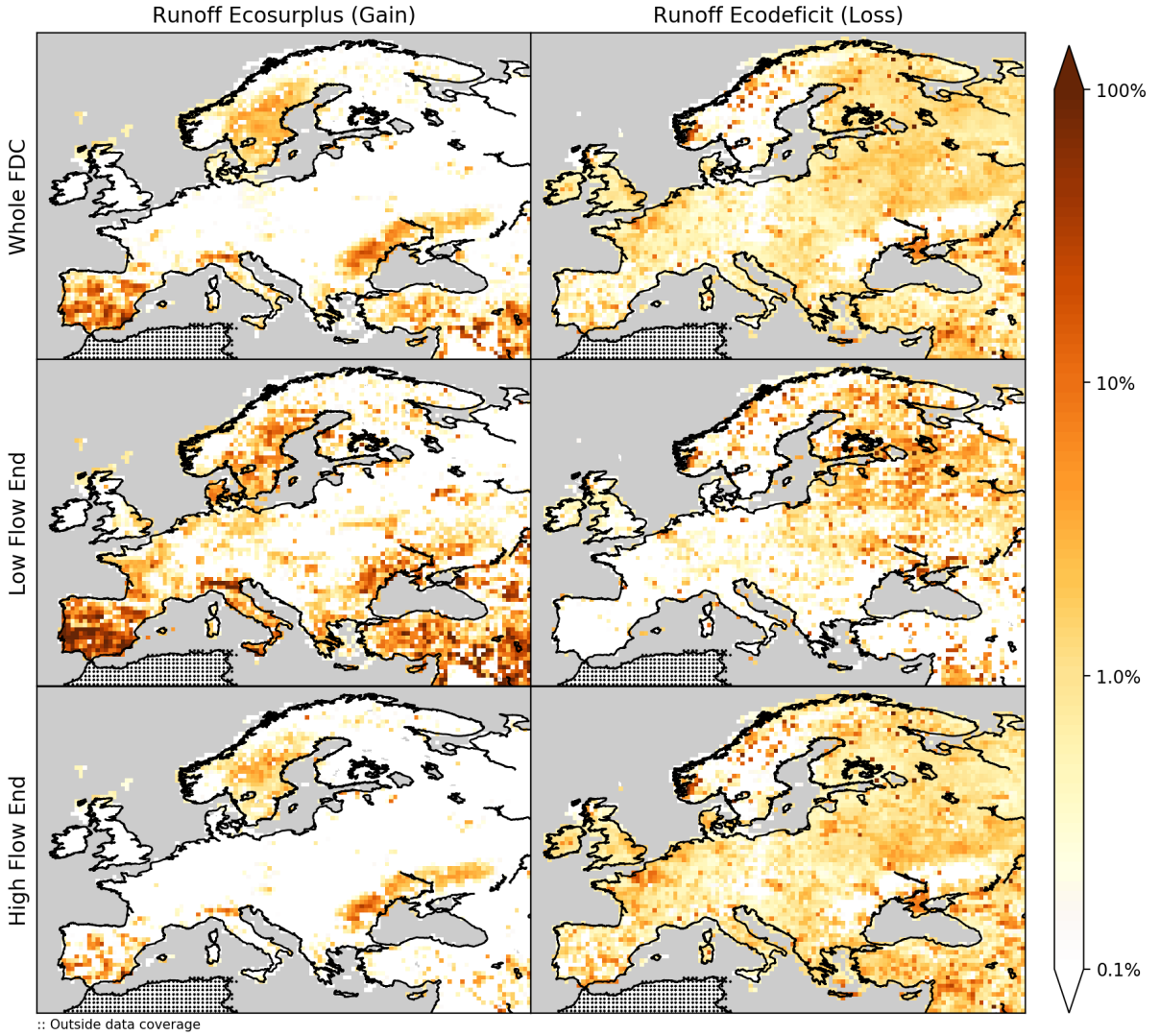


**Figure 23:** Runoff ecosurplus (left) and ecodeficit (right) for the whole FDC ($0^{th}$–$100^{th}$ percentile; top), low flow end FCD ($0^{th}$–$10^{th}$ percentile; middle) and high flow end FDC ($90^{th}$–$100^{th}$ percentile; bottom). The FDCs are based on simulated runoff using the WFDEI forcing data for the period 1901–2001.

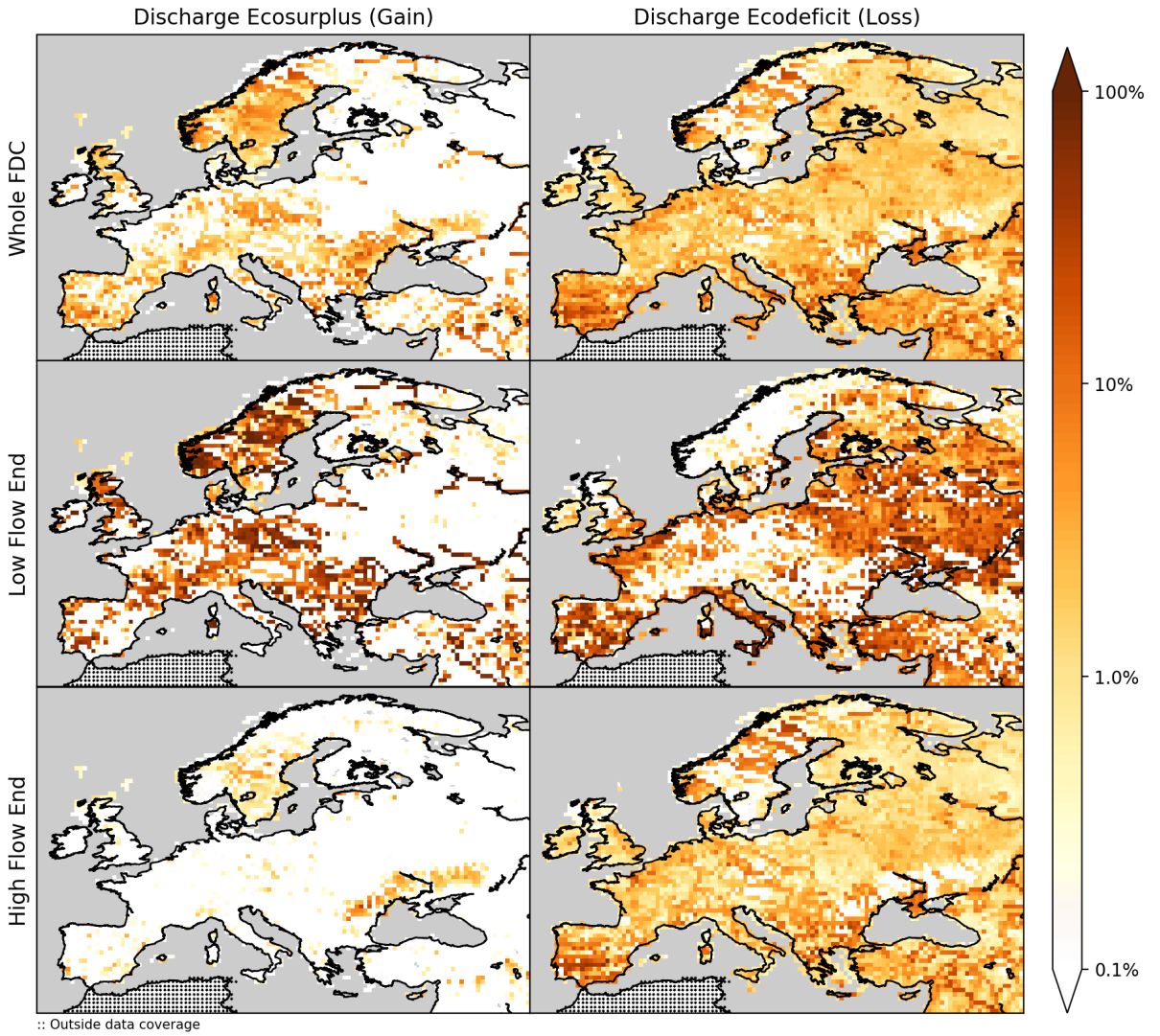


**Figure 24:** Discharge ecosurplus (left) and ecodeficit (right) for the whole FDC ($0^{th}$–$100^{th}$ percentile; top), low flow end FCD ($0^{th}$–$10^{th}$ percentile; middle) and high flow end FDC ($90^{th}$–$100^{th}$ percentile; bottom). The FDCs are based on simulated runoff using the WFDEI forcing data for the period 1901–2001.

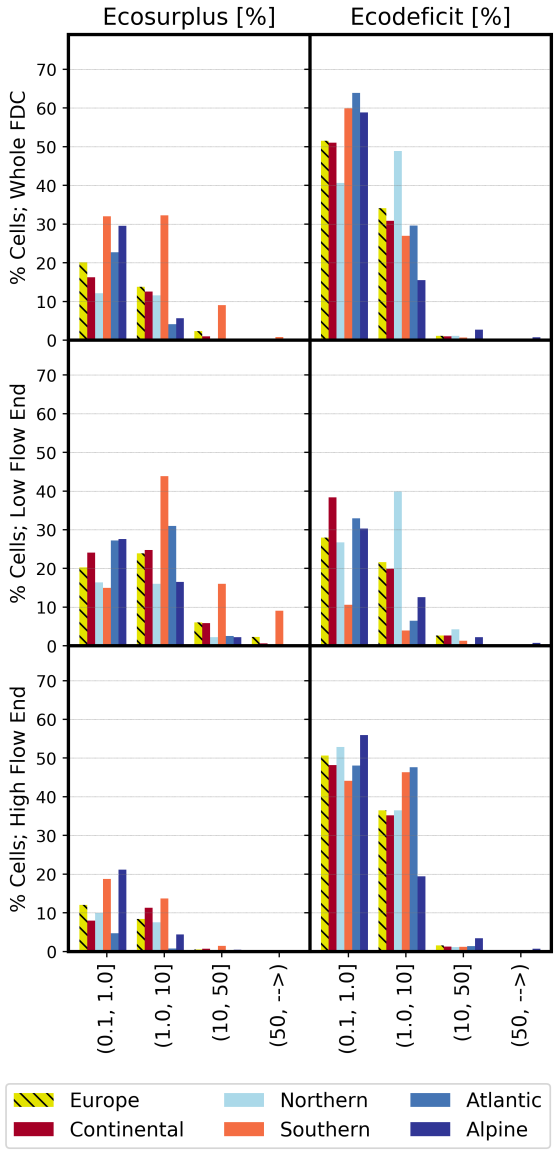


**Figure 25:** Europewide and regional runoff ecosurplus (left) and ecodeficit (right) in percent; for the whole FDC ($0^{th}$–$100^{th}$ percentile; top), low flow end FCD ($0^{th}$–$10^{th}$ percentile; middle) and high flow end FDC ($90^{th}$–$100^{th}$ percentile; bottom), corresponding to the maps in Figure 23. The ecometric values (e) larger than 0.1% are divided into four bins: $0.1<e\leq1.0$, $1.0>e\leq10$, $10<e\leq50$ and $e>50$. The FDCs are based on simulated runoff using the WFDEI forcing data for 1901–2001.

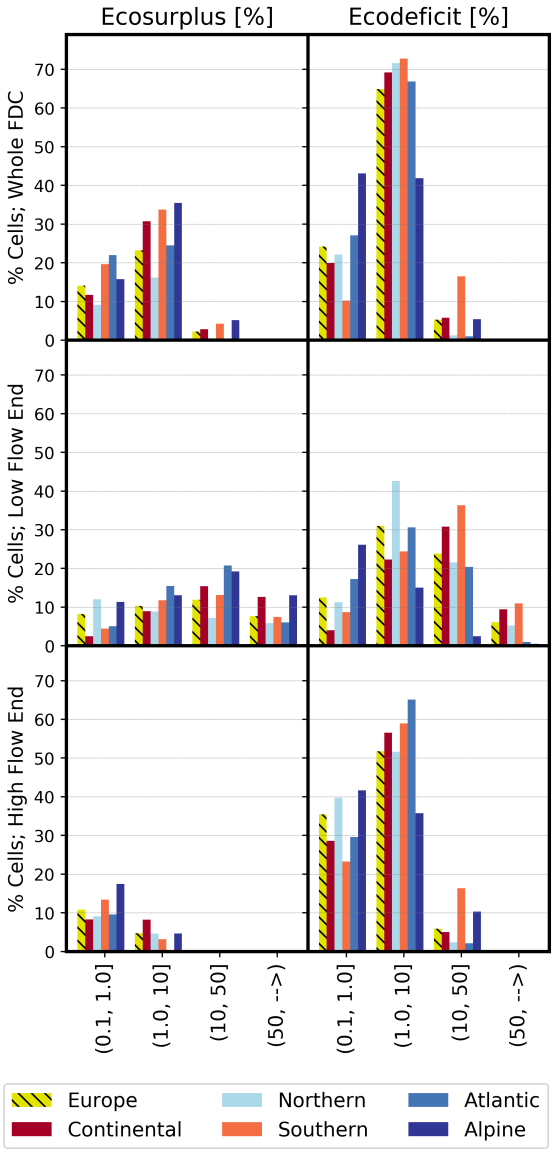


**Figure 26:** Europewide and regional discharge ecosurplus (left) and ecodeficit (right) in percent; for the whole FDC ($0^{th}$–$100^{th}$ percentile; top), low flow end FCD ($0^{th}$–$10^{th}$ percentile; middle) and high flow end FDC ($90^{th}$–$100^{th}$ percentile; bottom), corresponding to the maps in Figure 24. The ecometric values (e) larger than 0.1% are divided into four bins: $0.1<e\leq1.0$, $1.0>e\leq10$, $10<e\leq50$ and $e>50$. The FDCs are based on simulated discharge using the WFDEI forcing data for 1901–2001.

For runoff, the largest ecosurplus values for the whole FDC were found in the south of Europe, followed by a region north-west of the Black Sea, and Sweden (left plots of Figure 23 and 25). The same pattern was found in the ecosurplus values for the low and

high flow end FDC. For the low flow end, 25% of the cells in the Southern region had values larger than 10%, i.e. a water gain of more than 10% in the low flow end because of current HI. About 9% of the cells in the Southern region had low flow end ecosurplus values larger than 50%. Except for in the Southern region, the highest low flow end ecosurplus values were mostly in the range 1.0–10% found in the north-western region of the Black Sea, in Sweden, and along the western coast from Spain to Denmark. The largest high flow end ecosurplus values were in general smaller in magnitude compared to the ecosurplus values in the low flow end and in the whole FDC. Runoff ecosurplus values larger than 1.0% were found in only 9% of Europe for the high flow end, as opposed to 32% for the low flow end and 16% for the whole FDC.

The pattern of the highest runoff ecodeficit values for the whole FDC was similar to the pattern found for the high flow end (right plots of Figure 23 and 25). For both of these two FDC intervals, most of the runoff ecodeficit values were in the range 0.1–1.0% (in about half of the cells) and 1.0–10% (in about one third of the cells). Unaffected areas include the area north-west of the Black Sea, and areas in Norway and Sweden. Low flow end ecodeficit values were highest in the Northern region, with 44% of the cells having values larger than 1.0%. Generally, a contrasting pattern over Europe was found for areas of high ecodeficit and high ecosurplus.

In Europe, 37% of the cells had whole FDC discharge ecosurplus values in the range 0.1–10%, and only 2% of the cells had larger values (left plots of Figure 24 and 26). These higher values were located in the Iberian Peninsula, north-east of the Black sea, and in a large part of the Continental region between these two areas. In addition, Scotland, Norway, Sweden as well as many rivers in eastern Europe constituted values in the range 0.1–10%. Of the low flow end discharge ecosurplus results, 20% of the values were larger than 10%. These values were located in Scotland, Scandinavia, major rivers in eastern Europe (e.g. Dnieper, Volga and Euphrates), and large regions from France in west to the west-coast of the Black sea in Romania in the east. Since the highest values are distributed across most of Europe – except for large areas in the eastern part of the Northern region – the Continental, Southern, Alpine and Atlantic regions had values larger than 10% in more than 20% of their cells. High flow end discharge ecosurplus values were highest north-west of the Black Sea and in southern Sweden. However, overall only 5% of the ecosurplus values for the high flow end were larger than 1.0%.

For discharge, more cells are impacted by ecodeficit than ecosurplus for all FDC intervals and in all regions except for the low flow end in the Alpine region (Figure 24 and 26). Whole FDC discharge ecodeficit values between 0.1–10% covered approx. 90% the

European domain. The highest discharge ecodeficit results for the low flow end were mainly located in regions with very small discharge ecosurplus values for the low flow end. Values were larger than 50% in 11% of the cells in the Southern region and in 9% of the cells in the Continental region. More than 40% of the cells in these two regions had values larger than 10%. The Alpine region had the lowest values in the low flow end discharge ecodeficit, with 3% of the cells having values larger than 10%. Discharge ecodeficit for high flow end were found throughout Europe, except for the region with the highest discharge high flow end ecosurplus values (i.e. north-west of the Black Sea and southern Sweden). For this FDC interval, most of the values were in the range 0.1–10%. However, the Southern and Alpine regions had values larger than 10% for 16% and 10% of their cells, respectively.

The alternative forcing data sets had very similar pattern to WFDEI in terms of the direction of impact for all FDC intervals for both runoff and discharge (Figure 46–53 in Appendix E) Similar to WFDEI, the alternative forcing data sets had the highest runoff values in the Southern region for the low flow end. WFD had similar results to WFDEI, however showed a slight southward shift in the ecometric values for all FDC intervals, e.g. north-west of the Black Sea. The high values found in southern Sweden in the WFDEI results are not apparent in the GSWP3 results. Also, the region north-west of the Black Sea has "moved" south-west, and several other regions in Europe had different ecometric values for GSWP3 and WFDEI. The results using PGMFDv2 forcing data showed no clear cluster of high values in the region north-west of the Black Sea for any of the FDC intervals. The patterns of the highest ecosurplus and ecodeficit values were less spatially consistent compared to the WFDEI results. In general, for both runoff and discharge, the differences between forcing data sets were higher for the high flow end results compared to the low flow end results. Of the forcing data sets, PGMFDv2 gave the most deviating results, and of the regions, the Northern region showed the highest differences in ecometric values in all FDC intervals for both runoff and discharge.

# 7 Discussion

This chapter discusses the results of the analysis of impacts of human interventions (HI) on the water cycle and its extremes. It is organised as follows; the first three sections discuss the results following the same order as used when presenting the methods (in Chapter 5) and results (in Chapter 6). Then, the sensitivity of the results to the forcing data and other sources of uncertainties are discussed in Section 7.4 and 7.5, respectively. The two last sections attemp to take the results one step further, by connecting changes found in the water cycle and its extremes due to HI to climate induced changes (Section 7.6), and relating the findings to consequences they may have for society and ecology (Section 7.7).

## 7.1 Human Impacts on Regional Low, Mid and High Flow

The regional medians of low, mid and high flow (ref. Figure 19, 20 and 21, respectively) allow for direct comparison of regional variability in runoff over time, both with and without HI. The method also made it possible to use transient HI, i.e. non-stationary conditions in HI. As mentioned in methods (Section 5.2.1), only runoff was used for this part of the analysis because the discharge variable is highly spatial dependent and thus not suitable for computation of regional medians. Thus, only the local impacts are assessed here. Meteorological induced changes in regional median percentiles over time were found to be considerably larger than the induced changes by both transient and current HI. In addition, the time series for the five regions showed significant differences, irrespective of the meteorological or model scenario applied. The differences between model scenarios were in general very small, and notably smaller compared to the temporal and regional variability, thus indicating that HI have a minor impact on low, mid and high flow runoff. However, analyses on the runoff variable do not capture the aggregation of runoff within catchments that might lead to a stronger impact of HI towards basin outlets.

The regions used are classified based on meteorological conditions (Metzger et al. 2005), and since meteorology is one of the main controllers on runoff (in addition to e.g. storage capacity), the differences in percentile values between regions throughout the period (ref. lower right plot of Figure 19–21) were not unexpected. HI, on the contrary, are to a very small degree determined by climatic conditions, but rather determined by socio-economic and physiographic conditions and will usually be more variable within each climatic region (ref. maps in Figure 6–11 showing the spatial variability in HI across Europe vs the map in Figure 4 showing the climate regions). Thus, a high impact on runoff in a small percentage of the region will not be represented in the median for the whole region. Further, HI can

cause both increases and decreases in runoff, and thus the impact may be cancelled out in the regional median. A small direction-consistent shift in a regional median percentile or $\Delta$FDC due to HI is therefore potentially an indicator of a much larger impact at a smaller scale.

Despite this limitation of the regionalization, it provides valuable information regarding the impacts of HI. For example, it is apparent from the natural and current HI scenario that the impact of HI is also climate dependent. In the Alpine region, low flow under current HI was much lower compared to the natural low flow in the middle of the period when the percentile in general was lower. This may be due to higher water demand and more evaporation during warm and dry periods.

The direction of the shift in low flow by current HI indicates that low flows in the Continental, Southern and Alpine regions increase (i.e. higher $10^{th}$ percentile values) due to HI. These regions, in particular the Southern region, have large areas with irrigation (see Figure 6). The shift may be caused by the additional water on the irrigated fields that increases the runoff (more thoroughly explained in Section 7.3). Irrigated fields are sparse in the Northern and Alpine regions, and the shift towards lower low flows in these regions result mainly from groundwater abstractions for other sectors. A similar change towards lower flows was found for regional median mid flow, except for the Continental and Atlantic regions that had no clear direction in the shift. The median high flow decreased in all regions with the current HI, indicating that there is little irrigation during high flow periods and the impacts result mostly from water demand for other sectors.

An important reason for using time series analysis was to investigate the impacts of the historical development of HI represented by the transient HI scenario. The expected behaviour of the transient HI time series was that it would be very similar to the natural (no HI) time series in the beginning of the period, as the spin-up conditions were the same, and only difference in the two model scenarios would be the interventions during the 30 first years, and approaching the current HI time series towards the end of the period. This behaviour was found in the Southern low flow and mid flow. For the other regions and percentiles, however, the behaviour of the transient HI scenario was very similar to the natural scenario throughout the period. In some cases, the transient HI scenario percentiles were large than the natural scenario percentiles, whereas the current HI time series had lower percentile values than the natural time series, e.g. at the end of the Alpine median low flow time series.

The reason for the unexpected behaviour of the transient HI scenario is not clear, due to the complex model interactions in global hydrological models. The difference in direction of current and transient HI impact could be a consequence of a change over time in the dominant type of HI acting on the region, or that the results are very sensitive to the spin-up conditions, in which the transient HI scenario assumed no HI and current HI scenario assumed current HI. Different spin-up conditions can result in different groundwater and soil moisture levels which can further lead to differences in water use between the to scenarios. The reasons for the transient HI time series behaviour need more investigation, however, it is beyond the framework of this study.

## 7.2 Human Impacts on Regional Flow Variability

The largest change in flow variability (ref. Figure 22) was found in the Southern region where it decreased by 7.5% on average for the current HI scenario, indicating a human induced flattening of the runoff FDC. The low and high flow results indicated that this is a result of both an increase in low flow and a decrease in high flow. A shift towards lower variability was also found in the other regions except the Northern region, however to a lesser degree. In the Continental and Atlantic regions, as in the Southern region, both low and high flows were attenuated (i.e. high flows become lower and low flows become higher) for the current HI, whereas the Northern and Alpine regions had decreases in both extremes.

The same drawbacks apply here as for the regional median percentile time series, such as the loss of spatial variability in HI due to the regionalization and the unexpected behaviour of the transient HI time series. Accordingly, the results should be treated as indicative of dominant impacts within each region rather than looking at the actual magnitudes of the change. The Continental, the Atlantic, the Alpine and especially the Southern regions indicate an overall reduction in flow variability due to local HI, adding to the climatic induced reduction in flow variability seen in the last half of the century in three out of four of these regions. It is important to keep in mind the fact that impacts on runoff only stem from local HI, as one would expect HI in one location to also impact cells downstream. This was accounted for in the assessment of human impacts on whole period water gain and loss in discharge (ref. Section 7.3).

## 7.3 Human Impacts on Water Gain and Loss for the Whole Period

The ecometric (i.e. ecosurplus and ecodeficit) results revealed high spatial variability in the impact of current HI on the water cycle and it extremes given the $20^{th}$ century meteorological conditions (ref. Figure 23–26). The largest impacts on runoff were found in the Southern region, where a water gain of over 10% in the low flow end FDC (i.e. $0^{th}$–$10^{th}$ percentile) were found in one fourth of the region, mostly in the Iberian Peninsula (Spain and Portugal), northern Italy and Turkey. These are densely irrigated areas, as seen in Figure 6. Other densely irrigated areas, such as western France, north-west of the Black Sea, Denmark and some smaller clusters in the interior of Europe, also showed high runoff ecosurplus values. In the case of irrigation, water is withdrawn from surface- and groundwater, and added to the irrigated fields. This leads to an increase of water in the irrigated areas, and a reduction in the riverine and groundwater storage. Because runoff is estimated based on the water balance in each cell individually, the river system, and hence also its water losses, is not connected to the local water balance. Accordingly, the added water to the fields was taken into account in the local water balance without an equivalent reduction in the surface water source. Despite that a large proportion of the added water would infiltrate and evapotranspirate in water-limited regions, the net result is an increase in runoff compared to the situation of no irrigation. This effect is apparent as water gains in irrigated areas for both the low and the high flow end FDC, as well as for the water cycle in general (i.e. the whole FCD). However, irrigation during high flow periods is generally not taking place in the model unless the soil moisture is below the irrigation level (see irrigation scheme in Section 4.2.5). Irrigated areas north-west of the Black sea and in the Iberian Peninsula are nevertheless experiencing water gain in the high flow end. These regions are naturally dry and the water gain may be because irrigation increases the soil moisture in general or because the fields are irrigated even during high flow periods.

Irrigation was found to be the dominant source of most of the largest runoff ecosurplus (i.e. water gain) values across Europe, still runoff ecosurplus of 1–10% for all FDC intervals were found in unirrigated areas of Sweden. Here, the water gain may be due to the combination of return flow from (relatively low) domestic and industry water use, and very low natural runoff in the region (see Figure 5), causing a larger relative impact.

HI reduced runoff across most of Europe, however, rarely by more than 1%. Water losses results from water abstractions from groundwater when return flow is lower than the base flow change due to water withdrawals. As opposed to water use for irrigation where water withdrawals are added to the land surface, net water use (i.e. gross water use minus

return flow) for domestic, livestock and industry is not returned as runoff. Water losses in the low flow end FDC were mainly found in north-eastern parts of Europe (including Finland and large areas in Russia), whereas water losses in the high flow end FDC and whole FDC were found in eastern and western parts of Europe. It is possible for a cell to have both a significant ecosurplus and ecodeficit value if the associated HI have different impact on different intervals of the FDC. However, the regions dominated by HI induced water gain, overall had low or zero ecodeficit values, and vice versa.

All results regarding runoff is limited to the grid-cell scale, meaning that water abstractions upstream have no consequences for the downstream cell. This is also the case for lake and reservoir regulations. Thus, runoff results provide a picture of the local impacts of HI. However, the reality is different in terms of how HI affects the water cycle and discharge in particular. The discharge variable takes into account this spatial dependencies by representing the downstream accumulation of runoff along the river network.

The impact on the whole FDC for discharge are generally higher than for runoff in case of both water gains and water losses. Except for the areas in north-eastern Europe that are dominated by water losses, most of the domain is characterized by both water gains and water losses in the water cycle in general, and reflect HI that impact the water cycle differently for high and low flows. This mixed picture is therefore better understood by looking at the hydrological extremes.

For discharge, the pattern of largest water gains was similar to the patterns of cells affected by upstream regulations (ref. Figure 11). Regulated rivers in eastern Europe, such as Volga, Dnieper, Don, Euphates and Tigris, stand out with high ecosurplus values compared to the surroundings. Attributing the increased low flow volume to reservoir regulations is reasonable, since it is common to release water in dry periods to maintain minimum flow requirements. The model's reservoir regulation scheme assumes that reservoirs managers would like to keep a flow that is in general constant throughout the year, depending on the reservoir storage capacity and the downstream water demand (Hanasaki et al. 2006, Van Beek et al. 2011). The same effect has been found in studies on impacts of HI on streamflow drought, e.g. by Wanders & Wada (2015) and He et al. (2017). Several of the cells also have large reservoirs (ref. Figure 10). A high ecosurplus value is expected for cells containing reservoirs that have regulated water tables larger than the natural (i.e. no reservoir) water tables.

In some regions, large upstream reservoir capacity has only a minor impact on the discharge ecosurplus low flow results. This is the case for regions in the Iberian Peninsula

and Turkey. These areas have high water requirements, dominantly for irrigation, resulting in water losses downstream in the low flow end FDC. About 47% of the Southern region had water losses of more than 10% in the low flow end FDC. Large parts of western France, Belgium and the Netherlands, as well as large parts of eastern Europe, also had water losses of more than 10% in the low flow end. These areas have little reservoir regulations, and the water losses stem from water use and increased evapotranspiration (due to irrigation) with an accumulated effect downstream. These results are in accordance with existing literature. For example, Wada et al. (2013) found that human water use increases the drought frequency and intensified the drought intensity, mainly attributable to irrigation in southern Europe, whereas Wada et al. (2014) and Veldkamp et al. (2017) both stress the accumulated effect of HI on water availability downstream. As for runoff, discharge had water losses for the high flow end FDC over most of Europe due to current HI, except of north-west of the Black Sea and southern Sweden that had water gains in the high flow end. The water losses were larger for discharge, with 58% of the cells having more than 1% decrease, compared to runoff with 38%. This deviation is expected as discharge is affected by the sum of all water withdrawals in the upstream cells that are not returned as discharge. In addition, the water losses in the high flow end are a result of reservoir regulations that typically retain floods and high flows, either to decrease damage or to increase their water storage. The effect of reservoir regulations on discharge is also the reason for the watre losses in the high flow end FDC in Norway and Sweden that was not apparent in the ecodeficit results for runoff. The cells with high flow end ecosurplus for discharge are mostly cells located at the uppermost parts of the drainage network, so that they have little or no HI upstream, and thus act in a similar manner as the runoff results.

## 7.4 Sensitivity to the Meteorological Forcing Data

All results were sensitive to the meteorological forcing data applied (ref. Appendix C–E). Regional median low flow, mid flow, high flow and $\Delta$FDC results revealed large differences in percentiles, however the direction and to some degree the size of the impact of HI were similar. This means that the direction of change due to HI per region were stable, independent of the meteorological data. Differences in regional median percentiles between the forcing data sets result from differences in precipitation and temperature (ref. Figure 29 in Appendix B). PGMFDv2 has notably lower precipitation totals in all regions, likely due to the lack of precipitation undercatch correction, explaining the lower percentiles found for this forcing data. GSWP3 on the other hand, has in many cases

larger regional precipitation, resulting in higher percentile values. As WFD and WFDEI are the same data set until 1979, their results are equal until the 30-year window starts to include years after 1979, from which they are still very similar in percentile values and $\Delta$FDC.

Despite differences among the different forcing data sets when looking at whole period impacts of current HI on runoff, the forcing data sets were consistent in having high increases in low flow volumes in Southern Europe for runoff, and in the patterns of high increases and decreases in low flow volumes for discharge. This strengthens the confidence in the results of impacts of HI on low flows. The similarities were highest between WFD and WFDEI as expected, since the data sets are partly overlapping. However, WFD, as well as GSWP3 and PGMFDv2, showed different patterns of increases in water volumes in the region north-east of the Black Sea compared to WFDEI. This is a relatively dry area, and the differences may have occurred because the wetness in the areas is close to the soil moisture threshold for irrigation, thus making the HI very sensitive to small differences in meteorology. PGMFDv2 forcing data results showed no clear impacted region north-west of the Black Sea for any of the FDC intervals. The patterns of impacts were more spatially variable compared to WFDEI results. Because PGMFDv2 had the most deviating precipitation totals and the weakest validation results (ref. Section 6.1) of the four forcing data sets, less confidence are given to these results compared to the results of the other forcing data sets.

The Northern region, followed by the Alpine region, was the region with the largest sensitivity to the forcing data set. These are cold climate regions, characterized by a seasonal snow climate with temperatures falling below 0°C in 25–50% of each year (ref. Figure 14), and 0°C is the threshold temperature used in the PCR-GLOWB 2 runs to separate precipitation into snow or rain. When precipitation is set as snow, the water input is stored as snow and contributes to soil moisture and runoff first when it melts, whereas rain immediately contributes to soil moisture and runoff (if not evaporated). Thus, runoff is highly sensitive to this threshold temperature, and for regions where temperatures are close to 0°C, small differences in temperatures between the forcing data sets can give very different hydrological response.

In general, results for high flows appeared to be more sensitive to the choice of forcing data set compared to results for low flows. This was expected because high flows are more event-based flows resulting from intense precipitation or snow-melt (Smith & Ward 1998). As already mentioned, uncertainties are related to snow-rain partitioning, and in addition, precipitation is one of the largest causes of uncertainty in large-scale hydrological

modelling (Biemans et al. 2009, 2011). Low flows on the other hand is commonly a result of a prolonged lack of precipitation combined with the extent and properties of the storages in the catchment, and normally sustain for a longer period. Therefore, differences in precipitation events for the different forcing data sets cause larger differences in the results for high flows compared to low flow. Because the present study only used one hydrological model, the sensitivity of the results to the model is unknown. In a study of nine large-scale hydrological models driven with the same forcing data, Gudmundsson et al. (2012) found decreasing model performance from wet to dry conditions, and largest uncertainties were found for low flow percentiles. The combination of these findings with the findings of the present study implies that whether the choice of forcing data or model is the dominant source of uncertainty, depends on whether high flows or low flows are investigated.

## 7.5 Other Sources of Uncertainties

In addition to the uncertainties related to the meteorological data applied, the results are sensitive to several other choices, especially choices related to the metrics chosen and the model set-up.

The regional medians used in the percentile and $\Delta$FDC metrics aggregate across large areas such that much of the information of local scale impacts of HI were lost due to variable conditions within each region. An alternative could be to use regions based on "dominant type of HI", however, this would be most fitted for the runoff calculations as discharge is impacted by all upstream HI to various degrees. A HI based regionalization could also be challenging if investigating transient HI as the dominant type of HI may change over time.

Another metric-related aspect is how to quantify the impact of HI. This study has focused on relative changes rather than absolute changes, assuming that a relative change is more connected to the consequences, e.g. that the same absolute water loss for low flows would have a larger consequence in a river with already very little water during low flow compared to a river with more water-rich low flows. In addition, Relative variables allows comparison across regions that vary in hydro-climatic condition. A potential drawback of using relative changes is that high flow in general could be interpreted as "less impacted" than low flow due to their nature of being larger in magnitude, and thus a small deviation captured by an ecometric may stem from a large absolute impact of HI. However, whether this is a drawback or not is tightly connected to what kind of relation there is between

the changes in hydrology and the negative and positive consequences these changes have for society and nature (see Section 7.7).

Except for the discharge validation, all analyses were based on aggregated data over multiple years. Hence, the time component of low flows and high flows within the period is lost. However, impacts of HI on hydrological extremes can vary substantially per season (e.g. Wanders & Wada 2015). A natural next step could be to have multi-year analyses per season, to see whether some seasons have large or negligible impacts. Such findings would make it possible to connect seasonal impacts of HI to areas with certain periods of higher risk of negative consequences, e.g. for vulnerable freshwater ecosystems or problems with water scarcity.

A last remark regarding the metrics, concerns the use of percentile values as a basis for the analysis. This choice allowed a symmetric analysis of the hydrological extremes. However, the metrics used in this study are limited in the possibility to connect the extremes to their potential societal and nature-related consequences because the percentiles break the temporal dependence in the flow, and because metrics for other characteristics related to droughts and floods were not included as part of the analysis.

A model is a simplification of the system it tries to simulate, and the model output from PCR-GLOBWB 2 is a deterministic result of a set of model assumptions and simplifications made by the model developers. This make the results sensitive to the model set-up and choices, such as the snow-rain threshold temperature and conditions chosen for the spin-up period. In addition, the grid-cell size of 0.5° limits subregional or local applications (Sutanudjaja et al. 2017). Finer spatial resolution is available (Sutanudjaja et al. 2017, e.g.), however, there is a substantial lack of data on continental scale (e.g. for groundwater, water use and water transfers) that may constrain the possible subregional improvements by using a higher resolution (Wada et al. 2017).

When investigating impacts of HI on the water cycle, the implementation of HI in the model is a crucial factor, and potential future studies should preferably include several hydrological models with different implementations of HI to increase our understanding of uncertainties related to these types of assessments (Wanders & Wada 2015). It is important to note, however, that despite the simplifications of HI used, PCR-GLOBWB 2 is currently one of the Global hydrological models having the most sophisticated HI schemes implemented (Bierkens 2015, Wada et al. 2017).

Mainly due to a lack of sufficient information about HI globally, several general rules have been applied in PCR-GLOBWB 2. For example, the non-paddy irrigation scheme have implemented that water is filled to field capacity when soil moisture falls below a given threshold. However, it is likely that many farmers won't fill the soil column completely up to field capacity in case of (heavy) rainfall in near future. The irrigation scheme may therefore overestimate the water use for irrigation.

Water is withdrawn from surface- and groundwater based on their relative water availability. However, reality may be very different, and in regions with a consistent deviation from this model assumption, the results will be biased. In the case of runoff, this is vital, as groundwater withdrawals reduce the runoff, whereas surface water does not. Because the recharge rate in groundwater generally is slower than surface water, an over- or underestimation of the groundwater withdrawal can yield a very different response to the impact in the discharge downstream.

The model assumption of reservoir management is another example affecting the results. In the model, water is released during dry periods and held back during high flow periods, and in this way representing an "ideal" dam operation regarding ecosystems and risk protection. However, reality may give a different story if regulators follow other priorities. For example, if water is saved for energy production during low flow periods as well, the lack of water releases will cause water losses in the low flow end FDC rather than water gains as found for the reservoir impacted rivers in this study. Another aspect are the potential inter-basin transfers of water, which is not implemented in the model. Because this study uses a relatively coarse grid, the number and impact of such transfers are expected to be low. When using models on a finer scale, however, the lack of water transfer in the model may be a significant source of uncertainty in the results in some areas.

## 7.6 Combined Impact of Humans and Climate

The analyses of this thesis compare natural and HI scenarios for the period 1901-2001 given the same meteorological data, which allowed for separation of impacts caused by HI and impacts caused by changes in the climate. Hydrology is impacted by the combination of the two, and will continue to do so in the future (Wanders & Wada 2015).

Southern Europe was found to be one of the most impacted regions by HI in terms of low flows, regardless of the metric used in the assessment. This region also has the most severe and widespread problems with water scarcity (Metzger et al. 2005), and is one

of the hot spots for climate induced changes in hydrological drought characteristics in future scenarios (e.g. Prudhomme et al. 2014, Wanders et al. 2015). Because of recent increases in temperature and evapotranspiration, meteorological drought frequencies have increased during the last six decades in southern parts of Europe(Stagge et al. 2017). This observed signal was, however, not captured by the Southern median low flow time series, where climate driven change seemed to decrease low flows percentile values only slightly in the last part of the period. The intensification of hydrological droughts is projected to increase in the future (Prudhomme et al. 2014, Wanders et al. 2015). The discharge ecometric results indicate that HI will further aggravate this trend in many southern areas, as water withdrawals for irrigation cause large water losses downstream in the low flow end. Exceptions, where this climate driven trend is alleviated by HI in southern Europe, are found downstream of large reservoirs, as also recognized by Wanders & Wada (2015), and in irrigated areas that are not themselves affected by upstream withdrawals. The compensating effect on climate and water use driven increases in drought severity relies on dam operations that release water during low flow periods. In some southern areas, reservoir capacity are not always enough to compensate for the projected climate and HI induced increases in future hydrological droughts (Wanders & Wada 2015).

Much of northern Europe shows a decreasing trend in meteorological drought frequencies since mid $20^{th}$ century due to increased precipitation (Stagge et al. 2017). Projections for droughts in the $21^{st}$ century are more uncertain in this region compared to southern Europe, however, projections indicate a change towards dryer conditions, in particular in fall and winter season (Prudhomme et al. 2014, Wanders & Wada 2015). As for southern Europe, reservoir regulations may alleviate potential future increases in streamflow drought severity downstream if the dam operations include releases of water during low flow period. Human water use on the other hand, reduces water availability downstream, and will therefore likely aggregate the climate driven increases of drought severity downstream of where withdrawals occur.

In general, floods are decreasing in eastern Europe and increasing in central and atlantic regions, however the pattern varies among studies (Hall et al. 2014). These tendencies match to some extent the climate driven changes found in the regional median high flow results, where the Alpine region (parts of which constitute the Atlantic facing coastal region of Norway) and the Atlantic region show increases in high flows, and the Continental region and the Southern region show decreases in high flows. In the $21^{st}$ century, flood will likely increase in western Europe due to increases in intense rainfall, and decrease in some regions with snow cover during winter because of reduced snowmelt induced floods

(Rojas et al. 2012). Discharge results in this study showed that high flows are reduced in almost all of Europe due to HI, regardless of the type of intervention. Based on these findings, HI will likely reinforce the climate driven reduction in floods in snow-rich regions and alleviate increases in floods in western Europe.

Human interventions are not constant. In addition to projected changes in climate, changes in HI are also expected in the future. As already seen in the $20^{th}$ century, increased water demand is expected as a result of a growing population (Wada et al. 2013). Taking this aspect into account, the current HI scenario used in the present study may be regarded as the "minimum-HI-scenario" (i.e. no increase in HI) in studies of future impacts of HI. In addition, there are interactions and feedbacks in the human-water system. Whereas this study only looks at one direction in the feedback between humans and hydrology (i.e. the impacts of HI on hydrology), humans act dynamically and are both impacted by and drivers for hydrology and hydrological extremes (Montanari et al. 2013, Di Baldassarre et al. 2017). Such dependencies would be valuable to address in future studies, to better understand the reality of the human-water system.

## 7.7 Consequences of Changes in Flow Extremes and Variability

Consequences of hydrological extremes and their changes are dependent on both the hazard and the vulnerability (Blauhut et al. 2015). Flood hazard mapping can be made by combining flood water levels with topography because socio-economic consequences of floods are often related to the vulnerability of the flooded area (e.g. Van Alphen et al. 2009, Alfieri et al. 2014). For example, the observed growth in population and economic activities in flood-prone areas, results in more negative consequences of floods (Winsemius et al. 2016). Thus, the decreases in high flows seen in most of Europe due to HI may have a positive effect on society and economy if it reduces water levels in vulnerable flood-prone areas. However, the connection between high flows and water level is not trivial. There is also a possibility that a decrease in high flow will have a negative consequence for society, e.g. in water short regions with no risk of flood reaching hazardous water levels. Droughts may have many different types of negative consequences, including water quality and water deficit in agriculture, industry, navigation and water supply among others (Kundzewicz & Kaczmarek 2000, Blauhut et al. 2015). As opposed to floods, few of the numerous definitions of drought are tailored to the potential consequences (Blauhut et al. 2015). This limitation applies for the metrics used in this study as well, however, overall lower low flows reflect more severe droughts and thereby likely higher risk of negative consequences. Accordingly, the regions dominated by upstream reservoir management

experience a positive effect of HI, whereas regions with large water withdrawals a negative effect of HI.

Whereas a reduction in flow variability (i.e. higher low flow and/or lower high flow) seems to be positive for humans and society, the picture is more mixed in terms of consequences for biology. Freshwater ecosystems are often highly vulnerable to changes in low flows, high flows and flow variability in addition to a sensitivity to temperature changes that can result from changes in low flow magnitude (van Vliet et al. 2013, EEA 2017). The flow duration curve based metrics used in this study may therefore be more related to the consequences for ecosystems compared to socio-economic consequences, and changes in the water cycle and it extremes, regardless of the direction, may be treated as potentially negative for the species that are naturally adapted to the pristine conditions.

# 8 Conclusions

In this study, the sensitivity in the water cycle and its extremes to human interventions (HI) were investigated at the European scale. HI included water use for irrigation, industry, domestic and livestock, as well as reservoirs and dam regulations. Impacts of HI on runoff (based on water balance at the grid-cell scale) and discharge (i.e. routed runoff along the drainage networks) were analyzed by comparing time series of natural conditions (no HI) with transient HI (HI introduced on an annual basis) and current HI (whole period simulated with the HI per 2010). Whereas the transient HI scenario represented the actual development of HI throughout the $20^{th}$ century and thus aimed at simulating the historical impacts of HI, the current HI scenario represented the impacts the HI of 2010 given the meteorological conditions of the $20^{th}$ century. All three models scenarios (natural, transient HI and current HI) were simulated with the global hydrological model PCR-GLOBWB 2 using meteorological data for the period 1901-2001 by using four different forcing data sets; GSWP3, PGMFDv2, WFD and WFD+WFDEI (named WFDEI in the following for simplicity).

Monthly simulated discharge time series stemming from the different forcing data sets were validated against GRDC observed discharge time series. The simulated discharge values showed a good agreement with the observations for nearly all the forcing datasets, with the exception of PGMFDv2. The WFDEI was among the forcing data sets providing the best performance, and the rest of the study focus its presentation on results based on this forcing data set.

Non-exceedance runoff percentiles for the different HI scenarios were computed for 30-years moving windows throughout the period, and regional (i.e. Continental, Northern, Southern, Atlantic and Alpine) median $10^{th}$, $50^{th}$, $90^{th}$ and $20^{th}/80^{th}$ percentile time-series representing low, mid and high flow percentiles and flow variability (i.e. $\Delta$FDC), respectively, were assessed. Because regional medians are not well fitted for highly spatial dependent variables, discharge was excluded from this part of the analysis, and thus, only the impacts of the local HI (by using the runoff variable) were investigated. Regional median time series proved to be valuable in terms of detecting differences in the variability and magnitude of regional runoff over time, between different climate regions, model scenarios and forcing data sets. The transient HI scenario time series had an unexpected behaviour for most percentiles and regions (the Southern region being an exception), being very similar to the natural scenario time series throughout the period. Accordingly, the current HI was mainly used to assess the results. In general, the results indicated

that HI cause an overall increase in runoff for low flow, and to a lesser degree extent mid flow, in the Continental, Atlantic and Southern regions, and an overall decrease in the Northern and Alpine regions. High flows generally decreased in all regions as a result of HI. The highest regional median impact of current HI on runoff percentiles and $\Delta$FDC was found in the Southern region. The impact of HI was in general weak, and interannual variability, different climate regions and meteorological forcing data showed a stronger signal of impact on runoff. The low HI impacts can partly be explained by the aggregation of many types of impacts within each region, because diverging impacts and smaller highly impacted within a region could be cancelled out in the regional medians.

The last part of the analysis investigated the impact of current HI in Europe on both runoff and discharge given the meteorological conditions of the $20^{th}$ century. For this purpose, the metrics ecosurplus and ecodeficit were applied to detect water gains and water losses, respectively, in the water cycle in general (whole flow duration curve; FDC), in the low flow end FDC ($0^{th}$ –$10^{th}$ percentile of the FDC) and the high flow end FDC ($90^{th}$ –$100^{th}$ percentile of the FDC). In the case of runoff, the low flow end had the largest ecosurplus values, and one fourth of the Southern region was found to have a water gain of more that 10% in this end of the FDC. Water gains in the high flow end were only found in dry regions like Sweden and highly irrigated areas of the Iberian Peninsula, Turkey, northern Italy and north-east of the Black Sea. The largest water losses were found in regions that are affected by water abstractions from other sectors than irrigation. Because changes in runoff are attributed to HI in the same cell, this flow variable showed to be a valuable tool to attribute changes in the water cycle to its HI sources. However, to get a realistic picture of the impacts of HI throughout major river basins, changes in discharge must be investigated.

For discharge across Europe, a decrease of more than 10% in low flow volumes due to current HI were found for 30% of the area, whereas an increase of more than 10% in low flow volumes due to current HI were found for 20% of the area. Whereas changes in runoff are dominated by irrigation, impacts on discharge are dominated by reservoirs that exist in many of the large rivers throughout Europe. As reservoirs are part of the river network, this type of HI does not affect the runoff. Reservoir management as implemented in the model, retains water during high flow periods and releases water during low flow periods, and thus reduces the flow variability downstream. Thus, water gains in the low flow end and water losses in the high flow end were found downstream of regulations. The other types of HI (i.e. water use for irrigation, industry, domestic and livestock) generally caused relatively large water losses for the discharge variable in areas in the Atlantic region and

north-eastern Europe. Large water losses were also found in several areas in the Southern region where both irrigation and reservoir regulations were apparent. In these areas, the impact of irrigation seems to dominate over the impact of water releases from reservoir.

All results were found sensitive to the meteorological forcing data applied. The magnitude of the flow variables was found to be more sensitive to the forcing data than the impact of HI. The results stemming from the different forcing data sets were more variable in northern regions than southern regions, and more variable for high flows than low flows. The former may be attributable to different downscaling methods and sensitivity to temperature in the snow-rain partitioning, whereas the latter may result from the difficulties in climate models to accurately simulate intense precipitation events as the high flows are often the results of intense rainfall.

Future analyses are needed to investigate changes in the water cycle and its extremes due to HI using other types of metrics, hydrological models and regional divides to support or challenge the findings of this study. Also, assessment on a seasonal basis could provide more information into systematic differences in the intensity and/or direction of the impacts. Further, it would be of value to connect metrics of impact of HI on the water cycle and its extremes to consequences of such impacts on ecology and society. This will help water managers and policy makers to prepare and potentially reduce unwanted effects of HI on the hydrological system.

To the author's knowledge, this study was the first of its kind to investigate the impacts of human interventions on both hydrological extremes. The work revealed how different types of HI affect the two extremes, both in the direction and size of the impacts. Despite their differences, both extremes and changes in them have potentially devastating effects on society and ecosystems. It is therefore of importance to take into account the full flow range when aiming at reducing the negative consequences of the impacts of human interventions on hydrology. The findings in this study advance the knowledge on the impacts of HI on both hydrological extremes which in turn can aid policy makers and water managers in making sustainable and successful risk reduction strategies.

# References

Adam, J. C. & Lettenmaier, D. P. (2003), 'Adjustment of global gridded precipitation for systematic bias', *Journal of Geophysical Research: Atmospheres* **108**(D9).

Alcamo, J., Döll, P., Henrichs, T., Kaspar, F., Lehner, B., Rösch, T. & Siebert, S. (2003), 'Development and testing of the WaterGAP 2 global model of water use and availability', *Hydrological Sciences Journal* **48**(3), 317–337.

Alcamo, J., Döll, P., Kaspar, F. & Siebert, S. (1997), 'Global change and global scenarios of water use and availability: an application of WaterGAP 1.0', *Center for Environmental Systems Research (CESR), University of Kassel, Germany* **1720**.

Alfieri, L., Salamon, P., Bianchi, A., Neal, J., Bates, P. & Feyen, L. (2014), 'Advances in pan-European flood hazard mapping', *Hydrological Processes* **28**(13), 4067–4077.

Allen, R. G., Pereira, L. S., Raes, D., Smith, M. et al. (1998), 'Crop evapotranspiration-Guidelines for computing crop water requirements-FAO Irrigation and drainage paper 56', *FAO, Rome* **300**(9), D05109.

Arnell, N. W. (1999), 'Climate change and global water resources', *Global environmental change* **9**, S31–S49.

Biemans, H., Haddeland, I., Kabat, P., Ludwig, F., Hutjes, R., Heinke, J., Von Bloh, W. & Gerten, D. (2011), 'Impact of reservoirs on river discharge and irrigation water supply during the 20th century', *Water Resources Research* **47**(3).

Biemans, H., Hutjes, R., Kabat, P., Strengers, B., Gerten, D. & Rost, S. (2009), 'Effects of precipitation uncertainty on discharge calculations for main river basins', *Journal of Hydrometeorology* **10**(4), 1011–1025.

Bierkens, M. F. (2015), 'Global hydrology 2015: State, trends, and directions', *Water Resources Research* **51**(7), 4923–4947.

Blauhut, V., Gudmundsson, L. & Stahl, K. (2015), 'Towards pan-European drought risk maps: quantifying the link between drought indices and reported drought impacts', *Environmental Research Letters* **10**(1), 014008.

Blyth, E. (2001), 'Relative influence of vertical and horizontal processes in large-scale water and energy balance modelling', *IAHS-AISH PUBL.* (270), 3–10.

Chow, V. T. (1956), 'Hydrologic studies of floods in the United States', *International Association of Scientific Hydrology* **42**, 134–170.

Compo, G. P., Whitaker, J. S., Sardeshmukh, P. D., Matsui, N., Allan, R. J., Yin, X., Gleason, B. E., Vose, R. S., Rutledge, G., Bessemoulin, P. et al. (2011), 'The twentieth century reanalysis project', *Quarterly Journal of the Royal Meteorological Society* **137**(654), 1–28.

Cox, S. J., Stackhouse Jr, P. W., Gupta, S. K., Mikovitz, J. C. & Zhang, T. (2017), NASA/GEWEX shortwave surface radiation budget: Integrated data product with reprocessed radiance, cloud, and meteorology inputs, and new surface albedo treatment, *in* 'AIP Conference Proceedings', Vol. 1810, AIP Publishing, p. 090001.

De Graaf, I., Van Beek, L., Wada, Y. & Bierkens, M. (2014), 'Dynamic attribution of global water demand to surface water and groundwater resources: Effects of abstractions and return flows on river discharges', *Advances in water resources* **64**, 21–33.

Dee, D. P., Uppala, S. M., Simmons, A. J., Berrisford, P., Poli, P., Kobayashi, S., Andrae, U., Balmaseda, M. A., Balsamo, G., Bauer, P., Bechtold, P., Beljaars, A. C. M., van de Berg, L., Bidlot, J., Bormann, N., Delsol, C., Dragani, R., Fuentes, M., Geer, A. J., Haimberger, L., Healy, S. B., Hersbach, H., Hólm, E. V., Isaksen, L., Kållberg, P., Köhler, M., Matricardi, M., McNally, A. P., Monge-Sanz, B. M., Morcrette, J.-J., Park, B.-K., Peubey, C., de Rosnay, P., Tavolato, C., Thépaut, J.-N. & Vitart, F. (2011), 'The ERA-Interim reanalysis: configuration and performance of the data assimilation system', *Quarterly Journal of the Royal Meteorological Society* **137**(656), 553–597.

Di Baldassarre, G., Martinez, F., Kalantari, Z. & Viglione, A. (2017), 'Drought and flood in the Anthropocene: feedback mechanisms in reservoir operation', *Earth System Dynamics* **8**(1), 225.

Di Baldassarre, G., Viglione, A., Carr, G., Kuil, L., Salinas, J. & Blöschl, G. (2013), 'Socio-hydrology: conceptualising human-flood interactions', *Hydrology and Earth System Sciences* **17**(8), 3295.

Dirmeyer, P. A., Dolman, A. & Sato, N. (1999), 'The pilot phase of the global soil wetness project', *Bulletin of the American Meteorological Society* **80**(5), 851–878.

Dirmeyer, P. A., Gao, X., Zhao, M., Guo, Z., Oki, T. & Hanasaki, N. (2006), 'GSWP-2: Multimodel analysis and implications for our perception of the land surface', *Bulletin of the American Meteorological Society* **87**(10), 1381–1397.

Döll, P., Fiedler, K. & Zhang, J. (2009), 'Global-scale analysis of river flow alterations due to water withdrawals and reservoirs', *Hydrology and Earth System Sciences* **13**(12), 2413.

Doorenbos, J. & Pruitt, W. (1977), 'FAO Irrigation and drainage Paper 24: crop water requirements', *FAO, Roma* **156**.

EEA, O. (2007), 'Europe's environment – The fourth assessment', *European Environment Agency (EEA), Office for Official Publications of the European Communities (OPOCE), Copenhagen, Denmark* .

EEA, O. (2009), 'Water resources across Europe—confronting water scarcity and drought (EEA Report No. 2/2009)', *European Environment Agency (EEA), Office for Official Publications of the European Communities (OPOCE), Copenhagen, Denmark* .

EEA, O. (2017), 'Climate change, impacts and vulnerability in Europe 2016 (EEA Report No. 1/2017)', *European Environment Agency (EEA), Office for Official Publications of the European Communities (OPOCE), Copenhagen, Denmark* .

European Commission (2012), 'Communication from the commission to the European Parlament, the Council, the European Economic and Social Commitee of the Regions: A Blueprint to Safeguard Europe's Water Resources'. [Online; accessed March 1st, 2018].
**URL:** *http://eur-lex.europa.eu/LexUriServ/LexUriServ.do?uri=COM:2012:0673:FIN:EN:PDF*

Fleig, A., Andreassen, L., Barfod, E., Haga, J., Haugen, L., Hisdal, H., Melvold, K. & Saloranta, T. (2013), 'Norwegian Hydrological Reference Dataset for climate change studies', *NVE Report* pp. 2–2013.

Food and Agriculture Organization of the United Nations (2012), 'FAOSTAT statistics database'. Database URL: `http://www.fao.org/faostat/en/#home`.

Forzieri, G., Feyen, L., Rojas, R., Flörke, M., Wimmer, F. & Bianchi, A. (2014), 'Ensemble projections of future streamflow droughts in Europe', *Hydrology and Earth System Sciences* **18**(1), 85.

Gao, Y., Vogel, R. M., Kroll, C. N., Poff, N. L. & Olden, J. D. (2009), 'Development of representative indicators of hydrologic alteration', *Journal of Hydrology* **374**(1-2), 136–147.

Gesch, D. B., Verdin, K. L. & Greenlee, S. K. (1999), 'New land surface digital elevation model covers the Earth', *EOS, Transactions American Geophysical Union* **80**(6), 69–70.

Gleick, P. H. (1993), 'Water in crisis: a guide to the worlds fresh water resources.'.

Gosling, S. N. & Arnell, N. W. (2016), 'A global assessment of the impact of climate change on water scarcity', *Climatic Change* **134**(3), 371–385.

Gosling, S. N., Zaherpour, J., Mount, N. J., Hattermann, F. F., Dankers, R., Arheimer, B., Breuer, L., Ding, J., Haddeland, I., Kumar, R. et al. (2017), 'A comparison of changes in river runoff from multiple global and catchment-scale hydrological models under global warming scenarios of 1 C, 2 C and 3 C', *Climatic Change* **141**(3), 577–595.

GRDC: The Global Runoff Data Centre (data retrieved 2014), 'The Global Runoff Database and river discharge data'. Database URL: `http://www.bafg.de/GRDC`.

Gudmundsson, L., Tallaksen, L. M., Stahl, K., Clark, D. B., Dumont, E., Hagemann, S., Bertrand, N., Gerten, D., Heinke, J., Hanasaki, N. et al. (2012), 'Comparing large-scale hydrological model simulations to observed runoff percentiles in Europe', *Journal of Hydrometeorology* **13**(2), 604–620.

Haddeland, I., Clark, D. B., Franssen, W., Ludwig, F., Voß, F., Arnell, N. W., Bertrand, N., Best, M., Folwell, S., Gerten, D. et al. (2011), 'Multimodel estimate of the global terrestrial water balance: setup and first results', *Journal of Hydrometeorology* **12**(5), 869–884.

Haddeland, I., Heinke, J., Biemans, H., Eisner, S., Flörke, M., Hanasaki, N., Konzmann, M., Ludwig, F., Masaki, Y., Schewe, J. et al. (2014), 'Global water resources affected by human interventions and climate change', *Proceedings of the National Academy of Sciences* **111**(9), 3251–3256.

Hagemann, S. (2002), 'An improved land surface parameter dataset for global and regional climate models'.

Hagemann, S., Botzet, M., Dümenil, L. & Machenhauer, B. (1999), 'Derivation of global GCM boundary conditions from 1 km land use satellite data', *MPI Report* **289**, 34.

Hagemann, S., Chen, C., Clark, D., Folwell, S., Gosling, S. N., Haddeland, I., Hannasaki, N., Heinke, J., Ludwig, F., Voss, F. et al. (2013), 'Climate change impact on available water resources obtained using multiple global climate and hydrology models', *Earth System Dynamics* **4**, 129–144.

Hall, J., Arheimer, B., Borga, M., Brázdil, R., Claps, P., Kiss, A., Kjeldsen, T., Kriauciuniene, J., Kundzewicz, Z., Lang, M. et al. (2014), 'Understanding flood regime changes in Europe: A state of the art assessment', *Hydrology and Earth System Sciences* **18**(7), 2735–2772.

Hamon, W. R. (1960), Estimating potential evapotranspiration, PhD thesis, Massachusetts Institute of Technology.

Hanasaki, N., Kanae, S. & Oki, T. (2006), 'A reservoir operation scheme for global river routing models', *Journal of Hydrology* **327**(1-2), 22–41.

Hanasaki, N., Kanae, S., Oki, T., Masuda, K., Motoya, K., Shirakawa, N., Shen, Y. & Tanaka, K. (2008), 'An integrated model for the assessment of global water resources–Part 1: Model description and input meteorological forcing', *Hydrology and Earth System Sciences* **12**(4), 1007–1025.

Harding, R., Best, M., Blyth, E., Hagemann, S., Kabat, P., Tallaksen, L. M., Warnaars, T., Wiberg, D., Weedon, G. P., Lanen, H. v. et al. (2011a), 'WATCH: Current knowledge of the terrestrial global water cycle', *Journal of Hydrometeorology* **12**(6), 1149–1156.

Harding, R. & Blyth, E. (2009), Current knowledge of the terrestrial Global water Cycle-past and future, *in* 'EGU General Assembly Conference Abstracts', Vol. 11, p. 4567.

Harding, R., Warnaars, T., Weedon, G., Wiberg, D., Hagemann, S., Tallaksen, L., van Lanen, H., Blyth, E., Ludwig, F. & Kabat, P. (2011b), Executive summary of the completed WATCH Project, Technical report, European Commission.

Harris, I., Jones, P., Osborn, T. & Lister, D. (2014), 'Updated high-resolution grids of monthly climatic observations–the CRU TS3. 10 Dataset', *International Journal of Climatology* **34**(3), 623–642.

He, X., Wada, Y., Wanders, N. & Sheffield, J. (2017), 'Intensification of hydrological drought in California by human water management', *Geophysical Research Letters* **44**(4), 1777–1785.

Hirabayashi, Y., Kanae, S., Motoya, K., Masuda, K. & Döll, P. (2008), 'A 59-year (1948-2006) global meteorological forcing data set for land surface models. Part II: Global snowfall estimation', *Hydrological Research Letters* **2**, 65–69.

IPCC (2013), *Summary for Policymakers*, Cambridge University Press, Cambridge, United Kingdom and New York, NY, USA, book section SPM, p. 1–30.
**URL:** *www.climatechange2013.org*

Kalnay, E., Kanamitsu, M., Kistler, R., Collins, W., Deaven, D., Gandin, L., Iredell, M., Saha, S., White, G., Woollen, J. et al. (1996), 'The NCEP/NCAR 40-year reanalysis project', *Bulletin of the American meteorological Society* **77**(3), 437–471.

Kim, H. (2014), 'Global Soil Wetness Project Phase 3'.
**URL:** *http://hydro.iis.u-tokyo.ac.jp/GSWP3/index.html*

Kistler, R., Collins, W., Saha, S., White, G., Woollen, J., Kalnay, E., Chelliah, M., Ebisuzaki, W., Kanamitsu, M., Kousky, V. et al. (2001), 'The NCEP–NCAR 50–year reanalysis: Monthly means CD–ROM and documentation', *Bulletin of the American Meteorological society* **82**(2), 247–267.

Köppen, W. (1900), 'Versuch einer Klassifikation der Klimate, vorzugsweise nach ihren Beziehungen zur Pflanzenwelt', *Geographische Zeitschrift* **6**(11. H), 593–611.

Kottek, M., Grieser, J., Beck, C., Rudolf, B. & Rubel, F. (2006), 'World map of the Köppen-Geiger climate classification updated', *Meteorologische Zeitschrift* **15**(3), 259–263.

Kovats, R., Valentini, R., Bouwer, L. M., Georgopoulou, E., Jacob, D., Martin, E., Rounsevell, M. & Soussana, J.-F. (2014), *Europe*, Cambridge University Press, Cambridge, United Kingdom and New York, NY, USA, pp. 1267–1326.

Krasovskaia, I., Arnell, N. & Gottschalk, L. (1994), 'Flow regimes in northern and western Europe: development and application of procedures for classifying flow regimes', *IAHS Publications-Series of Proceedings and Reports-Intern Assoc Hydrological Sciences* **221**, 185–192.

Kundzewicz, Z. W. (2003), 'Water and Climate–The IPCC TAR Perspective: Paper presented at the Nordic Hydrological Conference (Røros, Norway 4-7 August 2002)', *Hydrology Research* **34**(5), 387–398.

Kundzewicz, Z. W. & Kaczmarek, Z. (2000), 'Coping with hydrological extremes', *Water International* **25**(1), 66–75.

Lehner, B. & Döll, P. (2004), 'Development and validation of a global database of lakes, reservoirs and wetlands', *Journal of Hydrology* **296**(1-4), 1–22.

Lehner, B., Liermann, C. R., Revenga, C., Vörösmarty, C., Fekete, B., Crouzet, P., Döll, P., Endejan, M., Frenken, K., Magome, J. et al. (2011), 'High-resolution mapping of the world's reservoirs and dams for sustainable river-flow management', *Frontiers in Ecology and the Environment* **9**(9), 494–502.

Lehner, B., Verdin, K. & Jarvis, A. (2008), 'New global hydrography derived from spaceborne elevation data', *Eos, Transactions American Geophysical Union* **89**(10), 93–94.

Loon, A. & Lanen, H. (2013), 'Making the distinction between water scarcity and drought using an observation-modeling framework', *Water Resources Research* **49**(3), 1483–1502.

Loveland, T. R., Reed, B. C., Brown, J. F., Ohlen, D. O., Zhu, Z., Yang, L. & Merchant, J. W. (2000), 'Development of a global land cover characteristics database and IGBP DISCover from 1 km AVHRR data', *International Journal of Remote Sensing* **21**(6-7), 1303–1330.

Maisch, M. (2000), 'The long-term signal of climate change in the Swiss Alps: Glacier retreat since the end of the Little Ice Age and future ice decay scenarios', *Geogr. Fis. Dinam. Quat* **23**, 139–151.

McDonald, R. I., Weber, K., Padowski, J., Flörke, M., Schneider, C., Green, P. A., Gleeson, T., Eckman, S., Lehner, B., Balk, D. et al. (2014), 'Water on an urban planet: Urbanization and the reach of urban water infrastructure', *Global Environmental Change* **27**, 96–105.

McKay, S. K. & Fischenich, J. C. (2016), Development and application of flow duration curves for stream restoration, Technical report, US Army Engineer Research and Development Center (ERDC) Vicksburg United States.

Metzger, M. J., Bunce, R. G. H., Jongman, R. H., Mücher, C. & Watkins, J. W. (2005), 'A climatic stratification of the environment of Europe', *Global ecology and biogeography* **14**(6), 549–563.

Milly, P. C. D., Wetherald, R. T., Dunne, K. & Delworth, T. L. (2002), 'Increasing risk of great floods in a changing climate', *Nature* **415**(6871), 514.

Mitchell, T. D. & Jones, P. D. (2005), 'An improved method of constructing a database of monthly climate observations and associated high-resolution grids', *International journal of climatology* **25**(6), 693–712.

Montanari, A., Young, G., Savenije, H., Hughes, D., Wagener, T., Ren, L., Koutsoyiannis, D., Cudennec, C., Toth, E., Grimaldi, S. et al. (2013), '"Panta Rhei—everything flows": change in hydrology and society—the IAHS scientific decade 2013–2022', *Hydrological Sciences Journal* **58**(6), 1256–1275.

Müller Schmied, H., Adam, L., Eisner, S., Fink, G., Flörke, M., Kim, H., Oki, T., Portmann, F. T., Reinecke, R., Riedel, C. et al. (2016), 'Variations of global and continental water balance components as impacted by climate forcing uncertainty and human water use', *Hydrology and Earth System Sciences* **20**(7), 2877–2898.

Müller Schmied, H., Eisner, S., Franz, D., Wattenbach, M., Portmann, F. T., Flörke, M. & Döll, P. (2014), 'Sensitivity of simulated global-scale freshwater fluxes and storages to input data, hydrological model structure, human water use and calibration', *Hydrology and Earth System Sciences* **18**(9), 3511–3538.

Mulligan, D., Bouraoui, F., Grizzetti, B., Aloe, A. & Dusart, J. (2006), An atlas of pan-European data for investigating the fate of agrochemicals in terrestrial ecosystems, Technical report, Institute for Environment and Sustainability, Rural, Water and Ecosystem Resources Unit, European Commision, Joint Research Centre.

Nasonova, O. & Gusev, E. (2008), 'Investigating the ability of a land surface model to reproduce river runoff with the accuracy of hydrological models', *Water Resources* **35**(5), 493–501.

Oki, T. & Kanae, S. (2006), 'Global hydrological cycles and world water resources', *science* **313**(5790), 1068–1072.

Olson, J. (1994*a*), Global ecosystem framework-definitions: USGS EROS, Technical report, Data Center Internal Report, Sioux Falls, SD.

Olson, J. (1994*b*), 'Global ecosystem framework-translation strategy', *USGS EROS Data Center Internal Report, Sioux Falls, SD* **39**, 1994.

Portmann, F. T., Siebert, S. & Döll, P. (2010), 'MIRCA2000—Global monthly irrigated and rainfed crop areas around the year 2000: A new high-resolution data set for agricultural and hydrological modeling', *Global Biogeochemical Cycles* **24**(1).

Prudhomme, C., Giuntoli, I., Robinson, E. L., Clark, D. B., Arnell, N. W., Dankers, R., Fekete, B. M., Franssen, W., Gerten, D., Gosling, S. N. et al. (2014), 'Hydrological droughts in the 21st century, hotspots and uncertainties from a global multimodel

ensemble experiment', *Proceedings of the National Academy of Sciences* **111**(9), 3262–3267.

Prudhomme, C., Parry, S., Hannaford, J., Clark, D. B., Hagemann, S. & Voss, F. (2011), 'How well do large-scale models reproduce regional hydrological extremes in Europe?', *Journal of Hydrometeorology* **12**(6), 1181–1204.

Remo, J. W., Carlson, M. & Pinter, N. (2012), 'Hydraulic and flood-loss modeling of levee, floodplain, and river management strategies, Middle Mississippi River, USA', *Natural hazards* **61**(2), 551–575.

Rizzi, J., Nilsen, I. B., Stagge, J. H., Gisnås, K. & Tallaksen, L. M. (2017), 'Five decades of warming: impacts on snow cover in Norway', *Hydrology Research* p. nh2017051.

Rojas, R., Feyen, L., Bianchi, A. & Dosio, A. (2012), 'Assessment of future flood hazard in Europe using a large ensemble of bias-corrected regional climate simulations', *Journal of Geophysical Research: Atmospheres* **117**(D17).

Rosenzweig, C., Arnell, N. W., Ebi, K. L., Lotze-Campen, H., Raes, F., Rapley, C., Smith, M. S., Cramer, W., Frieler, K., Reyer, C. P. et al. (2017), 'Assessing inter-sectoral climate change risks: the role of ISIMIP', *Environmental Research Letters* **12**(1), 010301.

Savenije, H. H., Hoekstra, A. Y. & van der Zaag, P. (2014), 'Evolving water science in the Anthropocene', *Hydrology and earth system sciences* **18**(1), 319–332.

Schneider, U., Becker, A., Finger, P., Meyer-Christoffer, A., Rudolf, B. & Ziese, M. (2011a), 'GPCC Monitoring Product: Near Real-Time Monthly Land-Surface Precipitation from Rain-Gauges based on SYNOP and CLIMAT data'.

Schneider, U., Becker, A., Finger, P., Meyer-Christoffer, A., Rudolf, B. & Ziese, M. (2011b), 'GPCC Full Data Reanalysis Version 6.0 at 0.5°: Monthly Land-Surface Precipitation from Rain-Gauges built on GTS-based and Historic Data'.

Sheffield, J., Goteti, G. & Wood, E. F. (2006), 'Development of a 50-year high-resolution global dataset of meteorological forcings for land surface modeling', *Journal of Climate* **19**(13), 3088–3111.

Siebert, S., Burke, J., Faures, J.-M., Frenken, K., Hoogeveen, J., Döll, P. & Portmann, F. T. (2010), 'Groundwater use for irrigation–a global inventory', *Hydrology and Earth System Sciences* **14**(10), 1863–1880.

Siebert, S. & Döll, P. (2010), 'Quantifying blue and green virtual water contents in global crop production as well as potential production losses without irrigation', *Journal of Hydrology* **384**(3-4), 198–217.

Smith, K. & Ward, R. (1998), *Floods: physical processes and human impacts*, John Wiley and Sons Ltd.

Sood, A. & Smakhtin, V. (2015), 'Global hydrological models: a review', *Hydrological sciences journal* **60**(4), 549–565.

Stagge, J. H., Kingston, D. G., Tallaksen, L. M. & Hannah, D. M. (2017), 'Observed drought indices show increasing divergence across Europe', *Scientific Reports* **7**(1), 14045.

Stahl, K., Tallaksen, L. M., Hannaford, J. & Van Lanen, H. (2012), 'Filling the white space on maps of European runoff trends: estimates from a multi-model ensemble', *Hydrology and Earth System Sciences* **16**(7), 2035–2047.

Steffen, W., Grinevald, J., Crutzen, P. & McNeill, J. (2011), 'The Anthropocene: conceptual and historical perspectives', *Philosophical Transactions of the Royal Society of London A: Mathematical, Physical and Engineering Sciences* **369**(1938), 842–867.

Sutanudjaja, E. H., Van Beek, L., Drost, N., de Graaf, I., De Jong, K., Peßenteiner, S., Straatsma, M., Wada, Y., Wanders, N., Wisser, D. et al. (2017), 'PCR-GLOBWB 2.0: a 5 arc-minute global hydrological and water resources model', *Geoscientific Model Development Discussions* .

Tallaksen, L. M. & Stahl, K. (2014), 'Spatial and temporal patterns of large-scale droughts in Europe: Model dispersion and performance', *Geophysical Research Letters* **41**(2), 429–434.

Tallaksen, L. M. & Van Lanen, H. A. (2004), *Hydrological drought: processes and estimation methods for streamflow and groundwater*, Vol. 48, Elsevier.

Thirel, G., Andréassian, V. & Perrin, C. (2015), 'On the need to test hydrological models under changing conditions'.

Uppala, S. M., Kållberg, P., Simmons, A., Andrae, U., Bechtold, V. d., Fiorino, M., Gibson, J., Haseler, J., Hernandez, A., Kelly, G. et al. (2005), 'The ERA-40 re-analysis', *Quarterly Journal of the royal meteorological society* **131**(612), 2961–3012.

USGS EROS Data Center (2006), 'HYDRO1k Elevation Derivative Database'. Database URL: `http://edcdaac.usgs.gov/gtopo30/hydro/`.

Van Alphen, J., Martini, F., Loat, R., Slomp, R. & Passchier, R. (2009), 'Flood risk mapping in Europe, experiences and best practices', *Journal of Flood Risk Management* **2**(4), 285–292.

Van Beek, L. & Bierkens, M. F. (2009), 'The global hydrological model PCR-GLOBWB: conceptualization, parameterization and verification', *Utrecht University, Utrecht, The Netherlands* .

Van Beek, L., Wada, Y. & Bierkens, M. F. (2011), 'Global monthly water stress: 1. Water balance and water availability', *Water Resources Research* **47**(7).

Van Der Knijff, J., Younis, J. & De Roo, A. (2010), 'LISFLOOD: a GIS-based distributed model for river basin scale water balance and flood simulation', *International Journal of Geographical Information Science* **24**(2), 189–212.

Van Loon, A. F., Gleeson, T., Clark, J., Van Dijk, A. I., Stahl, K., Hannaford, J., Di Baldassarre, G., Teuling, A. J., Tallaksen, L. M., Uijlenhoet, R. et al. (2016), 'Drought in the Anthropocene', *Nature Geoscience* **9**(2), 89.

van Vliet, M. T., Franssen, W. H., Yearsley, J. R., Ludwig, F., Haddeland, I., Lettenmaier, D. P. & Kabat, P. (2013), 'Global river discharge and water temperature under climate change', *Global Environmental Change* **23**(2), 450–464.

Veldkamp, T. I. E., Zhao, F., Ward, P. J., de Moel, H., Aerts, J. C., Schmied, H. M., Portmann, F. T., Masaki, Y., Pokhrel, Y. N., Liu, X. et al. (2018), 'Human impact parameterizations in global hydrological models improves estimates of monthly discharges and hydrological extremes: a multi-model validation study', *Environmental Research Letters* .

Veldkamp, T. I., Wada, Y., de Moel, H., Kummu, M., Eisner, S., Aerts, J. C. & Ward, P. J. (2015), 'Changing mechanism of global water scarcity events: Impacts of socioeconomic changes and inter-annual hydro-climatic variability', *Global Environmental Change* **32**, 18–29.

Veldkamp, T., Wada, Y., Aerts, J., Döll, P., Gosling, S., Liu, J., Masaki, Y., Oki, T., Ostberg, S., Pokhrel, Y. et al. (2017), 'Water scarcity hotspots travel downstream due to human interventions in the 20th and 21st century', *Nature communications* **8**, 15697.

Verdin, K. L. & Greenlee, S. (1996), Development of continental scale digital elevation models and extraction of hydrographic features, *in* 'Proceedings, third international conference/workshop on integrating GIS and environmental modeling, Santa Fe, New Mexico', pp. 21–26.

Verzano, K., Bärlund, I., Flörke, M., Lehner, B., Kynast, E., Voß, F. & Alcamo, J. (2012), 'Modeling variable river flow velocity on continental scale: Current situation and climate change impacts in Europe', *Journal of hydrology* **424**, 238–251.

Vogel, R. M., Sieber, J., Archfield, S. A., Smith, M. P., Apse, C. D. & Huber-Lee, A. (2007), 'Relations among storage, yield, and instream flow', *Water Resources Research* **43**(5).

Vörösmarty, C. J., Federer, C. A. & Schloss, A. L. (1998), 'Potential evaporation functions compared on US watersheds: Possible implications for global-scale water balance and terrestrial ecosystem modeling', *Journal of Hydrology* **207**(3-4), 147–169.

Vörösmarty, C. J., Meybeck, M., Fekete, B., Sharma, K., Green, P. & Syvitski, J. P. (2003), 'Anthropogenic sediment retention: major global impact from registered river impoundments', *Global and planetary change* **39**(1-2), 169–190.

Wada, Y., Bierkens, M. F., De Roo, A., Dirmeyer, P. A., Famiglietti, J. S., Hanasaki, N., Konar, M., Liu, J., Schmied, H. M., Oki, T. et al. (2017), 'Human–water interface in hydrological modelling: current status and future directions', *Hydrology and Earth System Sciences* **21**(8), 4169.

Wada, Y., Van Beek, L. & Bierkens, M. F. (2011a), 'Modelling global water stress of the recent past: on the relative importance of trends in water demand and climate variability', *Hydrology and Earth System Sciences* **15**(12), 3785–3805.

Wada, Y., Van Beek, L. P., Wanders, N. & Bierkens, M. F. (2013), 'Human water consumption intensifies hydrological drought worldwide', *Environmental Research Letters* **8**(3), 034036.

Wada, Y., Van Beek, L., Viviroli, D., Dürr, H. H., Weingartner, R. & Bierkens, M. F. (2011b), 'Global monthly water stress: 2. Water demand and severity of water stress', *Water Resources Research* **47**(7).

Wada, Y., Wisser, D. & Bierkens, M. (2014), 'Global modeling of withdrawal, allocation and consumptive use of surface water and groundwater resources', *Earth System Dynamics* **5**(1), 15.

Wanders, N. & Wada, Y. (2015), 'Human and climate impacts on the 21st century hydrological drought', *Journal of Hydrology* **526**, 208–220.

Wanders, N., Wada, Y. & Van Lanen, H. (2015), 'Global hydrological droughts in the 21st century under a changing hydrological regime', *Earth System Dynamics* **6**(1), 1.

Ward, P. J., Jongman, B., Aerts, J. C., Bates, P. D., Botzen, W. J., Loaiza, A. D., Hallegatte, S., Kind, J. M., Kwadijk, J., Scussolini, P. et al. (2017), 'A global framework for future costs and benefits of river-flood protection in urban areas', *Nature climate change* **7**(9), 642.

Warszawski, L., Frieler, K., Huber, V., Piontek, F., Serdeczny, O. & Schewe, J. (2014), 'The inter-sectoral impact model intercomparison project (ISI–MIP): project framework', *Proceedings of the National Academy of Sciences* **111**(9), 3228–3232.

Weedon, G., Gomes, S., Viterbo, P., Shuttleworth, W., Blyth, E., Østerle, H., Adam, J., Bellouin, N., Boucher, O. & Best, M. (2011), 'Creation of the WATCH forcing data and its use to assess global and regional reference crop evaporation over land during the twentieth century', *Journal of Hydrometeorology* **12**(5), 823–848.

Weedon, G., Gomes, S., Viterbo, P., Österle, H., Adam, J., Bellouin, N., Boucher, O. & Best, M. (2010), The WATCH forcing data 1958-2001: A meteorological forcing dataset for land surface- and hydrological models, Technical report, WATCH technical report.

Weedon, G. P., Balsamo, G., Bellouin, N., Gomes, S., Best, M. J. & Viterbo, P. (2014), 'The WFDEI meteorological forcing data set: WATCH Forcing Data methodology applied to ERA-Interim reanalysis data', *Water Resources Research* **50**(9), 7505–7514.

WFD (2000), 'Water Framework Directive'. Directive 2000/60/EC of the European Parliament and the Council of the European Union.

Winsemius, H. C., Aerts, J. C., van Beek, L. P., Bierkens, M. F., Bouwman, A., Jongman, B., Kwadijk, J. C., Ligtvoet, W., Lucas, P. L., van Vuuren, D. P. et al. (2016), 'Global drivers of future river flood risk', *Nature Climate Change* **6**(4), 381.

Wisser, D., Fekete, B. M., Vörösmarty, C. & Schumann, A. (2010), 'Reconstructing 20th century global hydrography: a contribution to the Global Terrestrial Network-Hydrology (GTN-H)', *Hydrology and Earth System Sciences* **14**(1), 1.

(WMO), W. M. O. (2009), 'Manual on low flow estimation and prediction'.

Wood, E. F., Roundy, J. K., Troy, T. J., Van Beek, L., Bierkens, M. F., Blyth, E., de Roo, A., Döll, P., Ek, M., Famiglietti, J. et al. (2011), 'Hyperresolution global land surface modeling: Meeting a grand challenge for monitoring Earth's terrestrial water', *Water Resources Research* **47**(5).

# Appendix A Mean Precipitation and Temperature by WFDEI Forcing Data

Appendix A includes Figure 27 that shows mean annual precipitation and Figure 28 that shows mean temperature in the period 1901–2001. The data stems from the WFDEI forcing data.

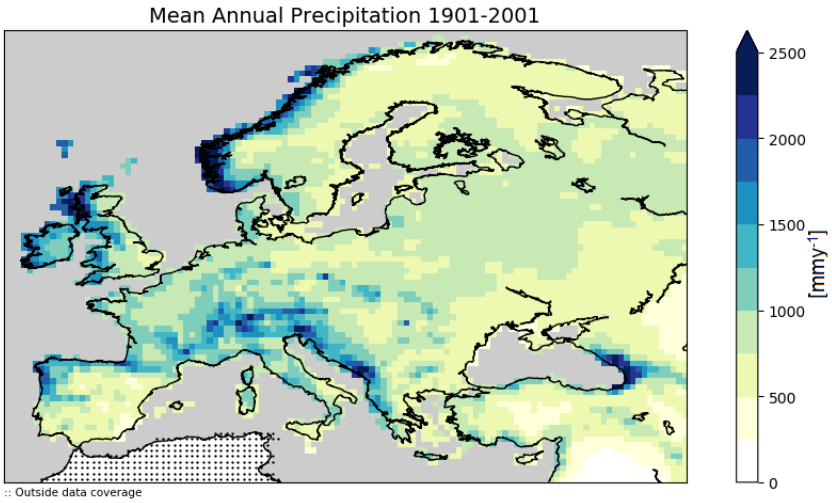


**Figure 27:** Mean annual precipitation in the period 1901-2001 by WFDEI forcing data.

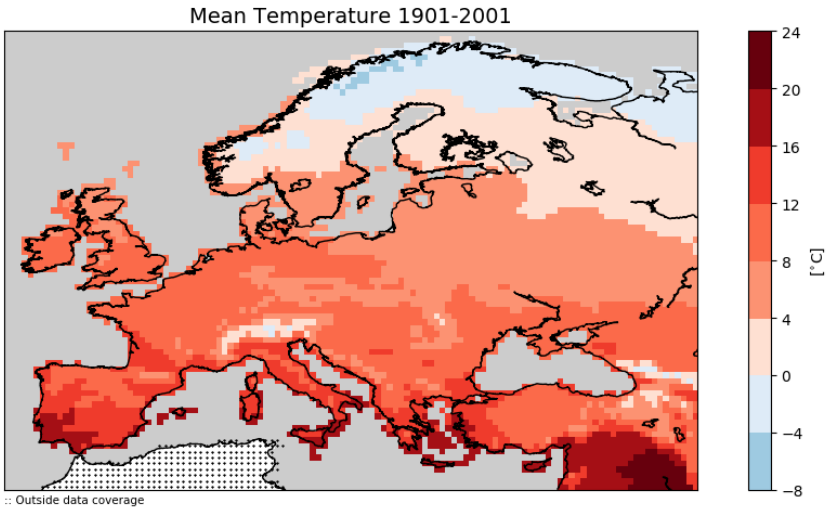


**Figure 28:** Mean temperature in the period 1901-2001 by WFDEI forcing data.

# Appendix B Regional Time Series of Precipitation and Temperature by Four Forcing Data Sets

Appendix B includes Figure 29 that shows regional time series of precipitation and temperature by the four forcing data sets used in the study; GSWP3, PGMFDv2, WFD and WFDEI.

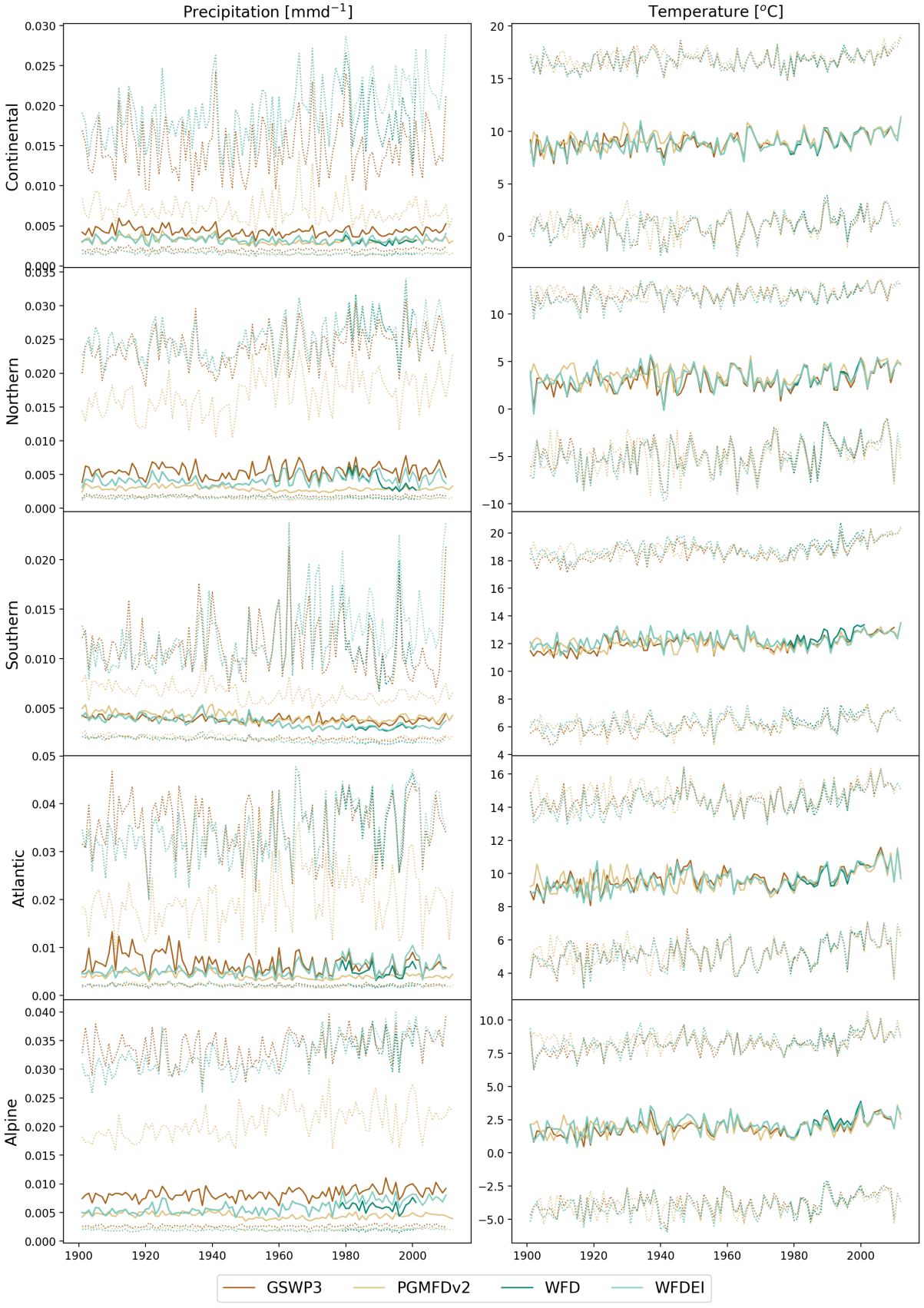


**Figure 29:** Regional annual medians of $1^{st}$, $2^{nd}$ and $3^{rd}$ quartile of precipitation (left) and temperature (right) derived from the four forcing data sets GSWP3, PGMFDv2, WFD and WFDEI.

# Appendix C Human Impacts on Regional Low, Mid and High Flow; Results by All Forcing Data Sets

Appendix C includes Figure 30–41 that provide the results by all four forcing data sets (GSWP3, PGMFDv2, WFD and WFDEI) and all three model scenarios (no human interventions, transient human intervention and current human interventions) of the runoff time series of regional median $10^{th}$, $50^{th}$ and $90^{th}$ percentiles, representing low flow, mid flow and high flow, respectively. The y-axis is fixed for the results by all forcing data sets for the same region and percentile, to easily compare the differences in results by the different forcing data sets. The y-axis increment is fixed for all regions for each percentile, to easily compare differences between model scenarios for the different regions.

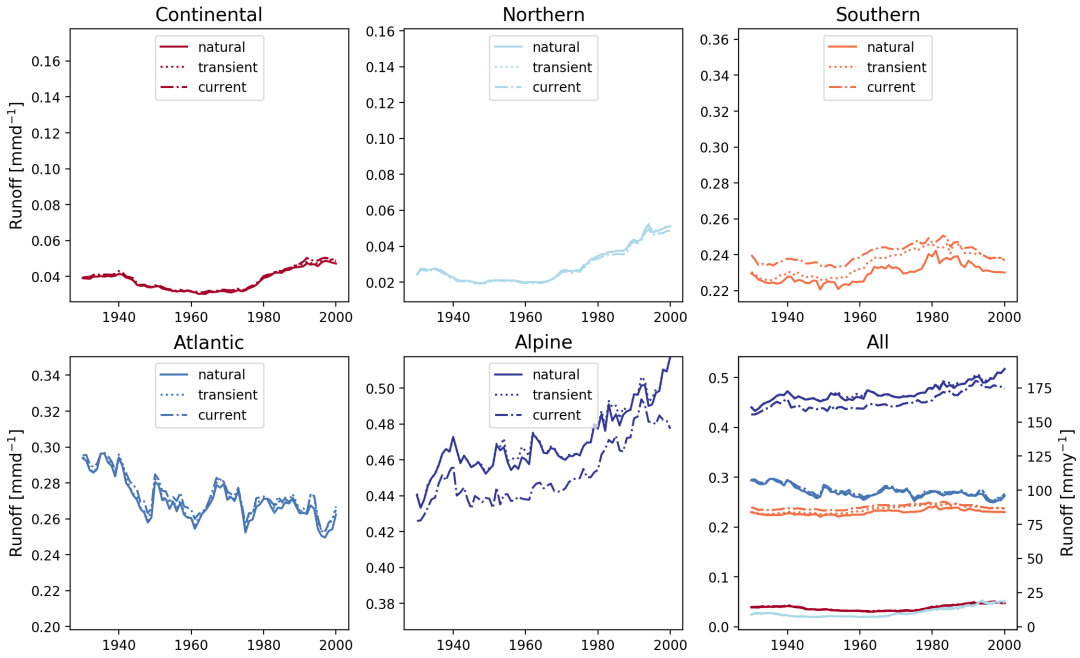


**Figure 30:** Regional median 30-years moving $10^{th}$ percentile runoff (i.e. low flow) for five climate regions in Europe over the period 1901–2001 using GSWP3 forcing data and three model scenarios; no human interventions, transient human interventions and current human interventions. The lower right plot shows all regions' results together.

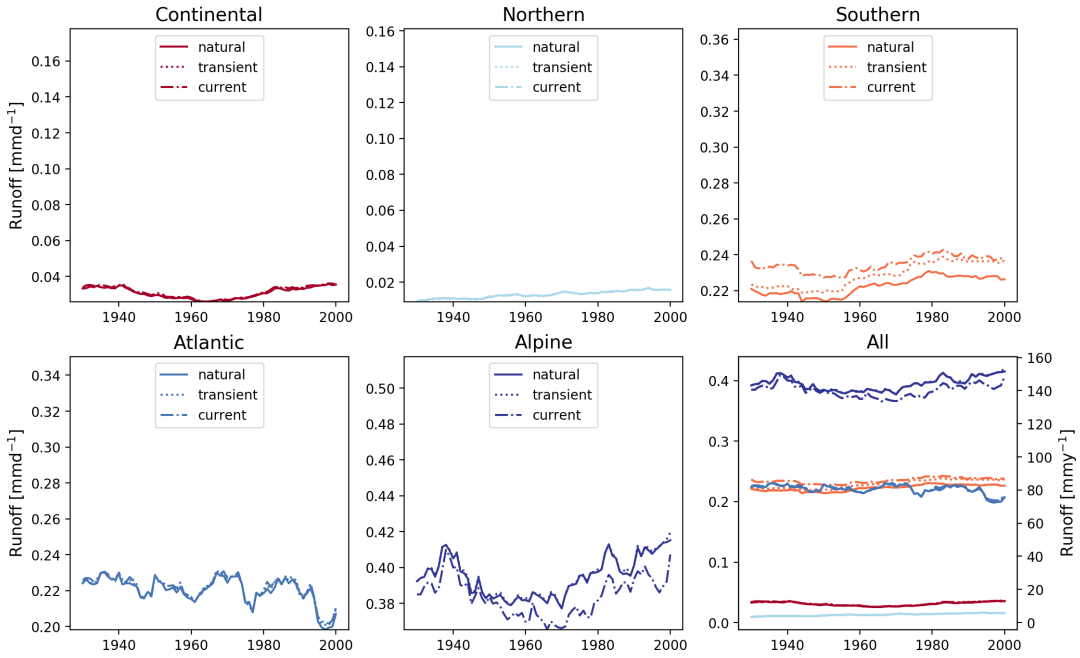


**Figure 31:** Regional median 30-years moving $10^{th}$ percentile runoff (i.e. low flow) for five climate regions in Europe over the period 1901–2001 using PGMFDv2 forcing data and three model scenarios; no human interventions, transient human interventions and current human interventions. The lower right plot shows all regions' results together.

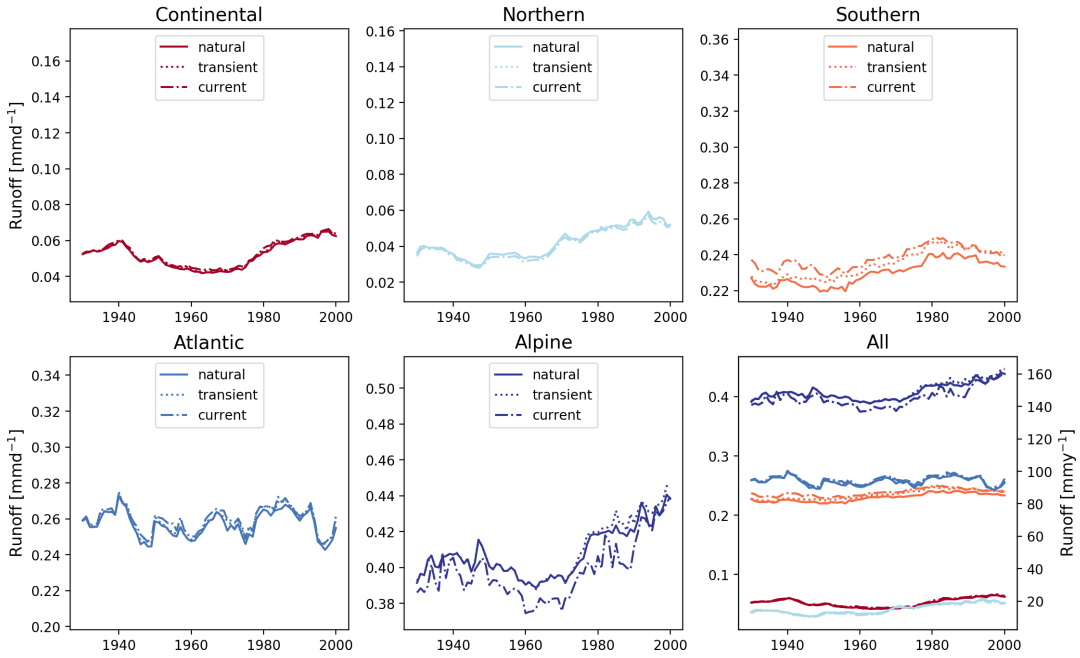


**Figure 32:** Regional median 30-years moving $10^{th}$ percentile runoff (i.e. low flow) for five climate regions in Europe over the period 1901–2001 using WFD forcing data and three model scenarios; no human interventions, transient human interventions and current human interventions. The lower right plot shows all regions' results together.

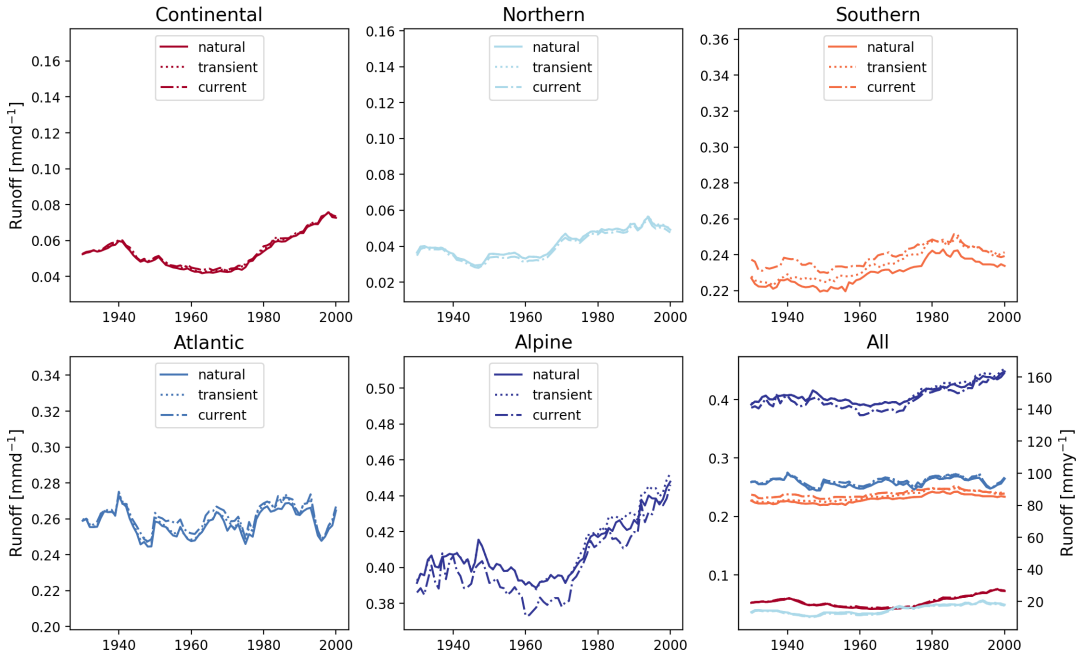


**Figure 33:** Regional median 30-years moving $10^{th}$ percentile runoff (i.e. low flow) for five climate regions in Europe over the period 1901–2001 using WFDEI forcing data and three model scenarios; no human interventions, transient human interventions and current human interventions. The lower right plot shows all regions' results together.

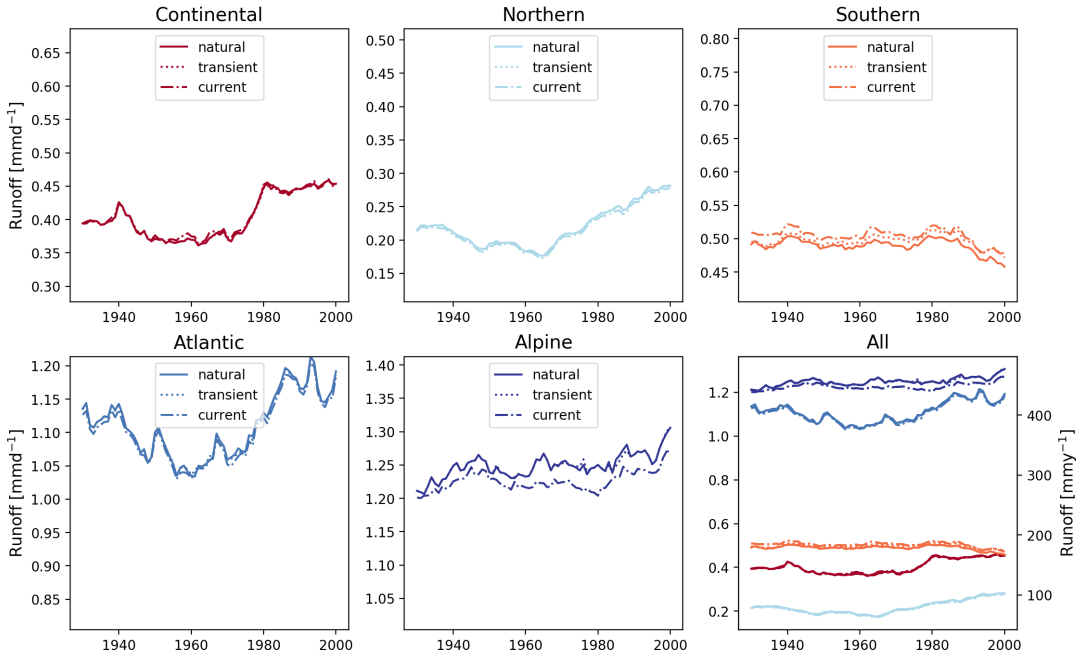


**Figure 34:** Regional median 30-years moving $50^{th}$ percentile runoff (i.e. mid flow) for five climate regions in Europe over the period 1901–2001 using GSWP3 forcing data and three model scenarios; no human interventions, transient human interventions and current human interventions. The lower right plot shows all regions' results together.

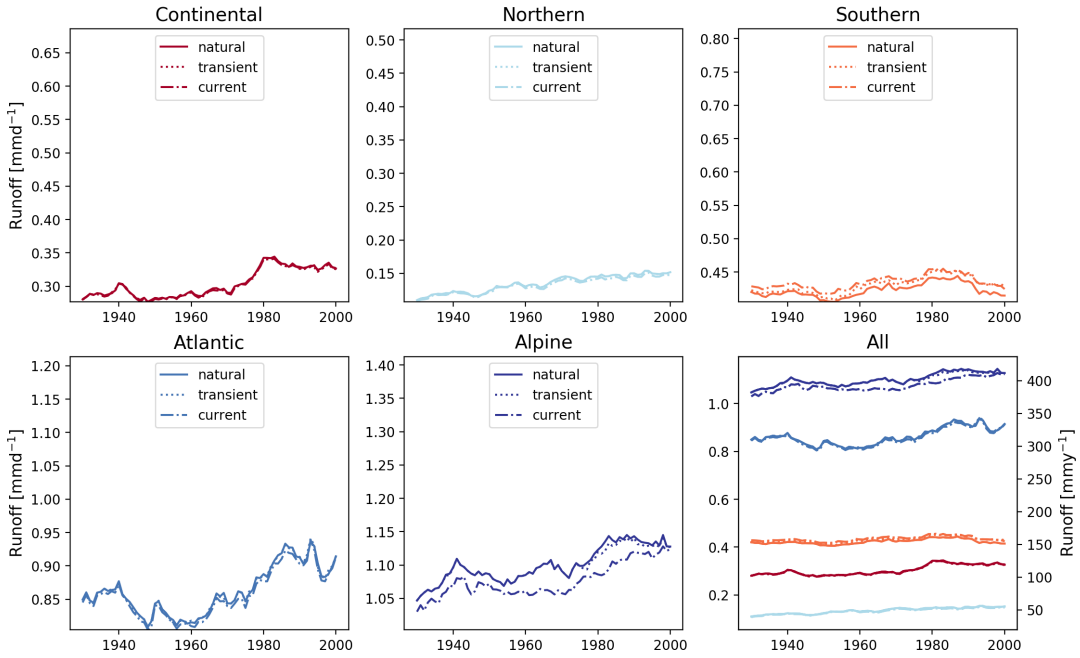


**Figure 35:** Regional median 30-years moving $50^{th}$ percentile runoff (i.e. mid flow) for five climate regions in Europe over the period 1901–2001 using PGMFDv2 forcing data and three model scenarios; no human interventions, transient human interventions and current human interventions. The lower right plot shows all regions' results together.

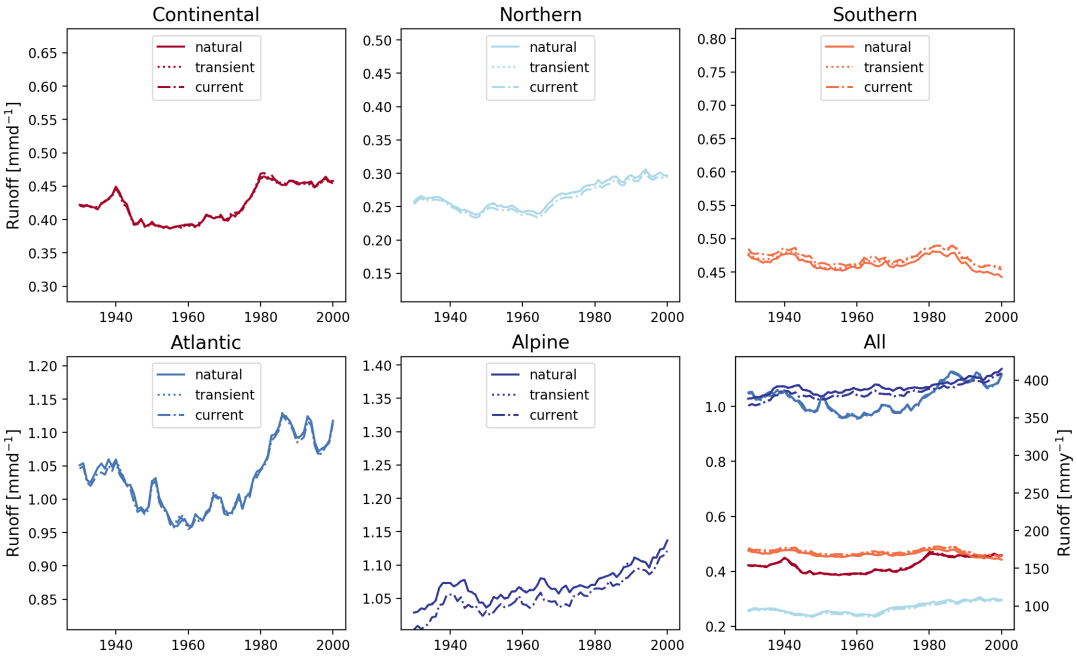


**Figure 36:** Regional median 30-years moving $50^{th}$ percentile runoff (i.e. mid flow) for five climate regions in Europe over the period 1901–2001 using WFD forcing data and three model scenarios; no human interventions, transient human interventions and current human interventions. The lower right plot shows all regions' results together.

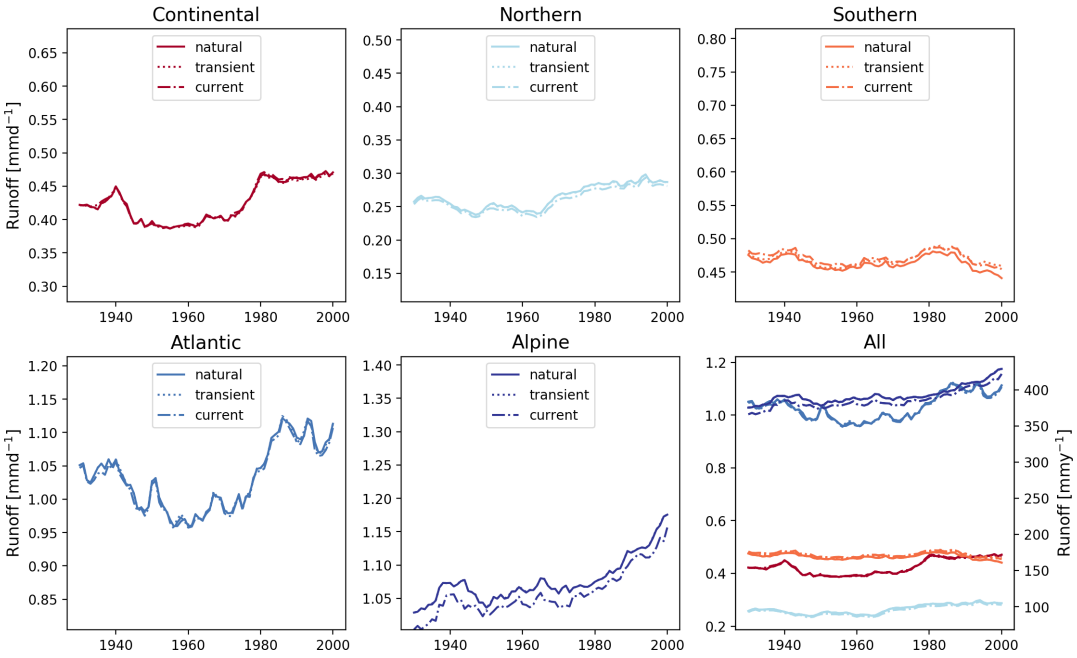


**Figure 37:** Regional median 30-years moving $50^{th}$ percentile runoff (i.e. mid flow) for five climate regions in Europe over the period 1901–2001 using WFDEI forcing data and three model scenarios; no human interventions, transient human interventions and current human interventions. The lower right plot shows all regions' results together.

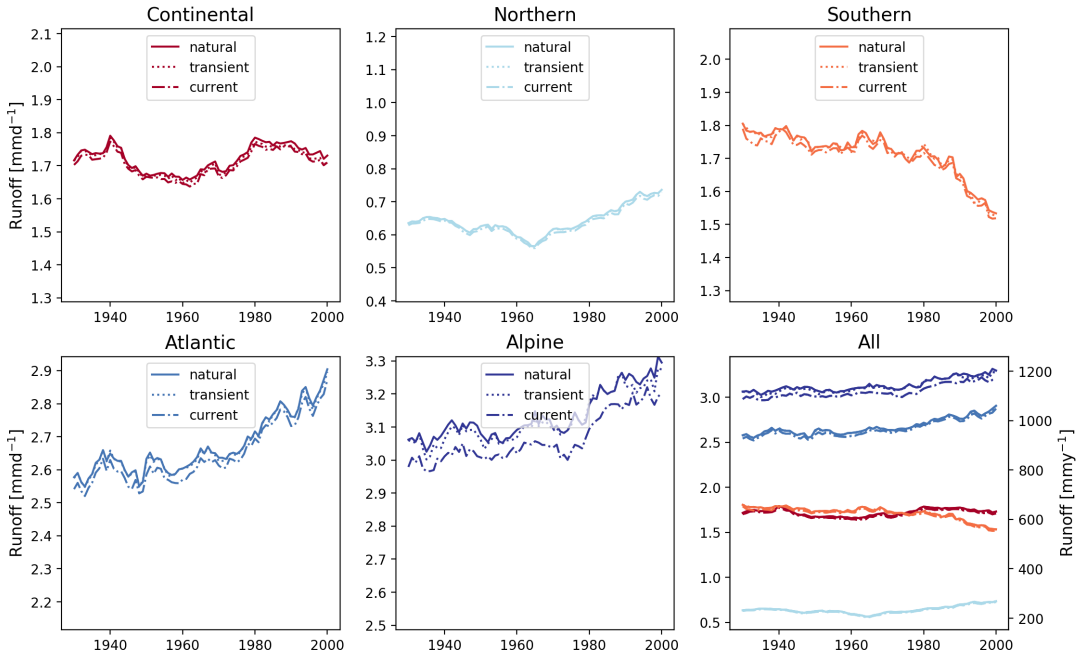


**Figure 38:** Regional median 30-years moving $90^{th}$ percentile runoff (i.e. high flow) for five climate regions in Europe over the period 1901–2001 using GSWP3 forcing data and three model scenarios; no human interventions, transient human interventions and current human interventions. The lower right plot shows all regions' results together.

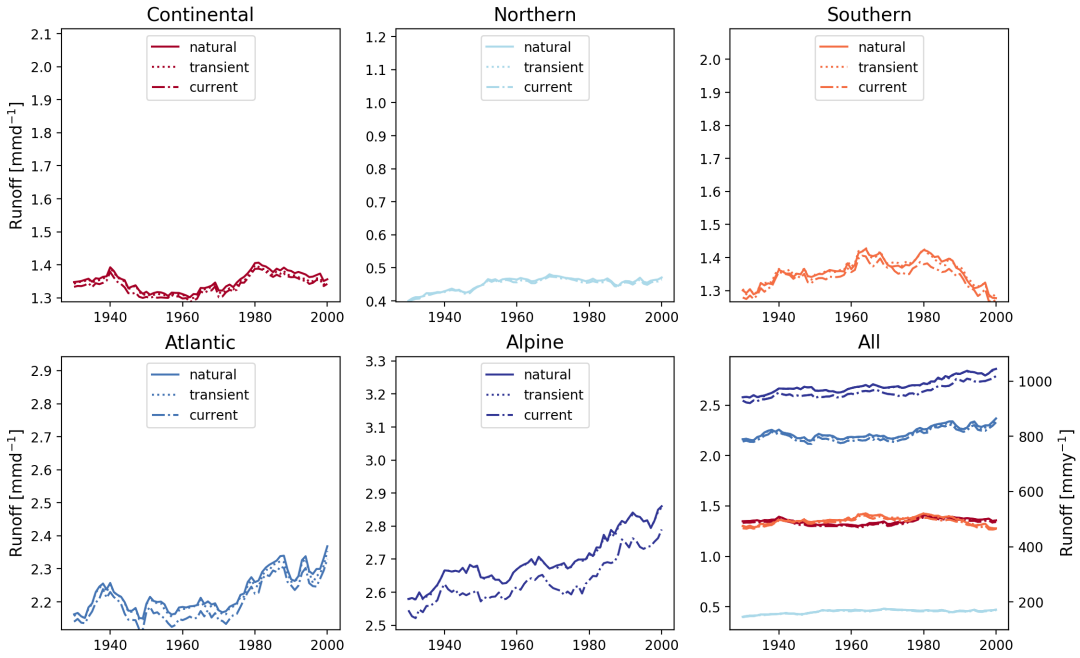


**Figure 39:** Regional median 30-years moving $90^{th}$ percentile runoff (i.e. high flow) for five climate regions in Europe over the period 1901–2001 using PGMFDv2 forcing data and three model scenarios; no human interventions, transient human interventions and current human interventions. The lower right plot shows all regions' results together.

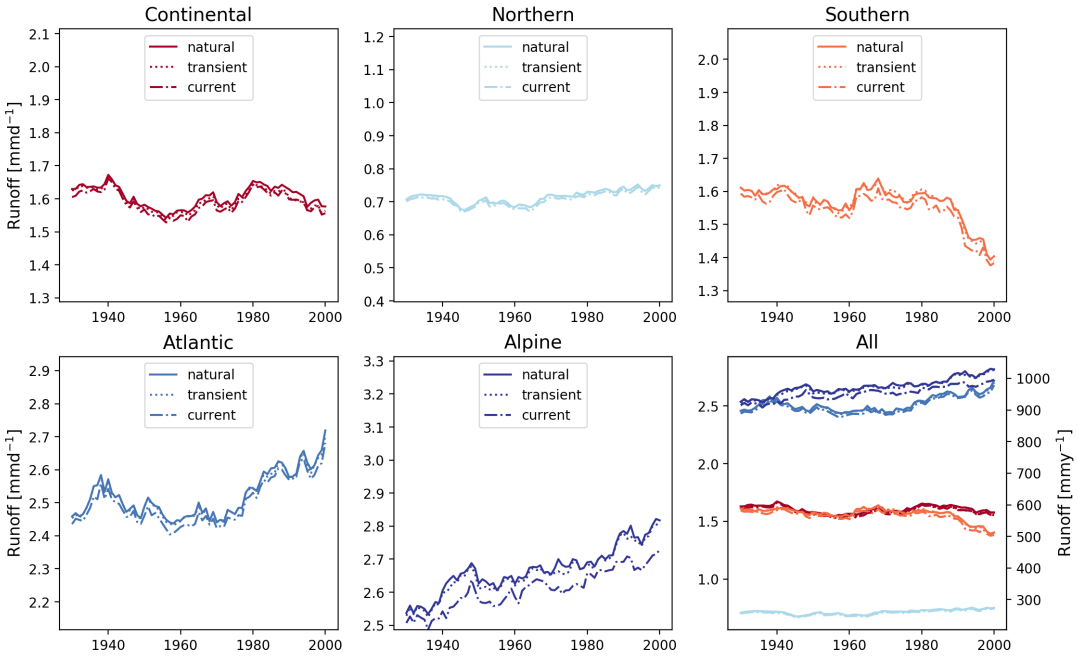


**Figure 40:** Regional median 30-years moving $90^{th}$ percentile runoff (i.e. high flow) for five climate regions in Europe over the period 1901–2001 using WFD forcing data and three model scenarios; no human interventions, transient human interventions and current human interventions. The lower right plot shows all regions' results together.

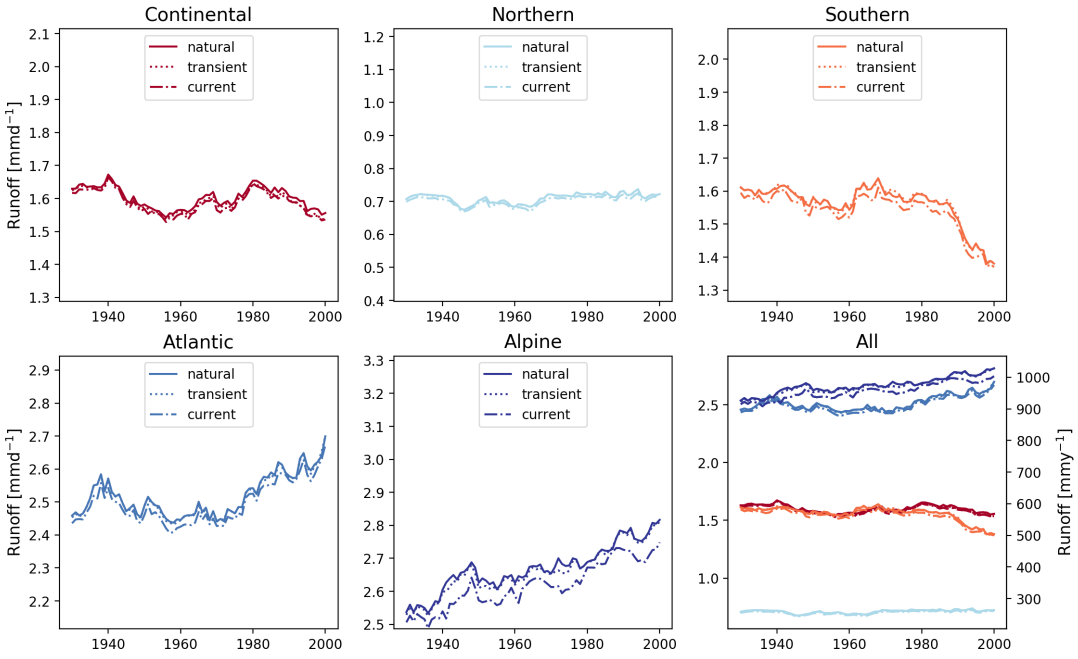


**Figure 41:** Regional median 30-years moving $90^{th}$ percentile runoff (i.e. high flow) for five climate regions in Europe over the period 1901–2001 using WFDEI forcing data and three model scenarios; no human interventions, transient human interventions and current human interventions. The lower right plot shows all regions' results together.

# Appendix D Human Impacts on Regional Flow Variability; Results by All Forcing Data Sets

Appendix C includes Figure 42–45 that provide the results by all four forcing data sets (GSWP3, PGMFDv2, WFD and WFDEI) and all three model scenarios (no human interventions, transient human intervention and current human interventions) of the time series of regional median $20^{th}/80^{th}$ percentile runoff (i.e. $\Delta$FDC representing flow variability). The y-axis is fixed for the results by all forcing data sets for the same region, to easily compare the differences between results by the different forcing data sets. The y-axis increment is fixed for all regions, to easily compare differences between model scenarios for the different regions.

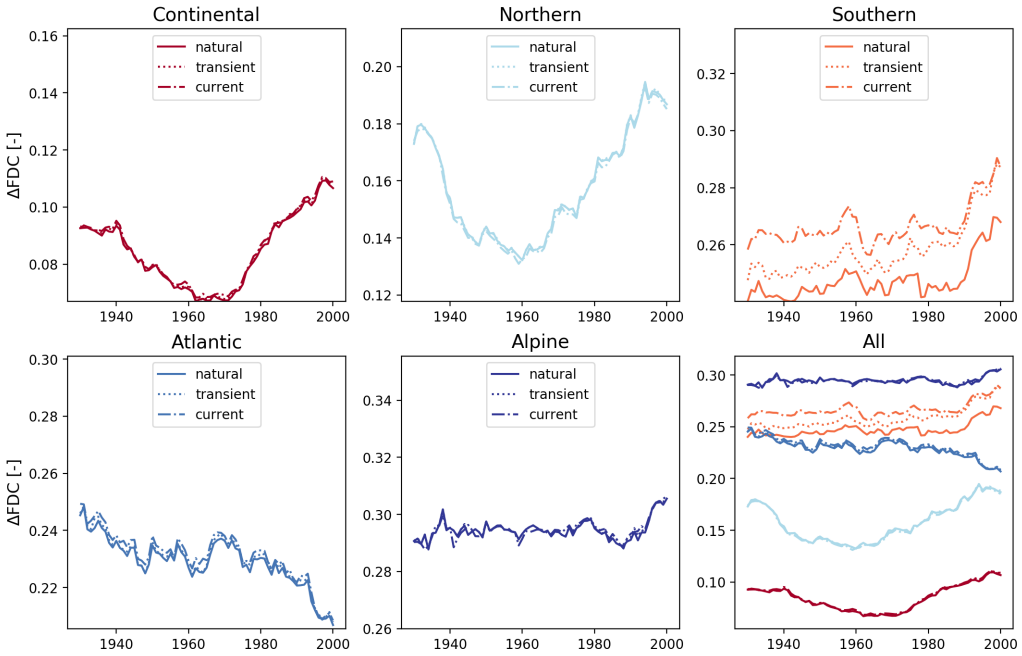


**Figure 42:** Regional median 30-years moving $20^{th}/80^{th}$ percentile runoff (ΔFDC) for five climate regions in Europe over the period 1901–2001 using GSWP3 forcing data and three model scenarios; no human interventions, transient human interventions and current human interventions. The lower right plot shows all regions' results together.

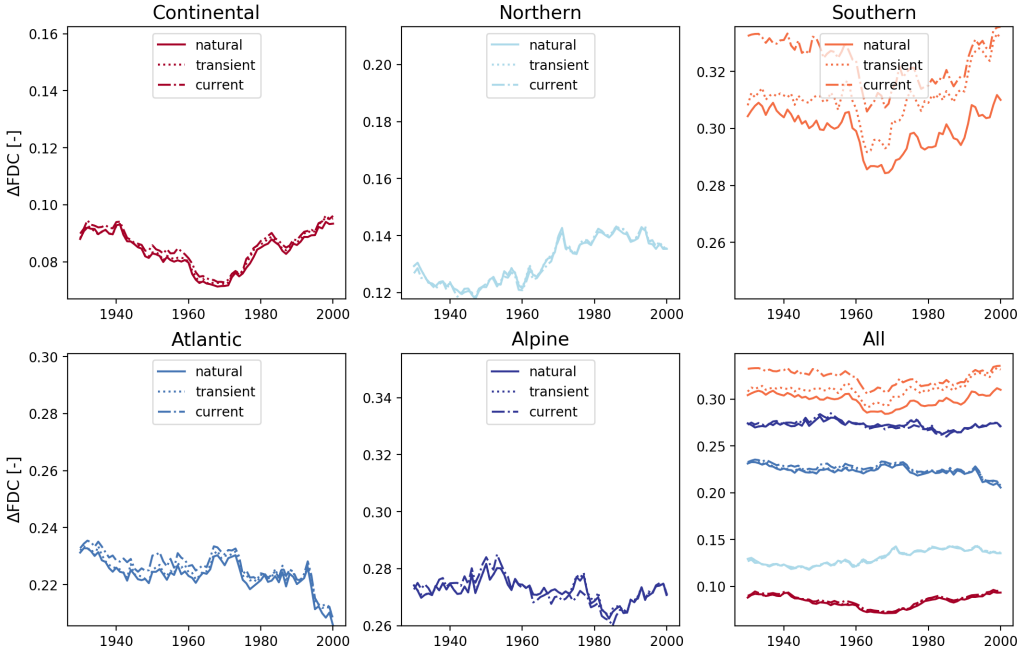


**Figure 43:** Regional median 30-years moving $20^{th}/80^{th}$ percentile runoff (ΔFDC) for five climate regions in Europe over the period 1901–2001 using PGMFDv2 forcing data and three model scenarios; no human interventions, transient human interventions and current human interventions. The lower right plot shows all regions' results together.

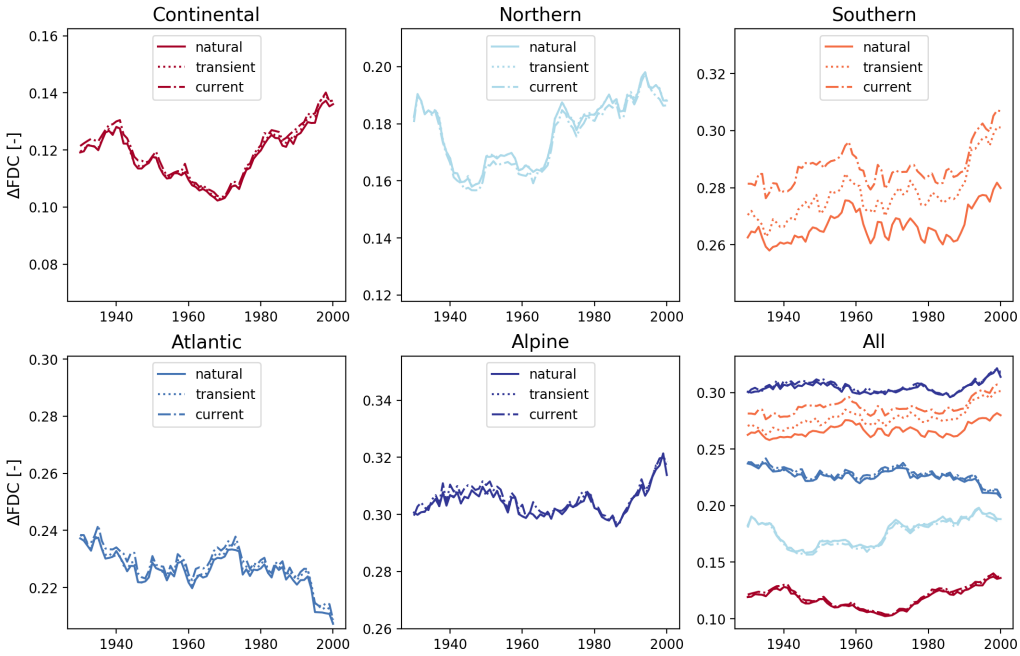


**Figure 44:** Regional median 30-years moving $20^{th}/80^{th}$ percentile runoff (ΔFDC) for five climate regions in Europe over the period 1901–2001 using WFD forcing data and three model scenarios; no human interventions, transient human interventions and current human interventions. The lower right plot shows all regions' results together.

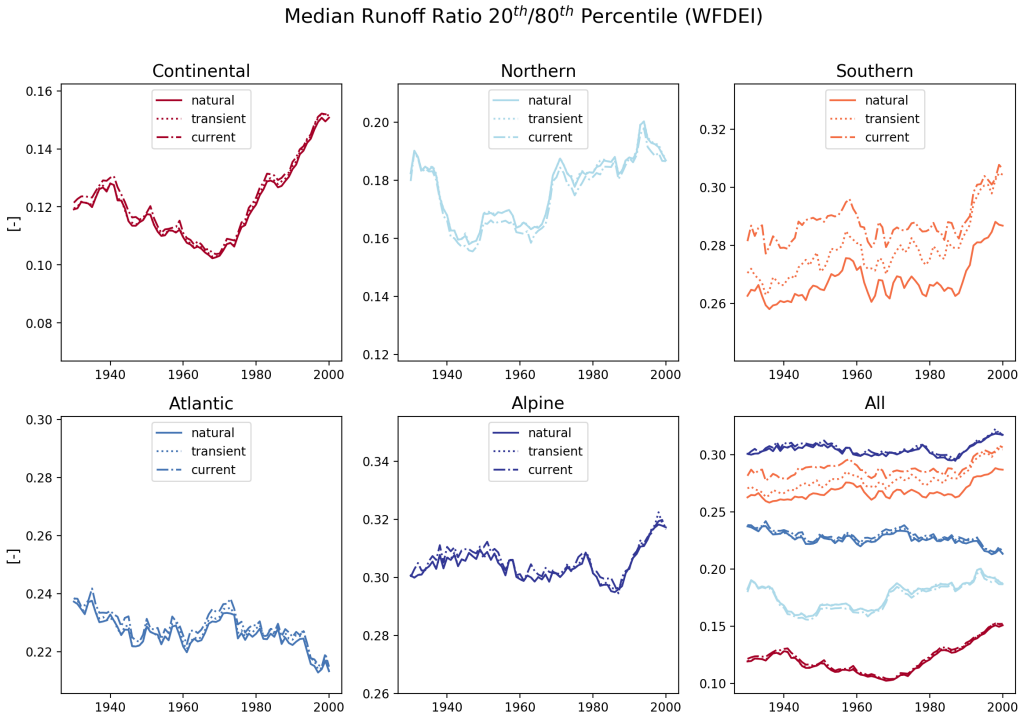


**Figure 45:** Regional median 30-years moving $20^{th}/80^{th}$ percentile runoff (ΔFDC) for five climate regions in Europe over the period 1901–2001 using WFDEI forcing data and three model scenarios; no human interventions, transient human interventions and current human interventions. The lower right plot shows all regions' results together.

# Appendix E Human Impacts on Water Gain and Loss for the Whole Period; Results by All Forcing Data Sets

Appendix E includes Figure 46–53 that provide all results of ecosurplus and ecodeficit, i.e. results for each of the four meteorological forcing datasets applied (GSWP3, PGMFDv2, WFD and WFDEI) for both runoff and discharge.

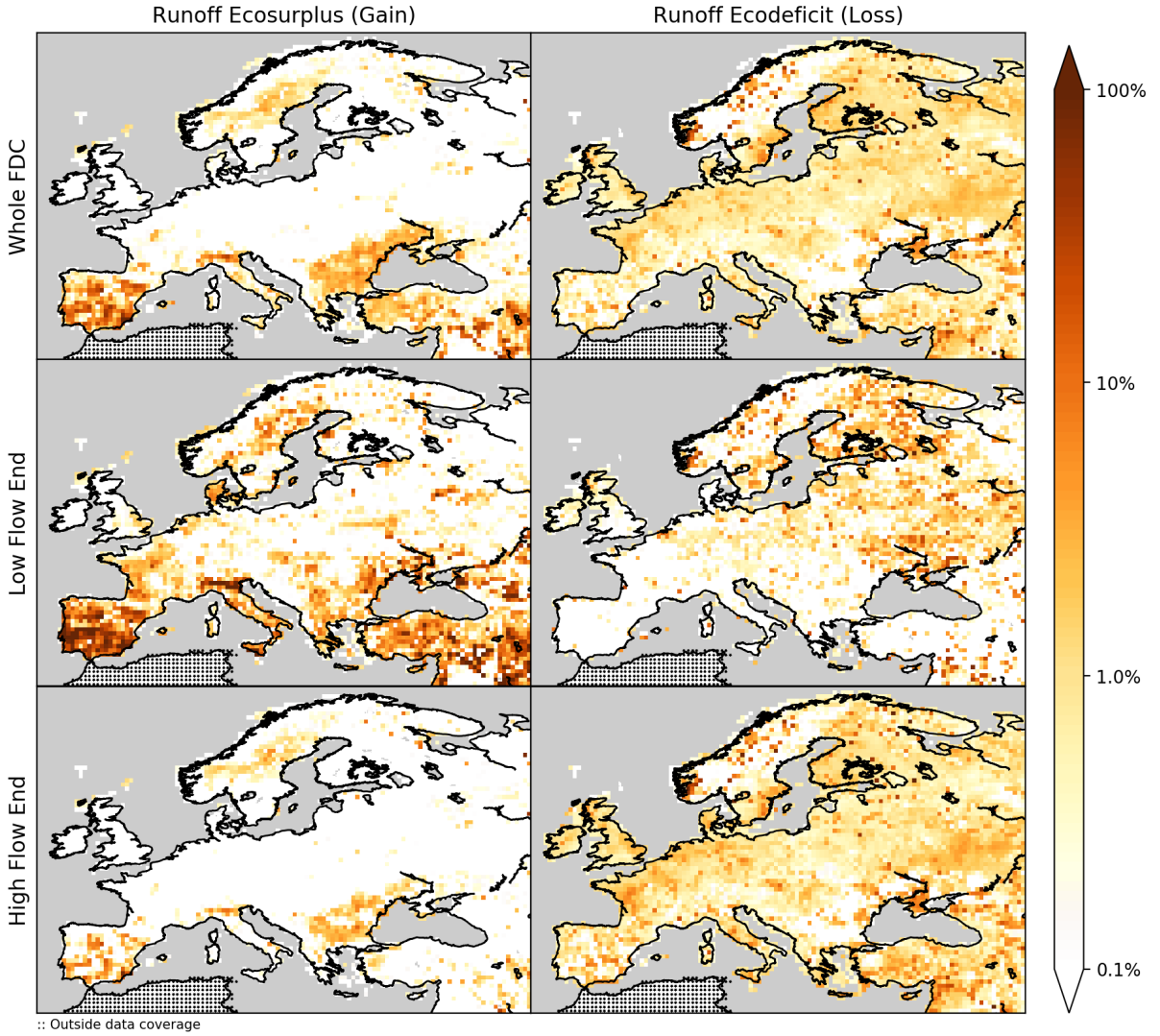


**Figure 46:** Runoff ecosurplus (left) and ecodeficit (right) for the whole FDC ($0^{th}$–$100^{th}$ percentile; top), low flow end FDC ($0^{th}$–$10^{th}$ percentile; middle) and high flow end FDC ($90^{th}$–$100^{th}$ percentile; bottom). The FDCs are based on simulated runoff using the GSWP3 forcing data for the period 1901-2001.

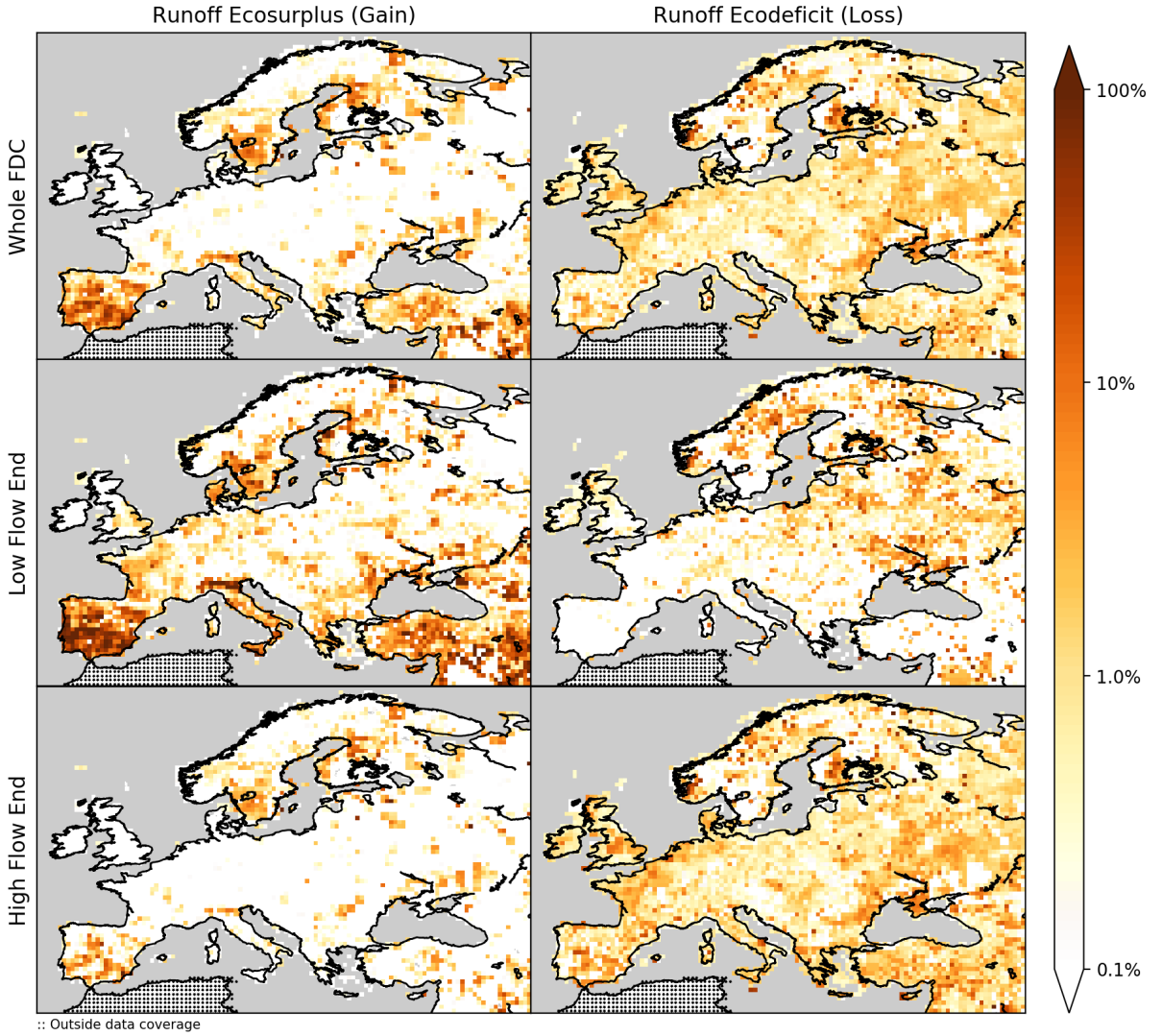


**Figure 47:** Runoff ecosurplus (left) and ecodeficit (right) for the whole FDC ($0^{th}$–$100^{th}$ percentile; top), low flow end FDC ($0^{th}$–$10^{th}$ percentile; middle) and high flow end FDC ($90^{th}$–$100^{th}$ percentile; bottom). The FDCs are based on simulated runoff using the PGMFDv2 forcing data for the period 1901-2001.

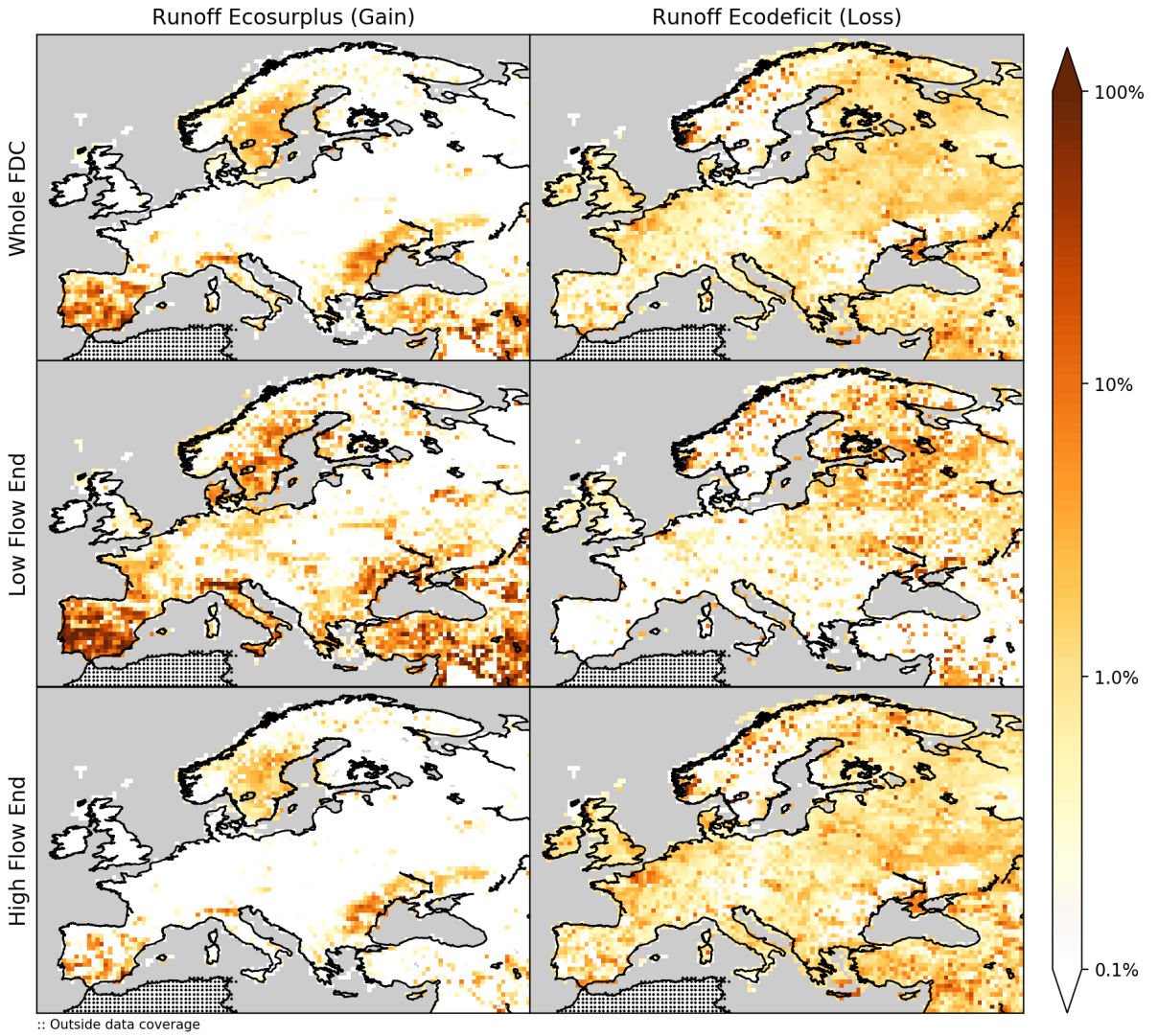


**Figure 48:** Runoff ecosurplus (left) and ecodeficit (right) for the whole FDC ($0^{th}$–$100^{th}$ percentile; top), low flow end FDC ($0^{th}$–$10^{th}$ percentile; middle) and high flow end FDC ($90^{th}$–$100^{th}$ percentile; bottom). The FDCs are based on simulated runoff using the WFD forcing data for the period 1901-2001.

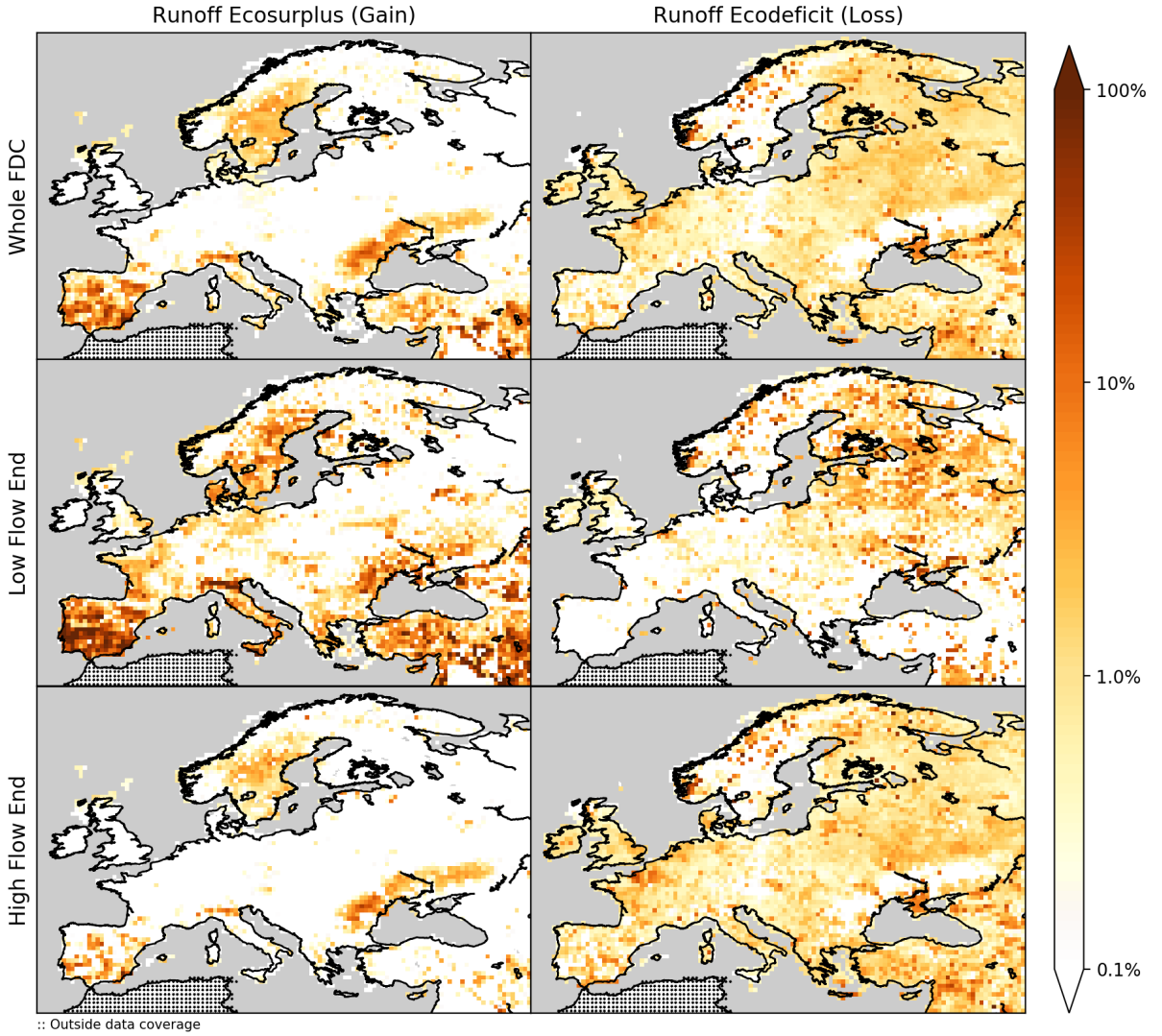


**Figure 49:** Runoff ecosurplus (left) and ecodeficit (right) for the whole FDC ($0^{th}$–$100^{th}$ percentile; top), low flow end FDC ($0^{th}$–$10^{th}$ percentile; middle) and high flow end FDC ($90^{th}$–$100^{th}$ percentile; bottom). The FDCs are based on simulated runoff using the WFDEI forcing data for the period 1901-2001.

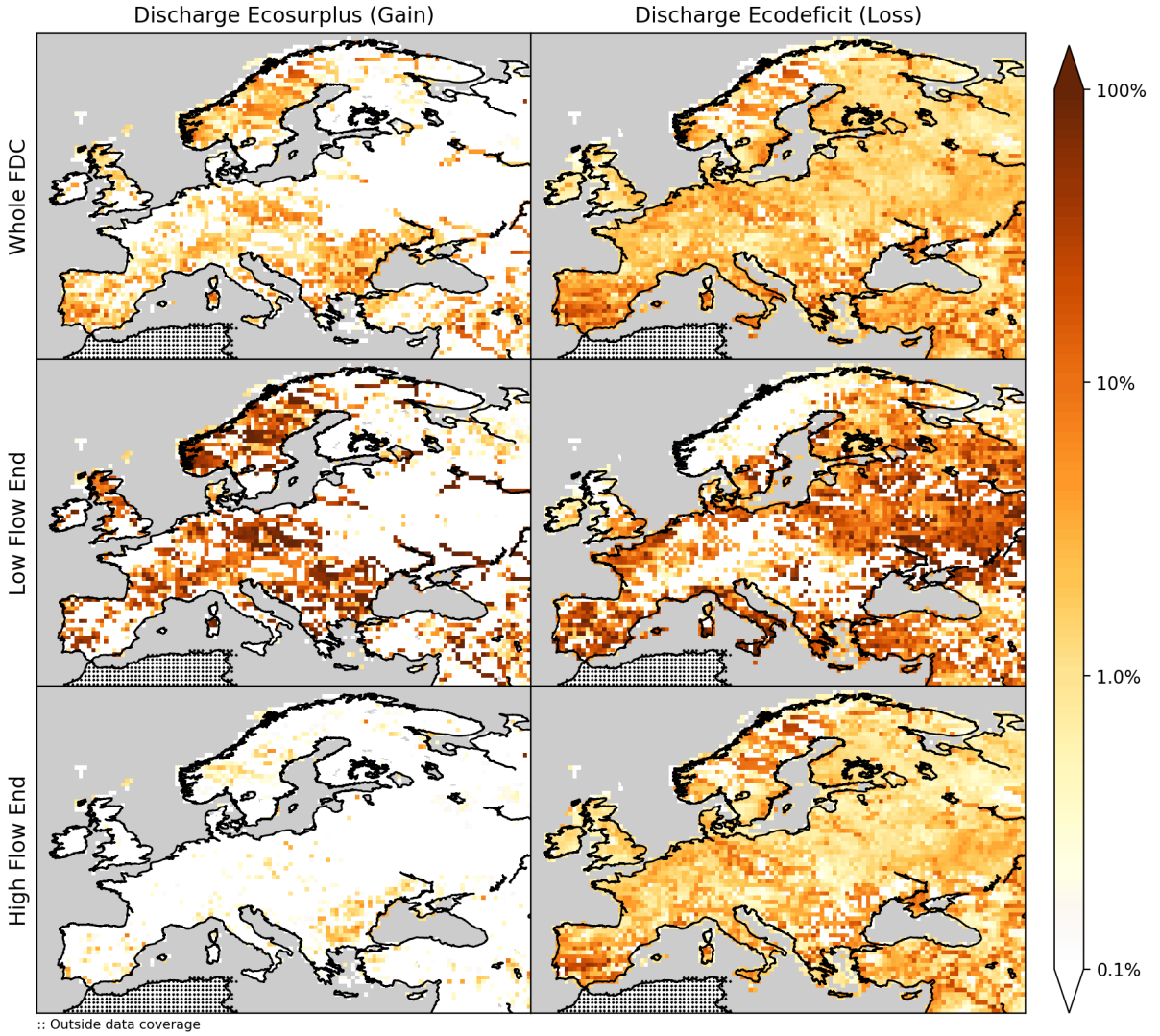


**Figure 50:** Discharge ecosurplus (left) and ecodeficit (right) for the whole FDC ($0^{th}$–$100^{th}$ percentile; top), low flow end FDC ($0^{th}$–$10^{th}$ percentile; middle) and high flow end FDC ($90^{th}$–$100^{th}$ percentile; bottom). The FDCs are based on simulated runoff using the GSWP3 forcing data for the period 1901-2001.

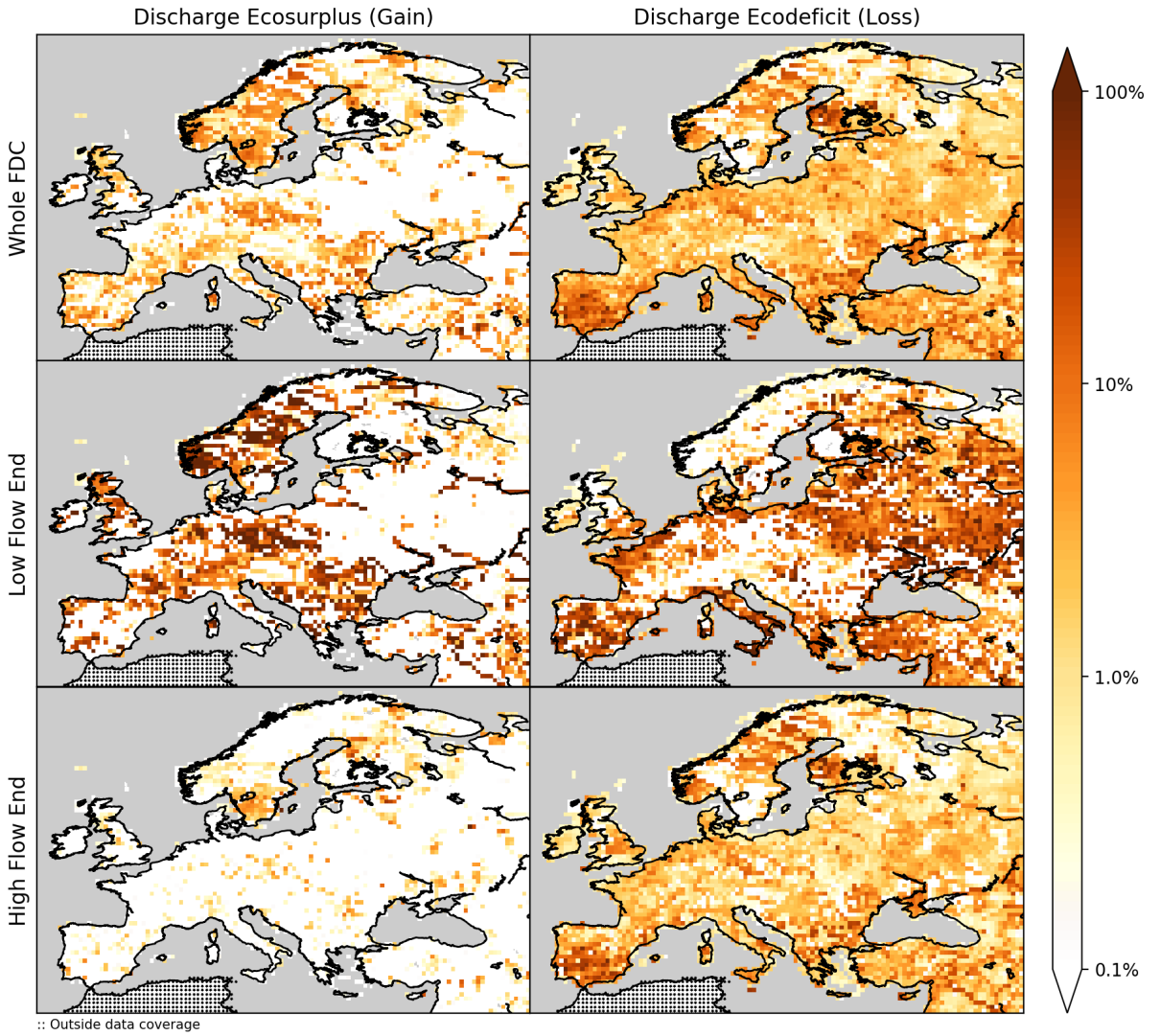


**Figure 51:** Discharge ecosurplus (left) and ecodeficit (right) for the whole FDC ($0^{th}$–$100^{th}$ percentile; top), low flow end FDC ($0^{th}$–$10^{th}$ percentile; middle) and high flow end FDC ($90^{th}$–$100^{th}$ percentile; bottom). The FDCs are based on simulated runoff using the PGMFDv2 forcing data for the period 1901-2001.

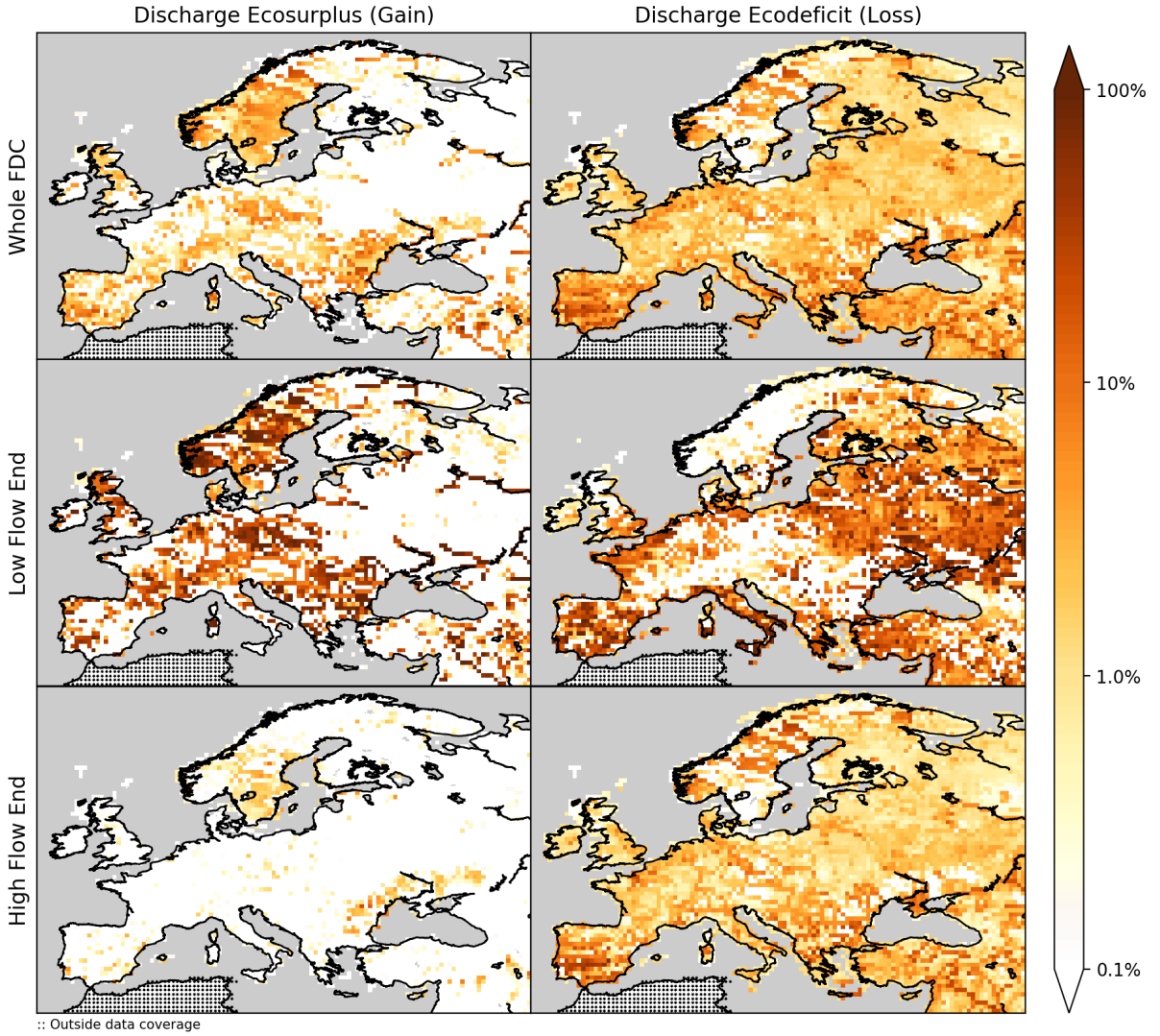


**Figure 52:** Discharge ecosurplus (left) and ecodeficit (right) for the whole FDC ($0^{th}$–$100^{th}$ percentile; top), low flow end FDC ($0^{th}$–$10^{th}$ percentile; middle) and high flow end FDC ($90^{th}$–$100^{th}$ percentile; bottom). The FDCs are based on simulated runoff using the WFD forcing data for the period 1901-2001.

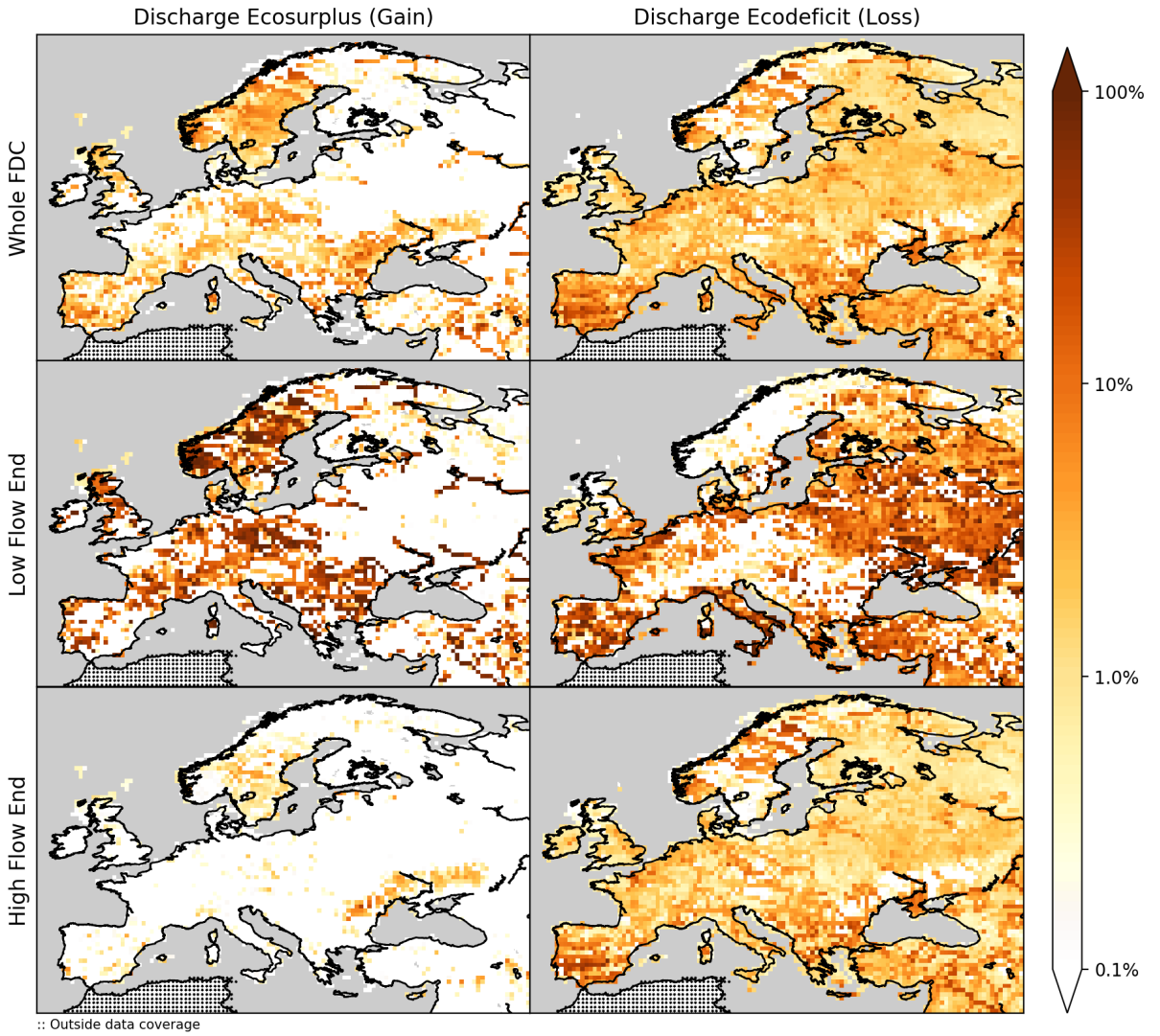


**Figure 53:** Discharge ecosurplus (left) and ecodeficit (right) for the whole FDC ($0^{th}$–$100^{th}$ percentile; top), low flow end FDC ($0^{th}$–$10^{th}$ percentile; middle) and high flow end FDC ($90^{th}$–$100^{th}$ percentile; bottom). The FDCs are based on simulated runoff using the WFDEI forcing data for the period 1901-2001.